UNIVERSIDAD COMPLUTENSE DE MADRID
FACULTAD DE FARMACIA

TESIS DOCTORAL

Funcionamiento y biocomplejidad de la cubierta criptogámica en zonas áridas y polares

Performance and bio complexity of the criptogamic cover in arid and polar regions

MEMORIA PARA OPTAR AL GRADO DE DOCTOR

PRESENTADA POR

Nuria Beltrán Sanz

Directores

Leopoldo García Sancho
Ruth del Prado Millán

Madrid

UNIVERSIDAD COMPLUTENSE DE MADRID
FACULTAD DE FARMACIA

TESIS DOCTORAL

FUNCIONAMIENTO Y BIOCOMPLEJIDAD DE LA CUBIERTA CRIPTOGÁMICA EN ZONAS ÁRIDAS Y POLARES

PERFORMANCE AND BIOCOMPLEXITY OF THE CRIPTOGAMIC COVER IN ARID AND POLAR REGIONS

MEMORIA PARA OPTAR AL GRADO DE DOCTORA

PRESENTADA POR

NÚRIA BELTRÁN SANZ

DIRECTORES

Leopoldo García Sancho,
Ruth del Prado Millán

UNIVERSIDAD COMPLUTENSE DE MADRID
FACULTAD DE FARMACIA

TESIS DOCTORAL

FUNCIONAMIENTO Y BIOCOMPLEJIDAD DE LA CUBIERTA CRIPTOGÁMICA EN ZONAS ÁRIDAS Y POLARES

PERFORMANCE AND BIOCOMPLEXITY OF THE CRIPTOGAMIC COVER IN ARID AND POLAR REGIONS

MEMORIA PARA OPTAR AL GRADO DE DOCTORA

PRESENTADA POR

NÚRIA BELTRÁN SANZ

DIRECTORES

Leopoldo García Sancho,
Ruth del Prado Millán

Acknowledgements

I want to thank some lovely people who made meaningful contributions to my sanity during the duration of this research project. I am grateful to my supervisors Dr. Leopoldo Garcia Sancho and Dr. Ruth del Prado Millán for the opportunity to take part in this project. Thank you Dr. Sancho too for introducing me to the scientific community promoting, thus, my first collaborations with other scientists, for allowing me to take part in the Antarctic expeditions, and for letting me take the chance of including some of my little ideas as thesis chapters. My sincere gratitude and appreciation to Dr. Francesco Dal Grande for always being there. Thanks Dr. Dal Grande for teaching me everything from Sanger to meta-barcoding sequencing, for your support in the laboratory and field experiments, for explaining to me the same issues hundreds of times without getting mad, and for making the effort of even supporting me in topics such as eco-physiology and modeling that are so distant to you. I really appreciate you and your family for hosting and treating me so kindly in Frankfurt. I am also grateful to Dr. Imke Schmitt's research group for providing me with more support than I could ever imagine. Thank you Dr. Imke Schmitt, Meike Schulz, Dr. Garima Singh, Junger Otten, Dr. Anjuli Cladera and Dr. Gregor Rolshausen.

It is impossible to not feel grateful for Dr. José Raggio who has invested countless hours and days, and effort into making this thesis better. Thanks Dr. Raggio for giving me feedback any time I needed it, for discussing my results for hours, for fixing all the issues that came along, and for being able to understand my ideas even in the unreadable first proofs. I will always appreciate all the time that you have invested in me, Dr. Raggio, in making me evolve and grow as a scientist. I am also grateful to Dr. Ana Pintado for, firstly, always being kind to me, and secondly, for having the best clinical eye for detecting even the smallest mistakes. It was a pleasure to share my first Antarctic expedition with you Dr. Pintado. Special thanks to Dr. Green, who despite being retired, has spent much of his time checking the data, the analysis and the writing of my chapters.

I am grateful to Dr. Isaac Garrido for checking my phylogenetic analysis and widening my knowledge about molecular methodologies. Also, I would like to say thanks

Contents

Summary

Introduction: The present thesis titled 'Performance and bio-complexity of the criptogamic cover in arid and polar regions' aims to understand how lichens and bryophytes modulate their physiological response pattern in order to maximize the fitness in the Tabernas Desert (south of Spain), and Livingston Island (maritime Antarctica). Lichens and bryophytes are widely spread in the most climatic extreme regions across the world due to their ability to cope with harsh environmental conditions. Their survival in these regions seems to be linked to physiological and phenotypical plasticity. Due to the symbiotic nature of lichens, adaptation strategies have to be assessed with a multidisciplinary approach, considering the bionts identity as important as morphology and micro-topography, since both might notably influence their physiologic performance. Unravelling how biotic and abiotic factors determine the adaptation strategies of species according to the local conditions is crucial for understanding the potential effects of climate change on biomes as vulnerable as polar and drylands.

Aims: This thesis addresses how the combination of different functional traits allows lichens and bryophytes to cope with hard abiotic conditions. Particularly, it aims to assess how environmental conditions modulate the physiological response pattern of lichens and bryophytes in extreme biomes. The specific aims are:

- Assessing the physiological plasticity of the cosmopolitan moss *Ceratodon purpureus* (Hedw.) Brid. under contrasting habitats along the Southern Hemisphere (Chapter 1).
- Investigating the functional traits of the two closely related species *Xanthoparmelia pulla* (Ach.) O. Blanco, A. Crespo, Elix, D. Hawksw. & Lumbsch and *X. pokornyi* (Körb.) O. Blanco, A. Crespo, Elix, D. Hawksw. & Lumbsch in the semi-arid region of Almería (Spain) from a molecular and eco-physiological perspective (Chapter 2).
- Studying the effects of climate change on metabolic activity and net primary productivity (NPP) of the lichen *Usnea aurantiaco-atra* (Jacq.) Bory in maritime Antarctica at different temporal and spatial resolutions (Chapter 3).

The present thesis has been organized inro three chapters, whose main results are:

- Populations of *C. purpureus* from maritime Antarctica and the semi-arid desert show thermal acclimation of respiration, while those from continental Antarctica

have a high sensitivity to temperature changes and no acclimation. There is a high dissimilarity between the tundra biomes, placing the population from the semi-arid desert in an intermediate position due to sharing functional traits with both of them. *C. purpureus* seems to be able to modulate the optimal temperature for net photosynthesis according to the environmental conditions of each ecosystem, and switch from shade- to sun- adapted forms.

- Our findings show that the mycobionts of *X. pulla* and *X. pokornyi* are highly similar, and use phenotypic plasticity - rather than genetic differentiation - as a strategy to better adapt to local environmental conditions. A similar photobiont community composition, low specificity between partner/s, and physiological convergence were found in both species. Nevertheless, there is a high genetic diversity of the lichen-associated algal communities on the coastal populations, as well as a potential complementary eco-physiological response between OTU1 and OTU2.

- The metabolic activity, the microclimate, and the type of hydric sources are crucial to predict the effects of climate change on the net primary productivity (NPP) in maritime Antarctica. Under climate change conditions, metabolic activity and NPP are predicted to increase in species with similar physiological tolerance to the lichen *U. aurantiaco-atra*.

*Conclusion*s: Over the chapters, we highlight how lichens and bryophytes exhibit different physiological strategies to better adapt to the local environmental conditions. Having high physiological plasticity allows the cosmopolitan moss *C. purpureus* to modulate respiration rates in habitats less climatically harsh like maritime Antarctica, and thus, maximize the carbon gain (Chapter 1). Nevertheless, in extreme regions such as continental Antarctica, this plasticity is constrained by the harsh climatic stresses of the region that promote species to acquire protection strategies and mechanisms to guarantee their survival. Finally, species from drylands like *X. pulla* and *X. pokornyi* show similar genetic backgrounds of both bionts, and physiological convergence (Chapter 2). This homogeneity in the physiological response pattern is also influenced by variations in growth form and by substrate switching which promote better harnessing of the hydric sources. Therefore, understanding how species cope with extreme environmental conditions allows us to predict the effects of climate change in vulnerable biomes such as drylands and the tundra. As long as liquid water is available in maritime Antarctica,

metabolic activity and NPP are predicted to increase under climate change scenarios in species with similar physiological tolerance ranges to *U. aurantiaco-atra* (Chapter 3). These changes are mainly driven by temperature, which significantly influences both metabolic activity duration and NPP on a daily basis.

Resumen

Introducción: La presente tesis titulada 'Funcionamiento y biocomplejidad de la cubierta criptogámica en zonas áridas y polares' tiene como objetivo general estudiar como los líquenes y los briófitos modulan su patrón de respuesta fisiológica para maximizar la *fitness* en regiones semi-áridas como el Desierto de Tabernas y en la tundra Antárctica. Los líquenes y los briófitos están ampliamente distribuidos en zonas climáticas extremas debido a su capacidad para hacer a frente a condiciones adversas. Para muchas especies, la supervivencia en estas regiones está ligada a la plasticidad fenotípica y fisiológica. Debido a la naturaleza simbiótica de los líquenes, las estrategias de adaptación deben ser además evaluadas des de un punto de vista interdisciplinar, considerando la identidad de los biontes como un factor de igual importancia que la morfología o la micro-topografía, ya que todos ellos pueden influir notablemente en el rendimiento fisiológico. Desentrañar como los factores bióticos y abióticos determinan las estrategias de adaptación de líquenes y briófitos, según las condiciones locales, es indispensable para entender los efectos potenciales del cambio climático en biomas tan vulnerables como la tundra y los desiertos.

Objetivos: Esta tesis aborda cómo la combinación de diferentes rasgos funcionales permite hacer frente a las duras condiciones climáticas en biomas extremos. Particularmente, se pretende evaluar cómo las condiciones ambientales modulan el patrón de respuesta fisiológica en los líquenes y los briófitos de zonas polares y desiertos. Los objetivos específicos son:

- Evaluar la plasticidad fisiológica del musgo cosmopolita *Ceratodon purpureus* (Hedw.) Brid. en hábitats contrastantes a lo largo del hemisferio sur (Capítulo 1).
- Investigar los rasgos funcionales de las especies estrechamente emparentadas *Xanthoparmelia pulla* (Ach.) O. Blanco, A. Crespo, Elix, D. Hawksw. & Lumbsch y *X. pokornyi* (Körb.) O. Blanco, A. Crespo, Elix, D. Hawksw. & Lumbsch en la región semi-árida de Almería (Sureste de la Península Ibérica) des de una perspectiva molecular y eco-fisiológica (Capítulo 2).
- Estudiar los efectos del cambio climático sobre la actividad metabólica y la productividad primaria neta (NPP) del líquen *Usnea aurantiaco-atra* (Jacq.) Bory en la Isla Livingston (Antártida marítima) a diferentes resoluciones temporales y espaciales (Capítulo 3).

Los resultados obtenidos para cada uno de los objetivos específicos son los siguientes:

- Las poblaciones de *C. purpureus* de la Antártida marítima y el desierto semi-árido muestran aclimatación de la respiración a la temperatura; sin embargo, la población de la Antártida continental tiene una elevada sensibilidad a los cambios de temperatura y no muestran aclimatación alguna. Hay una elevada disimilitud entre los biomas de tundra, lo que sitúa a la población del desierto semi-árido en una posición intermedia al compartir rasgos funcionales con ambas zonas de tundra. Además, *C. purpureus* es capaz de modular su óptimo de temperatura para la fotosíntesis neta según las condiciones ambientales de cada hábitat, e intercambiar de forma adaptada a la sombra a forma adaptada al sol.

- Nuestros resultados muestran que *X. pulla* y *X. pokornyi* tienen micobiontes genéticamente muy parecidos, y que utilizan la plasticidad morfológica y el intercambio de sustrato – en lugar de la diferenciación genética – como estrategia para adaptarse mejor a las condiciones ambientales locales. Ambas especies mantienen también similar composición del fotobionte, baja especificidad entre fotobionte y micobionte, y convergencia fisiológica. Sin embargo, hay una mayor diversidad genética de las comunidades algales asociadas al liquen en las poblaciones costeras, así como una potencial complementariedad eco-fisiológica entre los fotobiontes OTU1 y OTU2.

- La actividad metabólica, el microclima y el tipo de fuente hídrica son cruciales para predecir los efectos del cambio climático sobre la productividad primaria neta (NPP) en la Antártida marítima. Bajo los escenarios de cambio climático, la actividad metabólica y la NPP podría aumentar en especies como *U. aurantiaco-atra*.

Conclusión: A lo largo de los capítulos, se destaca como líquenes y briofitos utilizan diferentes estrategias fisiológicas para mejorar su adaptación a condiciones ambientales locales. Tener una elevada plasticidad fisiológica permite al musgo cosmopolita *C. purpureus* modular sus tasas de respiración en hábitats poco estresantes como la Antártida marítima y, por lo tanto, maximizar la ganancia de carbono (Capítulo 1). Sin embargo, en regiones más extremas como la Antártida continental, esta plasticidad se ve limitada debido al estrés ambiental, el cual provoca que las especies adopten estrategias y mecanismos de protección para no comprometer su supervivencia. Finalmente, en regiones áridas, especies como *X. pulla* y *X. pokornyi* mantienen una baja variabilidad

genética tanto en el fotobiontes como en el micobionte, y tienden a converger a nivel eco-fisiológico (Capítulo 2). Esta homogeneidad en la respuesta fisiológica está además influida por variaciones en la forma de crecimiento y cambios de sustrato que promueven un mejor aprovechamiento de los recursos hídricos. Por tanto, entender cómo las especies se enfrentan a condiciones ambientales extremas permite predecir los efectos del cambio climático en ecosistemas tan vulnerables como los desiertos y la tundra. Siempre que haya agua líquida presente en el medio, se prevé que la actividad metabólica y la NPP aumenten bajo escenarios de cambio climático en regiones como la Antártida marítima y en especies con similar plasticidad fisiológica que *U. aurantiaco-atra* (Capítulo 3). Estos cambios están principalmente impulsados por la temperatura la cual influye de forma significativa tanto en la duración de la actividad metabólica como la NPP diaria.

Introduction

1. Importance of the tundra and hot desert ecosystems

Biodiversity survives in searing temperatures, frosty environments, and even outer space. From Antarctica to torrid deserts, the study of inhospitable biomes is an exploration of the limits of life.

1.1. Maritime Antarctica

Antarctica has been characterized under criteria that are mostly biogeographic and climatic. Most of the ice-free areas in Antarctica are restricted to the maritime region (Oliva et al., 2017) where climatic conditions are more favourable for the species' survival. (Table 1; Peat et al., 2007; Casanovas et al., 2013). In comparison with the Antarctic plateau, the maritime region is under a narrower daily and seasonal thermal amplitude (Singh et al., 2018; Convey et al., 2014), greater precipitation events (Convey, 2013), and more cloudiness (Bölter et al., 2002).

The most species-rich plant communities tend to occur at low elevations like coastal regions (Green et al., 2007). This distribution pattern seems to be the result of both greater topographical variation and the absence of snow for at least three months of the year (Smith, 1972). Maritime Antarctica hosts a high diversity of bryophytes, lichens, algae, fungi, and bacteria, in addition to the only two angiosperm species present in Antarctica (Convey, 2005). Hence, cryptogams represent the main component of the tundra landscape (Fig. 1; Casanovas et al., 2015). This fact defines Antarctica as one of the simplest ecosystems in the world, providing, thus, a suitable study system due to the biotic-abiotic interactions being notably reduced.

Fig. 1 Cryptogamic communities located near Juan Carlos I Spanish Antarctic Station at Livingston Island (South Shetland Islands, maritime Antarctica).

The enormous interest in scientists studying Antarctica is justified by the fact that the continent has been warming up twice as much as the global average ever since the 1850's (Siegert et al., 2019). Particularly, the Antarctic Peninsula is experiencing one of the fastest rates of regional climate change on Earth, resulting in the collapse of ice shelves, the retreat of glaciers, and the emergence of new terrestrial habitats (Clarke et al., 2007). Therefore, Antarctica can provide baseline information to evaluate the potential effects of global climate change on biodiversity (Smith, 1990). According to previous studies, terrestrial biota is likely to benefit from reduced environmental stresses in the short term (Chwedorzewska, 2009). However, in the long-term, the colonization of the region by species from lower latitude and/or with greater competitive ability may become increasingly important, resulting in changes in the community composition and trophic complexity (Chwedorzewska, 2009). Moreover, the recent accelerated climate changes in the maritime Antarctic region, combined with increased human activity, could be modifying the dynamics of several non-native species (e.g. Smith and Richardson, 2011; Molina-Montenegro et al., 2014).

1.2. The Tabernas Desert

Drylands are one of the most ubiquitous biomes in the world, covering two-fifths of Earth's land surface (*ca.* 41%; Prăvălie, 2016). The specifics in precipitation and evapotranspiration (Bastin et al., 2017) for each desert determine their aridity index, and consequently, their floristic composition.

The south-eastern region of Spain is home to the most arid area in Europe, the Tabernas Desert (Raggio et al., 2014). It is classified as a hot semi-arid desert (Lázaro et al., 2008) and characterized by a broad daily and seasonal thermal amplitude, low precipitation (Chamizo et al., 2012), and frequent events of fog and dew (Rundel, 1978; Agam and Berliner, 2006; Kidron and Lázaro, 2020). However, climate conditions become milder along a gradient, from the inland desert toward the coastal areas due to the maritime influence of the Mediterranean Sea (Table 1). Climatic differences at those local scales depend on elevation, and the distance from inland to the coast (Lekouch et al., 2011).

The geomorphological processes in the Tabernas Desert have led to the formation of badlands with unique geo-ecologic characteristics that affect the species assemblage (Solé-Benet et al., 2009). The frequent changes in orientation of badlands favour a vegetation cover consisting of sparse shrubs, annuals plants, and lichens on the north- and east-facing hill slopes, while south- and west-facing slopes are barren or vegetation is highly degraded (Fig. 2; Canton et al., 2003).

Fig. 2 Typical landscape of the badlands from Tabernas Desert (Spain).

As with maritime Antarctica, vegetation in drylands is dominated by cryptogams, where they form the 'biocrust' consisting of communities made by lichens, bryophytes, bacteria, and fungi that cover the soil uppermost surface (Maestre et al., 2013). The biocrust provides stability and fertility to desert soils while facilitating colonization by vascular plants (Belnap, 2003). Therefore, the role of biocrust as pioneer colonizers is crucial to maintaining the biodiversity balance within this biome.

The increase in temperature and aridity of the 21st-century highlights the vulnerability of this ecosystem with regard to its dependence on water sources. The effects of climate change on drylands include changes in biocrust species composition (Lafuente et al., 2018), where cyanobacteria communities become favoured at the expense of bryophytes and lichens (Ferrenberg et al., 2015), along with changes in nitrogen (e g. Delgado-Baquerizo et al., 2014) and carbon cycling (Grote et al., 2010; Ladrón de Guevara et al., 2014; Maestre et al., 2013).

Table 1 Mean macroclimatic conditions from 2005 to 2020 in maritime Antarctica, Tabernas Desert, and Cabo de Gata. The superscript letters indicate the bibliographic details of their sources: (a) Longton (1988); (b) Spanish Meteorological Agency (AEMET); (c), Instituto Andaluz de Investigación y Formación Agraria, Pesquera, Alimentaria y de la Producción Ecológica (IFAPA) (d) Chamizo et al. (2015) (e) Smellie et al. (1995).

Climatic parameter	Ecosystem		
	Livingston Island (maritime Antarctica)	**Tabernas Desert (inland area)**	**Cabo de Gata (coastal area)**
Ecosystem	Tundra [a]	Semi-arid [d]	Semi-arid [d]
Temperature (ºC)	-1 [b]	16 [c]	19 [c]
Minimum temperature (ºC)	-22.6 [b]	-5 [c]	4 [c]
Maximum temperature (ºC)	15.5 [b]	40 [c]	38 [c]
Rainfall (mm)	402 [b]	232 [c]	212 [c]
Relative humidity (%)	82 [b]	61 [c]	66 [c]
Radiation (MJ m^{-2} day^{-1})	7 [b]	18 [c]	19 [c]
Substrate	Sedimentary and volcanic rock and soils [e]	Gypsum-calcareous mudstones and calcaric sandstones [d]	Thin soils, saturated in carbonates. Moderate rock fragment content [d]

2. From single individuals to biological communities in lichens

Traditionally, lichens have been defined as an intimate mutualistic interaction between two symbionts: the photobiont, and the mycobiont (Werth et al., 2015). More than 98% of the mycobiont species belong to the Phylum Ascomycota (Lutzoni and Miadlikowska, 2009), and about 90% of photobionts to the Phylum Chlorophyta, of which the genus *Trebouxia* is notably predominant (Muggia et al., 2016), and present in more than 50% of all known lichens (Barták, 2014). All lichen species with green alga as a photobiont are widely called 'chlorolichens' (Lange and Wagenitz, 2004).

However, technological advances have allowed unravelling the complexity of the lichen symbiosis, redefining it as a biological micro-ecosystem in which different species are assembled (Grube et al., 2013). This micro-ecosystem concept contributes to a better understanding of species interactions and their ecological and evolutionary dynamics. The loss of genetic variability is usually associated with a decline of ecosystem resilience, and may have negative impacts on species diversity, including the extinction of the less adapted species to changing environmental conditions (Werth et al., 2015).

Given the rapid and continuous advancements in sequencing technologies, analytical techniques and computational capabilities, the current molecular and phylogenetic approaches allow for a deeper study of the interactions between the host organisms and their symbiotic communities. Much of our current knowledge about fungus–alga associations in lichens relies on studies based on Sanger sequencing, which has been useful in determining the identity of the main photobiont (e.g. Fernández-Mendoza et al., 2011; Werth and Sork, 2014). Nevertheless, Sanger sequencing is not able to identify the genetic complexity of natural populations that meta-genomic approaches can (e.g. Hodkinson and Lendemer, 2013, Dal Grande et al., 2017a, 2017b; Onut-Brännström et al., 2018). Hence, the progress in genomic studies may offer new insights into the functional biology of lichens, which together with other analytical approaches, will improve our understanding of symbiosis.

3. Physiological plasticity in chlorolichens and bryophytes, and their contribution to the global carbon cycle

Poikilohydric organisms such as lichens and bryophytes depend largely on the availability of hydration sources to be metabolically active (Green and Lange, 1995). Without hydration sources, these organisms enter a dormant state in order to get through harsh and dry times (Green et al., 2011), and remain in this state for as long as such conditions persist. However, when moist conditions return, cryptogams become hydrated and resume all physiological processes (Lange, 2001; Green et al., 2011).

Metabolic activity is, therefore, related to the ability of cryptogams to uptake and retain water, optimizing the hydric sources available in their habitats as maximum as possible (Green and Proctor, 2016). Species from maritime Antarctica may be hydrated by rainfall and meltwater during the summer and spring, and by close contact with a layer of ice or snow during the winter (Kappen and Schroeter, 1997). The heterogeneity and frequency of hydric resources in this ecosystem allow species to be metabolically active almost the entire year (Schroeter et al., 2010). Nonetheless, the duration of metabolic activity changes seasonally, being higher during the winter and lesser during the summer (e.g. Pintado et al., 2010; Schroeter et al., 2010; Raggio et al., 2014). This seasonal pattern has also been observed in the Tabernas Desert, suggesting that high metabolic activity is usually concentrated during the cooler, wetter, and greyer times of the year (Pintado et al., 2010). Despite this similarity, the hydric sources available in the Tabernas Desert differ notably from maritime Antarctica. Both regions are highly influenced by rainfall events, but in the semi-arid desert fog and dew also play an important role as hydric sources (Kidron and Lázaro, 2020). However, the species inhabiting there spend several months without metabolic activity due to the dry summer (Pintado et al.,2010; Raggio et al., 2014).

The effect of hydric stress in both ecosystems leads to higher metabolic activity in the species from maritime Antarctica (Table 2). In general, species from cold habitats increase their thallus temperature when are active to be warmer than the surrounding environment. Meanwhile, those from hotter habitats decrease their thallus temperature to be cooler than their surroundings (Table 2). This leads to reduced temperature differences between maritime Antarctica and the Tabernas Desert.

Table 2 Long-term monitoring of chorolichens and bryophytes using chlorophyll *a* fluorescence measurements from maritime Antarctica and Tabernas Desert. The temperature in which species were active (Tact) is also included in the table. Only the papers in which activity was expressed as a percent of metabolic activity were included in the table. Neither metabolic activity data of cryptogams from Cabo de Gata nor bryophytes from Tabernas Desert were found.

Species	Division	Growth form	Substrate	Metabolic activity (%)	Period of time measured	Tact (°C)	Reference
MARITIME ANTARCTICA							
Parmelia saxatilis	Ascomycota	Foliose	Rock	59	Summer	3.2	Schroeter et al. (2017)
Ramalina terebrata	Ascomycota	Fruticose	Rock	61	Summer	NA	Kappen et al. (1988)
Stereocaulon alpinum	Ascomycota	Clump	Soil	38	Summer	3.7	Schlensog et al. (2013)
Umbilicaria antarctica	Ascomycota	Fruticose	Rock	46	Summer	1.1	Raggio et al. (2016)
				57	Summer	3.8	Schroeter et al. (2017)
Umbilicaria decussata	Ascomycota	Fruticose	Rock	22	Summer	3.1	Schlensog et al. (2013)
Umbilicaria umbilicarioides	Ascomycota	Fruticose	Rock	*ca.* 33	Summer	NA	Schlensog et al. (2013)
Usnea antarctica	Ascomycota	Fruticose	Rock	33	Summer	3.6	Schlensog et al. (2013)
				69	Summer	4	Schroeter et al. (2017)

Species	Phylum	Growth form	Substrate		Season		Reference
Usnea aurantiaco-atra	Ascomycota	Fruticose	Rock	42	Summer	1.1	Schroeter et al. (2010)
				51	Summer	3.5	Schroeter et al. (2017)
				65	Summer	4.8	Schroeter et al. (2021)
Andreaea gainii	Bryophyta	Cushion	Rock	67	Summer	5.5	Schroeter et al. (2017)
				37	Summer	4.1	Schlensog et al. (2013)
Bartramia patens	Bryophyta	Turf	Rock	99	Summer	3.9	Schroeter et al. (2017)
Brachythecium austrosalebrosum	Bryophyta	Turf	Scree	100	Summer	3.8	Schroeter et al. (2017)
			NA	86	Summer	2.4	Schlensog et al. (2013)
Bryum archangelicum	Bryophyta	Turf	Scree	99	Summer	3.6	Schroeter et al. (2017)
Bryum argenteum	Bryophyta	Turf	Rock	100	Summer	3.7	Schlensog et al. (2013)
Bryum pseudotriquetrum	Bryophyta	Turf	Scree	100	Summer	3.7	Schroeter et al. (2017)
			NA	100	Summer	5.1	Schlensog et al. (2013)
Ceratodon purpureus	Bryophyta	Turf	Soil	42	Summer	NA	Schlensog et al. (2013)
Hymenoloma crispulum	Bryophyta	Turf	Rock	96	Summer	4.0	Schroeter et al. (2017)
				68	Summer	5.0	Schroeter et al. (2021)
Pohlia cruda	Bryophyta	Turf	NA	95	Summer	4.4	Schlensog et al. (2013)
Polytrichum alpinum	Bryophyta	Individual stems	Soil	56	Summer	5.5	Schlensog et al. (2013)
			Scree	100	Summer	3.2	Schroeter et al. (2017)

23

Sanionia uncinata	Bryophyta	Turf	NA	97	Summer	2.8	Schlensog et al. (2013)
TABERNAS DESERT							
Biocrust complex 1	Several	Several	Soil	3	Summer	NA	Raggio et al. (2014)
				21	Annual	9.4	
Biocrust complex 2	Several	Several	Soil	12.7	Annual	8.8	Raggio et al. (2017)
Diploschistes diacapsis	Ascomycota	Crustose	Soil	20	Annual	8.8	Pintado et al. (2010)

The temperatures in which species are metabolically active in the field differ from the optimum temperature of net photosynthesis measured under laboratory conditions. The optimal temperature range changes according to the species and their habitat (Longton, 1988). For example, the optimal temperature range has been established from 10 to 28 °C in semi-arid deserts (Lange, 2001), and from 3 to 14 °C in Antarctica (Green et al., 2011).

Determining the metabolic activity response patterns allows for pinpointing when bryophytes and lichens are able to photosynthesise, which is considered a crucial process for the survival of autotrophic species. In long-term studies, net primary productivity (NPP) has been established as a standard measurement of the CO_2 balance (Chapin et al., 2006; Sancho et al., 2016).

Although NPP of terrestrial ecosystems are not saturated at present atmospheric CO_2 concentrations (Schimel, 1995), this could be the case if concentrations reach 800-1000 ppm CO_2, values that are likely to be reached by next century (Watson et al., 1996). Some predictions point that NPP may even exceed the current rates seen in some ecosystems due to higher temperatures (Duveneck and Thompson, 2017). Nevertheless, this temperature increase may also enhance microbial heterotrophic respiration (Kirschbaum, 1995). Hence, the combined effects of higher CO_2 concentrations, higher temperatures, and changes in hydric sources and moisture regimes lead to a considerable uncertainty about the ability of terrestrial ecosystems to mitigate the effects of climate change (e.g. Kennedy, 1995; Convey, 2001; Singh et al., 2018).

The spatial variability on NPP over the Earth is notorious, ranging from *ca.* 1000 g C m^{-2} for evergreen tropical rain forests to less than 30 g C m^{-2} for deserts (Running et al., 2000), which points out the importance of the type of vegetation cover and the ecosystem. It has been estimated that 7% of the Earth's total NPP is fixed by cryptogams (Elbert et al., 2012), in which biomes like deserts and tundras can reach to 1.72 and 1.83 Pg C y^{-1}, respectively (Porada et al., 2013).

The NPP of cryptogams has been estimated in several biomes (e.g. Uchida et al., 2006; Elbert et al., 2012; Porada et al., 2013). Particularly in maritime Antarctica, the NPP of lichens ranges from -0.64 to 85 mg CO_2 gDW^{-1} y^{-1} on a biomass basis (Schroeter, 1997), and around 250 g m^{-2} y^{-1} on an area basis (Smith, 1984). Nevertheless, the NPP of bryophytes in the same study area ranged from 223 to 893 g m^{-2} y^{-1} (Collins, 1973, 1977; Longton, 1970; Davis, 1983). In the case of arid and semi-arid deserts, the NPP for different biocrust types can reach up to 6.05 g C m^{-2} y^{-1} in the Mu Us Desert (Feng et al.,

2014), 16 g C m^{-2} y^{-1} in the Namib Desert (Lange et al., 1994), and 11.7 g C m^{-2} y^{-1} in the Mojave Desert (Brostoff et al., 2005).

4. Adaptations of chlorolichens and bryophytes to local environmental conditions

Spatial and temporal variations of abiotic factors make it difficult to understand the adaptation patterns of biodiversity (Smith and Dukes, 2013; Vanderwel et al., 2015). This is explained by the physiological, historical, and morphological traits of populations which may change with the resources available, and/or during diurnal or seasonal cycles (Chown and Convey, 2007). Such changes are often discussed under the rubric of phenotypic plasticity, which is defined as the capacity of a given genotype to render multiple phenotypes according to environmental conditions (Arnold et al., 2019).

Plastic responses reflect the effects of the environmental limits on growth and physiology of species (Sultan, 2000), and span across a broad variety of functional traits. The fact that these traits interplay with each other makes the establishment of a direct link between trait variation and fitness difficult. For instance, as a response to environmental pressures, the same lichen species is able to acquire different thallus morphologies (Szaniszlo, 1985), which determine the ratio between the surface area and the volume of the thallus. This is closely related to water absorption, water-holding capacity, and evaporation rates that –among other traits– (e.g. Giordani et al., 2014; Ure and Stanton, 2019) affect CO_2 exchange.

The rates of CO_2 exchange obtained by measuring under laboratory conditions are highly dependent on the species (e.g. Kappen and Redon, 1987) and the habitat (e.g. Ino, 1990a; Pintado et al., 1997). Green and Lange (1995) ranged the net photosynthesis of lichens from 0.5 to 2 mg CO_2 dm^{-2} h^{-1} on area bases and from 0.3 to 5 mg CO_2 mg^{-1} h^{-1} on dry weight bases. Nevertheless, moss rates were less than 3 mg CO_2 dm^{-2} h^{-1} on area bases and between 0.6 and 3.5 mg CO_2 mg^{-1} h^{-1} on dry weight bases. In terms of respiration, lichens and bryophytes maintained similar rates (Green and Lange, 1995), which range from -0.2 to -1.3 µmol CO_2 kg dwt^{-1} s^{-1} at 5 ºC and 400 µmols photons m^{-2} s^{-1} of PPFD in habitats such as maritime Antarctica and the Tabernas Desert (e.g. Kappen, 1985; Kappen and Redon, 1987; Kappen et al., 1988; Harrisson et al, 1986, 1989; Harrisson and Rothery, 1988; Schroeter et al., 1995; Convey, 1994; Davey and Rothery, 1997; Laguna-Defior et al., 2016; Del Prado and Sancho, 2000; Nakatsubo, 2002; Pintado et al., 2005; Raggio et al., 2018).

In lichenology, growth form and photobiont switching are the most studied functional traits (e.g. Giordano et al., 2012; Asplund and Wardle, 2017; Koch *et al.*, 2019) due to their role in water use efficiency and carbon balance (e.g. Green et al., 1997; Matos et al., 2015; Cao et al., 2015). Moreover, as a consequence of the environmental conditions of each habitat, the same mycobiont may associate with a new photobiont partner (Guzow-Krzemińska, 2006; Fernández-Mendoza et al., 2011; Williams et al., 2017), or even with multiple coexisting algal OTUs (Casano et al., 2011; Dal Grande et al., 2017a). This flexibility in the choice of photobiont is considered to be a strategy to survive under new selective pressures and to widen the species' ecological niche amplitude (Lutsak et al., 2016; Ertz et al., 2018).

Methods

In Chapter 1, samples of the moss *Ceratodon purpureus* were collected near the Juan Carlos I Spanish Antarctic Station in an ice-free area of Livingston Island (maritime Antarctica). After collecting the samples, CO_2 exchange measurements were carried out under controlled laboratory conditions using the GFS-3000 system. These measurements consisted of light response curves performed at several temperatures and light intensities, which allowed us to obtain the following physiological traits: dark respiration, net photosynthesis, photosynthetic efficiency, and gross photosynthesis. The traits were then included in a Principal Components Analysis (PCA), together with those already published by Pannewitz et al. (2005) and Weber et al. (2012). In order to evaluate whether there is thermal acclimation of respiration, respiration rates were represented as the total percent of the gross photosynthesis from 0 to 20ºC, and temperature sensitivity coefficient (Q_{10}) was calculated.

In Chapter 2, samples of the lichens *Xanthoparmelia pulla* and *X. pokornyi* were collected from Cabo de Gata and the Tabernas desert (southeast of Spain). CO_2 exchange measurements were later conducted under controlled laboratory conditions using the GFS-3000 system. These measurements consisted of (i) light response curves performed at several temperatures and light intensities, and (ii) desiccation response curves performed at 15 °C and 400µmol photons m^{-2} s^{-1} PPFD. Differences among eco-physiological traits were investigated though with one-way ANOVA tests. If data did not fit the assumptions, Kruskal Wallis test were performed.

The genetic background of the mycobiont was studied using Sanger sequencing. The markers nrITS, *β-tubulin*, and *MCM7* were selected for the amplification. The generated sequences of each marker were aligned and the genetic diversity indices and haplotype networks were determined. These sequences were also merged with two multi-locus datasets published in previous phylogenetic studies of *Xanthoparmelia* (Amo de Paz et al. 2012, Leavitt et al. 2018). The phylogenetic relationships of the combined datasets were inferred using both Maximum Likelihood and Bayesian Inference methods. Also, two different species delimitation analyses based on nrITS were performed (ABGD and GYMC).

Finally, for the study of the lichen-associated microalgal community, ITS2 was amplified and sequenced using Illumina MiSeq sequencing. In order to infer the phylogenetic

position of the *Trebouxia* OTUs found in *Xanthoparmelia* populations, we constructed a phylogenetic tree using OTUs from this study and those in Leavitt et al. (2015). This phylogenetic inference was based on a Maximum Likelihood method. The statistical analysis of the photobiont community consisted of a two-dimensional non-metric multidimensional scaling (NMDS), and a DeSeq analysis. Additionally, the influence of the climatic conditions, the physiological performance, and the host genetic diversity on the lichen-associated algal communities were analysed through correlation analysis.

In Chapter 3, the lichen *Usnea aurantiaco-atra* (Chapter 2) located near the Juan Carlos I Spanish Antarctic Station in an ice-free area of Livingston Island (maritime Antarctica), was monitored for several years at high temporal resolution. Long-term field monitoring of chlorophyll *a* fluorescence and microclimate was carried out using the non-invasive automatic MoniDA system. All data were simultaneously recorded at hourly intervals for 41 months. Metabolic activity and net primary productivity (NPP) were then predicted under two different climate change scenarios (RCP 4.5 and RCP 8.5) using sequential Generalized Additive Models (GAMs).

Chapter 1:

Physiological plasticity as a strategy to cope with harsh climatic conditions: eco-physiological meta-analysis of the cosmopolitan moss *Ceratodon purpureus* along the Southern Hemisphere

Abstract

Determining the physiological tolerance ranges of species allows for a better understanding of their adaptation patterns to both abiotic stresses and climate change. For this purpose, cosmopolitan species are a good model due to their wide geographic distribution throughout several biomes and habitats. In this study, we investigate the physiological plasticity of the cosmopolitan moss *Ceratodon purpureus* (Hedw.) Brid. from different and contrasting habitats along the Southern Hemisphere. The Succulent Karoo semi-arid Desert and Antarctica (both continental and maritime) were chosen as study areas in order to unravel how high radiation, heat, and freezing tolerance modulates the physiological response pattern of this species in each habitat. To carry out the study, a meta-analysis was designed by including the main physiological parameters obtained by CO_2 exchange measurements. Our findings demonstrated that *C. purpureus* has high physiological plasticity and is able to modulate its response range according to local environmental conditions. Contrary to populations from continental Antarctica, the populations from maritime Antarctica and the semi-arid desert show thermal acclimation of respiration and low respiration sensitivity to temperature increases. Thus, there is a high dissimilarity between maritime and continental Antarctica that leads the semi-arid desert population to occupy an intermediate position and share functional traits with both tundra habitats. Maritime Antarctica becomes a most suitable habitat for the physiological performance of *C. purpureus* likely due to the less abrupt climatic changes throughout the year, which allow species to maximize their carbon gain, and therefore, to increase their photosynthetic efficiency. The ability of *C. purpureus* to modulate the optimal temperature for net photosynthesis within the range of 7-20ºC is in concordance with the macroclimatic conditions of each habitat. This leads the semi-arid desert population to be heat-tolerant and to not have a decline in maximum net photosynthesis at high temperatures -even though *C. purpureus* performs better at low temperatures-. Furthermore, the ability to switch from shade- to sun-adapted forms, and to be highly light-use efficient at a wide temperature range, emphasizes the high radiation tolerance of this species. Hence, the cosmopolitan nature of *C. purpureus* makes this species highly resilient under abrupt climate changes.

Key words: Photosynthesis, CO_2 exchange, microclimate, tundra, drylands, Antarctica, bryophytes, cryptogams

1. Introduction

Cryptogams are widely spread and even dominant in the most climatic extreme regions around the world, where they are subjected to several stresses simultaneously. Due to poikilohydric nature, they can cope with harsh environmental conditions such as extreme temperatures, high radiation, and water scarcity at the same time.

Cryptogams are known for their ability to survive a wide range of temperatures in nature. Freeze-tolerant species have the capacity for supercooling and dehydrating rapidly in order to avoid internal ice formation, and therefore, reduce cell damage (Hoffman and Gates, 1970; Proctor, 1982; Longton, 1988; Lenné et al., 2010). Similarly, heat-tolerant species also accelerate their dehydration process in order to avoid tissue damage (He et al., 2016). Taking into account that lichens and bryophytes are important members of the cryptogamic communities from extreme biomes, their survival is thus linked to them being able to be metabolically activated at low water contents (Green et al., 2011). In fact, species from sun-exposed habitats are able to be metabolically active at lower water contents than those from shadow-exposed habitats (Longtom, 1988; Proctor, 2000; Kappen and Valladares, 2007). Hence, tolerance to extreme temperatures and high radiation levels leads species to maintain different physiological responses according to their ability to adapt to the surrounding environment.

Cryptogam's survival is also linked to their dehydration recovery speed (Oliver et al., 2005; Marschall, 2017). Species from deserts and steppes have a rapid recovery due to their frequent and severe drying, while species from moist habitats have a slow recovery (Kappen and Valladares, 2007; Green et al., 2011). Dry and moist cycles, thus result in changes in the frequency and duration of the physiological activity, which may notably affect the carbon balance of species (Davey, 1997a; Bjerke et al., 2013).

Nevertheless, acclimation of physiological processes may broaden the range of climatic conditions over which carbon gain occurs. Conceptually, this strategy is based on maintaining the photosynthetic rates relatively constant over a broad range of temperatures (Atkin et al., 2006a). If organisms were able to keep their respiration rates stable, net photosynthesis would increase with temperature until a plateau was reached. Only a few studies have addressed that issue in lichens and mosses (Hicklenton and Oechel, 1976; Oechel, 1976; Lange and Green, 2005; Wagner et al., 2013a, 2013b; Colesie et al., 2018). The vast majority of them concluded that there is no thermal acclimation of respiration in lichens and bryophytes from tropical and polar habitats (Hicklenton and Oechel, 1976; Wagner et al., 2013b, Colesie et al., 2018). However,

others pointed out that acclimation may be species-specific (Oechel, 1976; Larson and Kershaw, 1975). Only Lange and Green (2005) demonstrated that full acclimation may occur in lichens from steppes. Hence, due to the potential importance of temperature adjustments to climate change modelling, more information is needed on the type, magnitude, and timing of these adjustments.

Physiological plasticity is, then, closely related to the species' capacity to colonize different habitats (Valladares et al., 2002; Niinemets and Valladares, 2004). This plasticity is especially relevant in cosmopolitan species due to their wide geographic distribution. Therefore, determining the physiological tolerance of the cosmopolitan species may allow for a better understanding of the adaptation patterns of the species to stress.

Ceratodon purpureus (Hedw.) Brid. is one of the most widespread moss species. Its exceptionally wide geographic range includes a broad variety of biomes, habitats, and substrates, inhabiting several continents of both hemispheres (Schofield and Crum, 1972). From polar to tropical biomes (Ochyra et al., 2008), it is commonly found in harsh and ruderal habitats such as buildings, roofs, sidewalks, recently burnt soil, and barren glacial deposits (e.g. Jules and Shaw, 1994; Shaw and Beer, 1999). Therefore, it has been considered a suitable model organism for plant development (e.g. Cove et al., 1997, 2006), and population genetics studies (e.g. Wood et al., 2000; Skotnicki et al., 2004; McDaniel and Shaw, 2005; Clarke et al., 2009; Biersma et al., 2020).

C. purpureus has been widely analysed using CO_2 exchange techniques in order to address several questions such as tolerance to dehydration (Davey, 1997a, 1997b; Smith, 1999; Weber et al., 2012; Tamm et al., 2018), to freezing (Aro et al., 1987; Aro and Karunen, 1988), and to high radiation (Valanne, 1976a, 1976b, 1977; Valanne et al., 1978; Aro and Valanne, 1979; Aro, 1982; Post, 1990). Other studies have focused on unravelling photosynthetic responses under field conditions (Ino, 1983a, 1983b, 1990b, 1994) and under laboratory conditions (Ino, 1990a; Pannewitz et al., 2005; Weber et al., 2012; Tamm et al., 2018), as well as estimating the productivity rates at a local scale (Ino, 1983a; Castro-Perera et al., 2020). Light tolerance studies were carried out using spores of *C. purpureus* cultured under laboratory conditions (Valanne, 1976a, 1976b, 1977; Valanne et al., 1978; Aro, 1982; Aro et al., 1987, Aro and Karunen, 1988), as well as specimens collected in Finland forests (Aro and Valanne, 1979). Webber et al. (2012) performed both light and desiccation response curves to several light and temperature intensities in the Succulent Karoo Desert, and used this large dataset in back studies

(Tamm et al., 2018). Pannewitz et al. (2005) widely studied the CO_2 exchange of *C. purpureus* in continental Antarctica. Similarly, the photosynthetic profile of a mixture community of *C. purpureus* (Ino, 1983a, 1990b, 1994) and a turf community of only *C. purpureus* (Ino 1990a) was analysed in continental Antarctica (Ino, 1983a, 1990b, 1994) and Japan (Ino, 1990a). Finally, Davey and Rothery (1997) and Convey (1994) measured the maximum photosynthetic rates of several bryophyte species from maritime Antarctica.

Due to those studies addressing different questions, they required different methodologies. This fact hinders the comparison of the data obtained between studies and consequently, between habitats. Therefore, in order to investigate the physiological plasticity of *C. purpureus* from contrasting habitats along the Southern Hemisphere, we provide new data of this species in maritime Antarctica. Moreover, a meta-analysis was designed using the data from other two studies which measured functional traits comparable to the newly generated data in this study (Pannewitz et al., 2005; Weber et al., 2012). Due to the notorious macroclimatic differences between the study areas, *C. purpureus* has to cope with freezing temperatures, heat, prolonged dehydration and high radiation tolerance. Knowing the performance of this species under these stresses will allow us to better understand how environmental conditions modulate the physiological response ranges in cosmopolitan species.
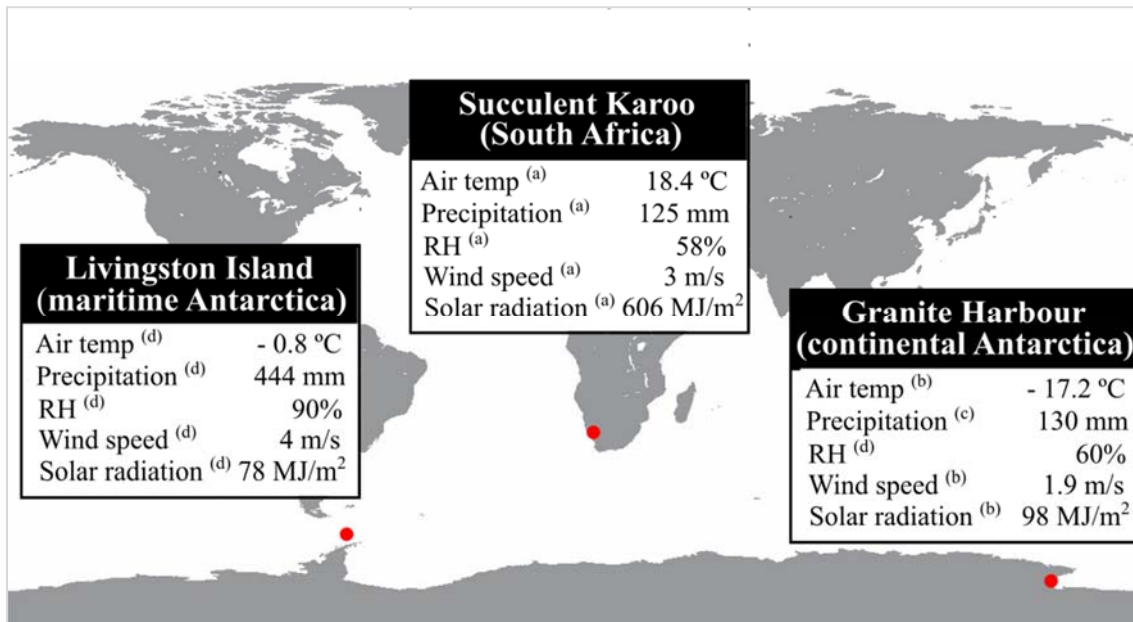
Fig. 1 Location of *C. purpureus* populations in the maritime Antarctica (62º39′ S, 60º23′ W), continental Antarctica (77°00′ S, 162°32′ E), and the semi-arid desert in South Africa (32°21′ S, 22°34′ E). Each red circle represents one population, in which macroclimatic conditions were summarized in the adjacent table. The letters indicate the references in which climate data were downloaded: [a] Soebatsfontein weather station (http://www.biota-africa.org) [b] Granite Harbour soil climate station (https://www.nrcs.usda.gov/wps/portal/nrcs/site/national/home/) [c] Ascaso et al. (2003) [d] AEMET (2019).

2. Methods

2.1. Research site and sampling

The study area was located in the vicinity of the Juan Carlos I Spanish Antarctic Station in an ice-free area of South Bay, Livingston Island, South Shetland Islands, maritime Antarctica (62° 39'' 46'' S; 60° 23' 20'' W). It consisted of an area of 200 m^2 located close to a glacier creek. Four samples of *C. purpureus* were collected from the sedimentary rocks present in the area. They were collected in pieces of *ca.* 5 cm^2 and the substrate attached to the moss was removed.

2.2. Climatic data

Microclimatic conditions were recorded every 30 minutes from February 27th to March 24th 2018 using I-buttons DS1923. Each of the four I-buttons installed measured

microclimatic temperature (range: -20 to +85°C) and relative humidity (range: 0 to 100%) simultaneously.

Macroclimatic conditions were obtained from the Spanish Meteorological Agency (AEMET; https://antartida.aemet.es/). The AEMET weather station is located in an open area about 400 m from the study area (AEMET, 2019). Air mean temperature (°C) and relative humidity (%) were downloaded for the same period of time and resolution as the microclimate.

2.3. CO_2 exchange

Immediately after collecting the samples, CO_2 exchange measurements were carried out under controlled laboratory conditions in the facilities of the Spanish Antarctic Base, using the GFS-3000 system (Walz Mess und Regeltechnik, Effeltrich, Germany). Samples were sprayed with water directly taken from the creek in order to hydrate them. When they reached their maximum net photosynthesis, samples were then weighted to determine their optimal water content. Afterwards, light response curves were performed at several temperatures (0, 5, 10, 15, 20 and 25°C). At each temperature level, net photosynthesis rates were obtained at eight different light intensities (0, 25, 50, 100, 200, 400, 800, 1300 µmol photons m^{-2} s^{-1}). Dark respiration rates at the optimal water content (DRopt) were measured at 0 µmol photons m^{-2} s^{-1} and the maximal net photosynthesis (NP_{1300}) at 1300 µmol photons m^{-2} s^{-1}. In order to facilitate the comparison with other studies already published, the 24 light response curves generated in this study were expressed on an area basis. After that, they were fitted to the best statistical model using CurveExpert Professional v.2.6.5 software (Table S1). From each fitted curve, we obtained the following physiological parameters: gross photosynthetic rate (GP = NP_{1300} + DRopt), photosynthetic efficiency (K_F = (NP_{1300} + DRopt)/DRopt, see Green and Lange, 1995), the light compensation point (LCP; defined as the light intensity in which the photosynthetic rate is zero), the light saturation point (LSP; defined as the light intensity in which net photosynthesis reaches 95% of the NP_{1300}), and the quantum yield of photosynthesis (Φ; defined as the slope between photosynthesis and light from 0 µmols photons m^{-2} s^{-1} to 32 µmols photons m^{-2} s^{-1}).

The temperature in which the net photosynthesis was maximum for each PPFDs was also obtained (optimal temperature). This parameter was obtained graphically representing the dependence of NP_{1300} on temperature.

2.4. Meta-analysis

The new data generated in this study was included with those from Pannewitz et al. (2005) and Weber et al. (2012) in the meta-analysis. These studies were selected because both showed similar methodologies for the measurement of the turf, the photosynthetic rates were expressed in an area basis, and both analysed a wide combination of temperatures and PPFD (see also Midgley et al., 1997). The study of Pannewitz et al. (2005) was carried out at Granite Harbour in continental Antarctica, while the study of Weber et al. (2012) was carried out in the semi-arid desert of Succulent Karoo in South Africa.

The NP_{1300} and DRopt measured at temperatures between 5 and 20ºC were extracted from the studies mentioned above, in order to calculate the GP and photosynthetic efficiency for each temperature and habitat. The calculus of both parameters is explained in the previous section. Afterwards, the Pearson's correlation coefficients among those four traits were checked using R package '*corrplot*' (Taiyun and Viliam, 2017; Fig. S1). Correlations with a p-value < 0.05 were considered statistically significant. The dimensionality of the variables was reduced using a Principal Components Analysis (PCA) on the data scaled.

In order to evaluate if there was a thermal acclimation of respiration, the respiration rates were represented as the total percent of the gross photosynthesis from 0 to 20ºC. We also calculated the temperature sensitivity coefficient (Q_{10}) as the proportional change in respiration per 10ºC rise in temperature. This coefficient is calculated as $Q_{10} = (R2/R1)^{[10/(T2-T1)]}$, in which R2 and R1 are rates of respiration measured at temperatures T2 (higher temperature) and T1 (lower temperature), respectively (Atkin and Tjoelker, 2003). The Q_{10} was calculated between 10-20ºC of all habitats, and between 0-10ºC for the tundra biomes.

The data at 0ºC was not included in the meta-analysis because it was not measured in the semi-arid desert. However, it was considered in the graphs due to the potential influence of low temperatures in the Antarctic populations of *C. purpureus*. Also NP_{1300} and DRopt at 25ºC from maritime Antarctica and the semi-arid desert were included in the graphs.

3. Results

3.1. Climatic data

Microclimatic conditions in maritime Antarctica showed a mean temperature of 2.72°C, which was similar to the macroclimatic temperature recorded by the AEMET (AEMET, 2019; Table 1). Both minimum and maximum microclimatic temperatures were higher than air temperature. The mean microclimatic relative humidity was 10% higher than the air relative humidity, with its median being 100%. See Table 1, Fig S2 and S3.

Table 1 Summary of the microclimatic measurements of *C. purpureus* at Livingston Island (maritime Antarctica) from February 27th to March 24th 2018, and the macroclimatic conditions for the same period downloaded from the Spanish Meteorological Agency (AEMET).

	MICROCLIMATIC CONDITIONS		MACROCLIMATIC CONDITIONS	
	Temperature	Relative Humidity	Temperature	Relative Humidity
	(°C)	(%)	(°C)	(%)
Mean ± standard deviation	2.72 ± 3.09	95.23 ± 8.17	2.15 ± 1.90	85.22 ± 8.42
Minimum	-1.25	57	-5.4	53
Median	2.81	100	2.50	87
Maximum	13.02	100	10.2	98

3.2. CO_2 exchange

Eco-physiological analysis of *C. purpureus* in maritime Antarctica showed a typical saturation-type response of net photosynthesis to light incidence (Fig. 2). The PPFD increase led to an increase in the optimal temperature of net photosynthesis. In fact, the optimal temperature ranged from close to 0°C at 25 μmol photons m^{-2} s^{-1} to 16.7 °C at 1300 μmol photons m^{-2} s^{-1}. NP_{1300} was maximal between 15 and 20°C, and declined drastically at 25°C (Fig. 2). Indeed, the NP_{1300} achieved at 25°C was similar to that at 5°C. Gross photosynthesis followed the same trend as NP_{1300}, reaching maximum value

between 15 and 20ºC (Table 2). The values of DRopt ranged from -0.26 µmol CO_2 m^{-2} s^{-1} at 0°C to -2.05 µmol CO_2 m^{-2} s^{-1} at 25°C (Fig. 2 and Table 2).
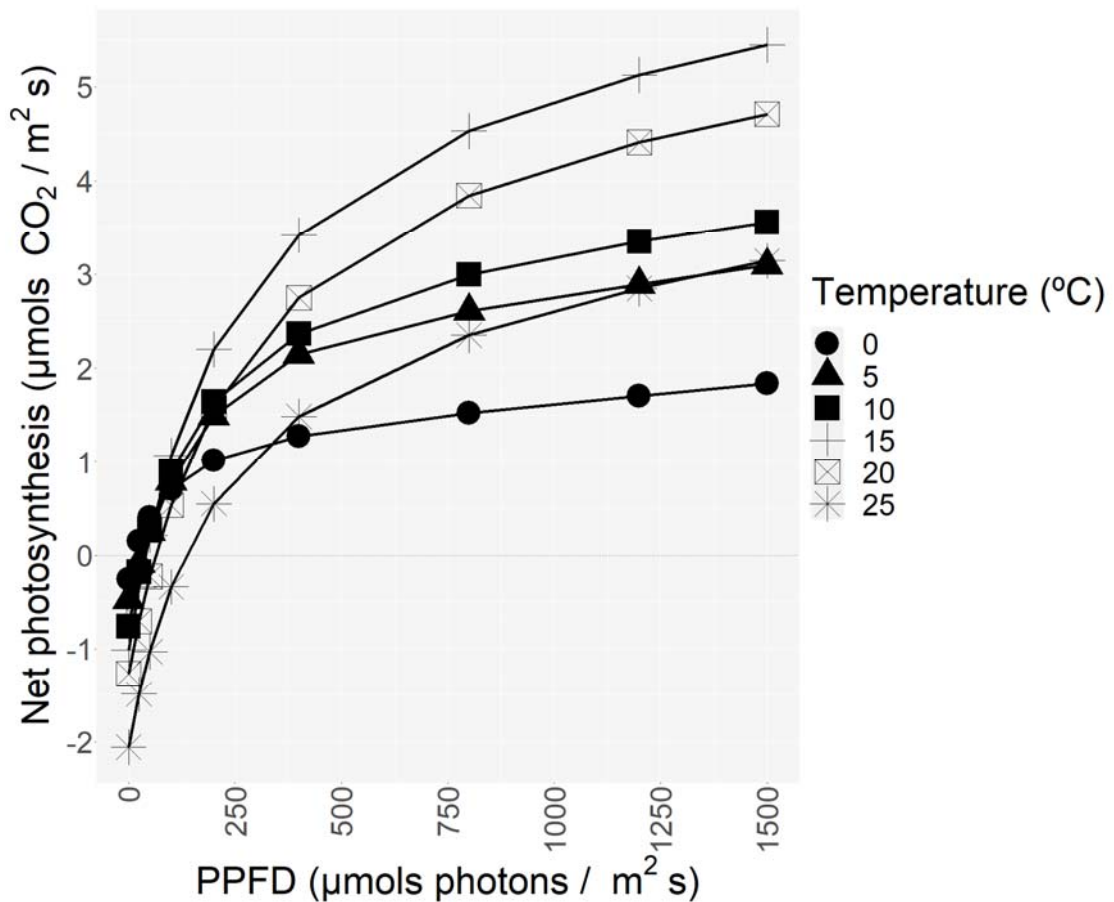
Fig. 2 Dependence of net photosynthesis to different PPFD at 0, 5, 10, 15, 20, 25°C of *C. purpureus* in maritime Antarctica. The R^2-adjust and standard error of each curve is detailed in Table S1.

The rise in temperature led to an increase in the light compensation points, which ranged from 14 to 132 µmol photons m^{-2} s^{-1} (Table 2). The light saturation points also increased with temperature from 428 µmol photons m^{-2} s^{-1} at 0°C to 911 µmol photons m^{-2} s^{-1} at 25°C (Table 2). The quantum yield of photosynthesis increased with temperature from 0.016 mol CO_2 mol^{-1} quanta at 0°C to 0.0226 mol CO_2 mol^{-1} quanta at 20°C. However, its value was stabilized to 0.0226 mol CO_2 mol^{-1} quanta at 20°C, reaching the same value at 25°C (Table 2). The photosynthetic efficiency decreased as temperature increased, showing its maximum rate at 0°C and its minimum at 25°C (Table 2).

Table 2 Means and standard deviations of the physiological parameters of *C. purpureus* from Livingston Island (maritime Antarctica) obtained from the fitted light response curves, and clustered according to the temperature measured.

Temperature	DRopt	NP$_{1300}$	GP	Photosynthetic efficiency	LCP	LSP	Φ
°C	μmol CO_2/ m^2 s			adimensional	μmol photons/ m^2 s		mol CO_2/ mols quanta
0	-0.26 ± 0.09	1.72 ± 0.69	1.96 ± 0.70	7.9 ± 2.8	14 ± 22	428 ± 572	0.016 ± 0.018
5	-0.48 ± 0.22	2.09 ± 0.44	3.31 ± 0.22	6.2 ± 5.9	31 ± 23	544 ± 137	0.019 ± 0.004
10	-0.76 ± 0.17	2.36 ± 0.26	3.15 ± 0.27	6.0 ± 1.2	35 ± 14	689 ± 142	0.023 ± 0.004
15	-1.01 ± 0.11	5.12 ± 0.94	6.14 ± 0.86	5.9 ± 1.4	39 ± 7	802 ± 75	0.027 ± 0.002
20	-1.27 ± 0.12	4.54 ± 0.90	5.91 ± 1.02	4.7 ± 1.0	62 ± 1	915 ± 67	0.023 ± 0.003
25	-2.05 ± 0.49	2.87 ± 1.13	4.92 ± 1.11	2.4 ± 0.6	132 ± 64	911 ± 55	0.023 ± 0.005

3.3. Meta-analysis

C. purpureus from maritime Antarctica had higher NP_{1300} and lower dark respiration compared to the other habitats (Fig. 3). In fact, the total proportion of dark respiration over gross photosynthesis showed stable proportions in maritime Antarctica, at values ranging between 13-21% from 0 to 20ºC (Fig. 4). In the Succulent Karoo semi-arid Desert, the proportion ranged between 15-37% from 5 to 20ºC. In continental Antarctica, the proportion is similar between 0-5ºC (*ca.* 40-47%), but it notably increased from 10ºC onwards. Moreover, Q_{10} from 10 to 20ºC was 1.68, 1.85 and 1.95 for maritime Antarctica, the Succulent Karoo semi-arid Desert, and continental Antarctica, respectively. The Q_{10} from 0 to 10ºC for the tundra biomes was 2.84 for both.
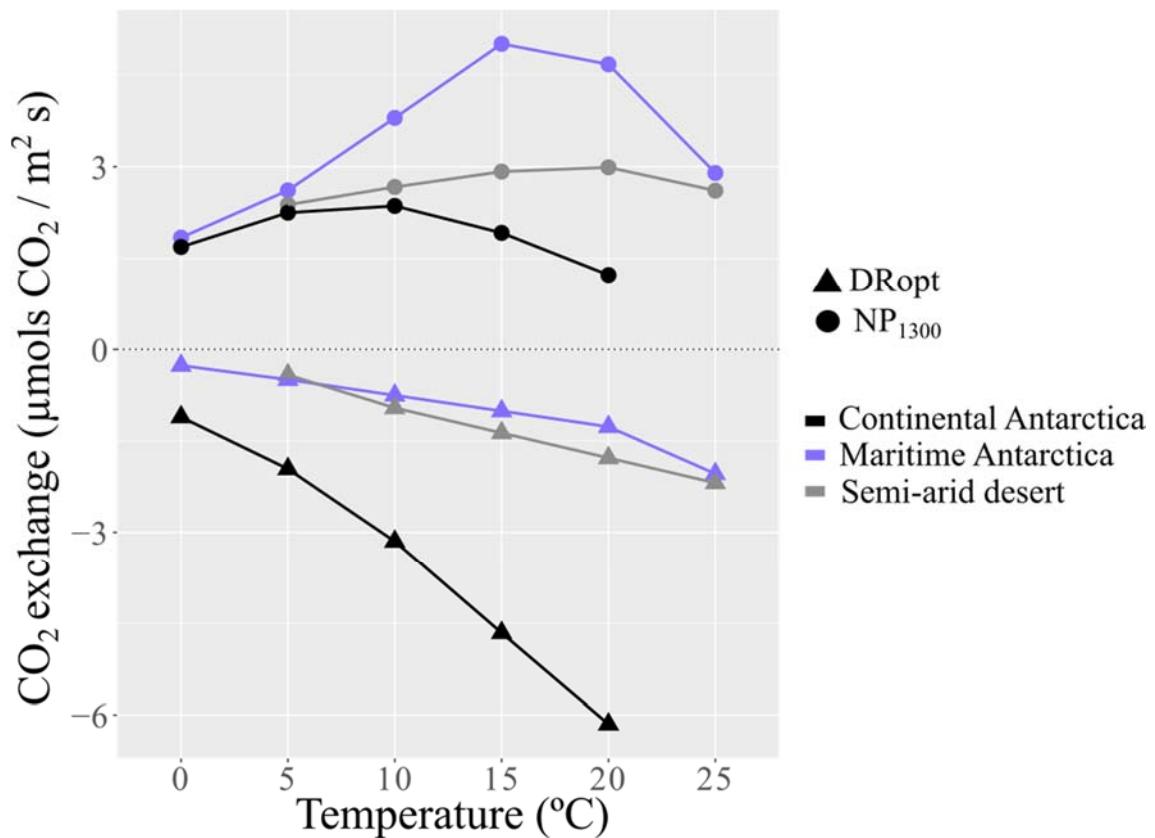
Fig. 3 Response of net photosynthesis measured 1300 µmol photons m^{-2} s^{-1} PPFD (NP_{1300}) and dark respiration at the optimal water content (DRopt) to different temperatures in the continental Antarctica, maritime Antarctica, and the Succulent Karoo semi-arid Desert.

Despite not having data available at 0ºC for the semi-arid desert specimens, the NP_{1300} measured at temperatures below 5ºC seemed to converge in all habitats (Fig. 3).

The NP_{1300} decline found at higher temperatures is more remarkable in specimens from maritime Antarctica, which highlights their sensitivity to temperatures higher than 20ºC (Fig. 3). This sensitivity was also shown in the optimal temperature for NP_{1300} measured under lab conditions, which changed according to the habitat, at *ca.* 7, 15, and 20ºC for specimens from continental Antarctica, maritime Antarctica, and the semi-arid desert, respectively (Fig. 3).
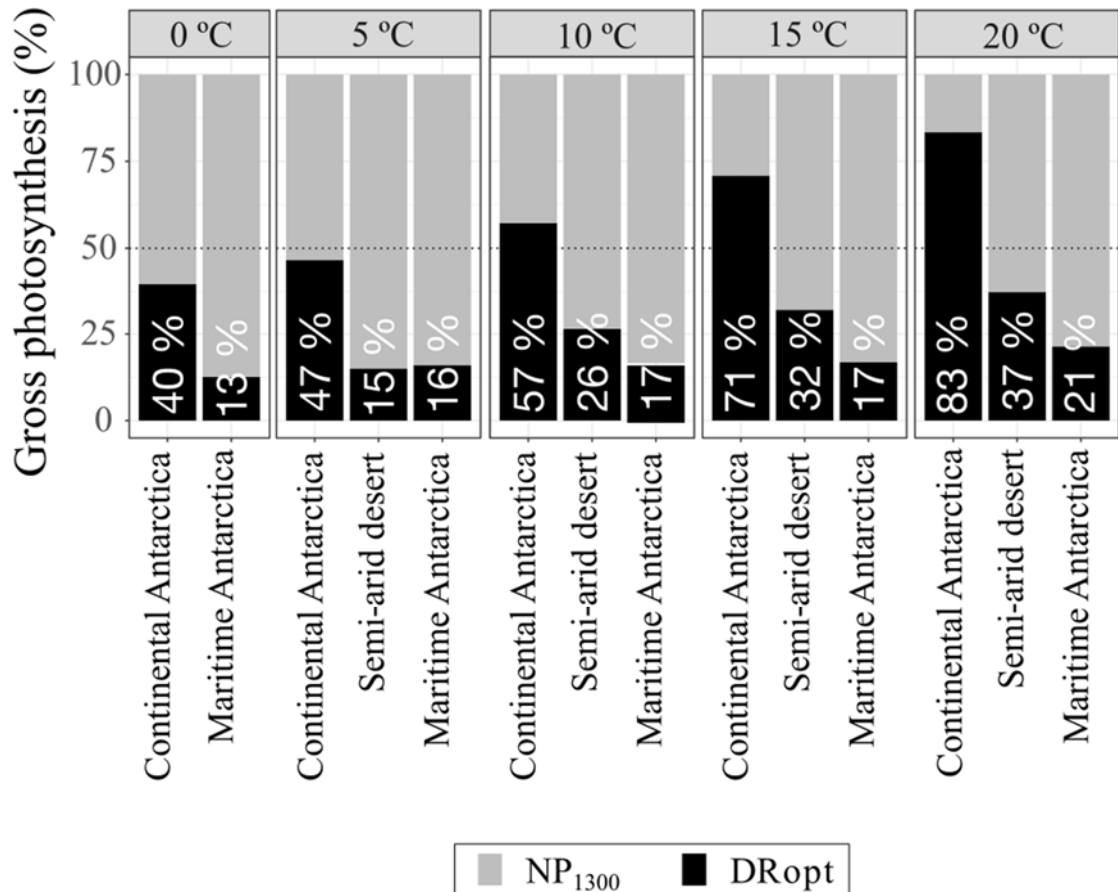
Fig. 4 Changes of dark respiration at the optimal water content (DRopt) as a proportion of gross photosynthesis for C. purpureus of continental Antarctica, maritime Antarctica, and Succulent Karoo semi-arid Desert. Data were measured at different temperatures (0-20ºC) and PPFD of 0 and 1300 µmol photons m^{-2} s^{-1} for DRopt and net photosynthesis (NP_{1300}), respectively.

The correlation analysis showed that all functional traits are highly positive or negatively correlated to each other (Fig. S1). However, no correlation is found between gross photosynthesis and NP_{1300} which have a correlation coefficient of 0.05 (Fig. S1).

The two axes of the PCA explained 94.2% of the total variance (Fig. 5). PC1 explained 68.8% of the variance, and it was positively correlated with NP_{1300} and photosynthetic efficiency (Fig. 5, Table S2). This meant that higher values of PC1 were related to higher carbon gain and higher photosynthetic efficiency. The PC1 split the specimens measured at maritime Antarctica from those of continental Antarctica. PC2 explained an additional 25.4% of the variance and was negatively correlated with DRopt and GP (Fig. 5, Table S2). This meant that higher values of PC2 were related to increased respiration and increased gross photosynthesis. Specimens from the semi-arid desert show an intermediate position between continental and maritime Antarctica, sharing functional traits with both tundra habitats.
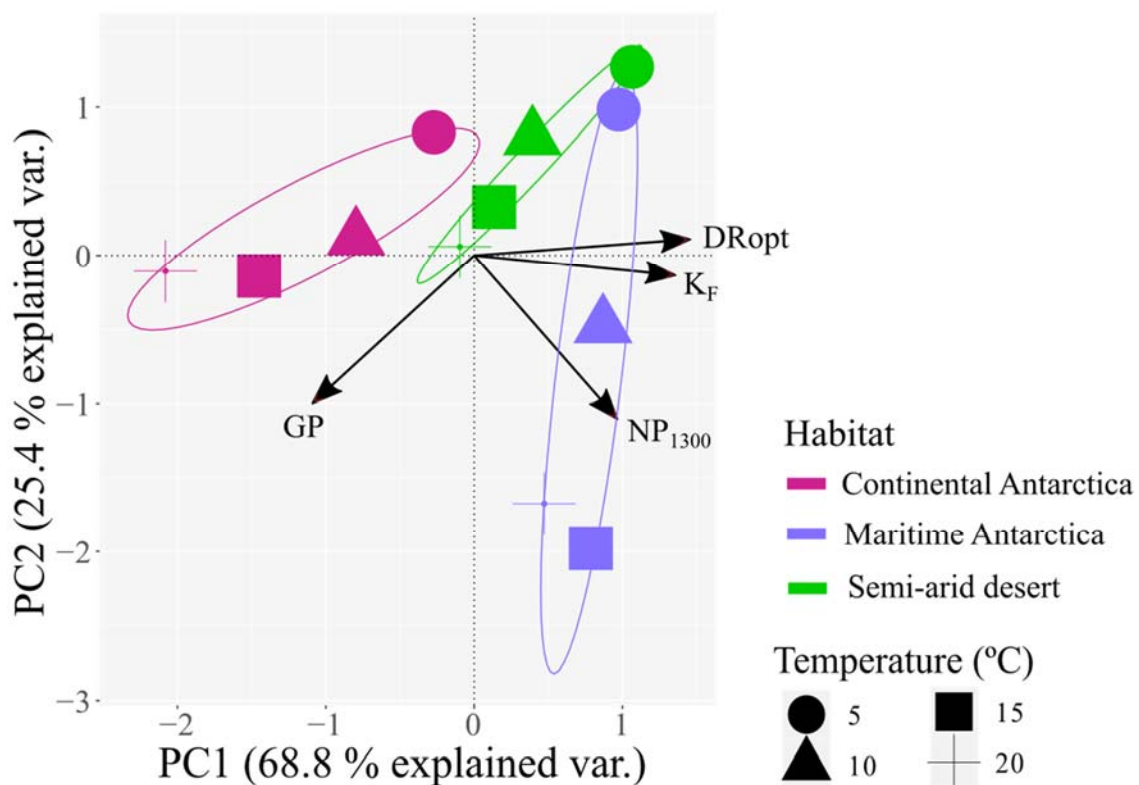
Fig. 5 Principal Component Analysis (PCA) of the photosynthetic parameters calculated for *C. purpureus* in the Succulent Karoo semi-arid Desert, maritime Antarctica, and continental Antarctica at four different temperatures (5-20ºC). Abbreviations correspond to gross photosynthesis (GP), net photosynthesis at 1300 μmol photons m^{-2} s^{-1} (NP_{1300}), dark respiration at the optimal water content (DRopt), and photosynthetic efficiency (K_F).

4. Discussion

The strategies of lichens and bryophytes to cope with extreme temperatures, high radiation, and water deficiency are highly dependent on micro-topographic factors (Schlensog et al., 2013; Schroeter et al., 2017; Raggio et al., 2017; Beltrán-Sanz et al., 2022). Microclimatic convergence when species are active allows the reduction of the macroclimatic differences between biomes, even up to 13ºC in temperature (Green et al., 2011; Raggio et al., 2017). The mean microclimatic temperatures during the active period of lichens and bryophytes have been established in *ca.* 0ºC in the tundra biomes (Davey et al., 1992; Schroeter et al., 2010, 2011), and 9ºC in semi-arid regions as the Tabernas Desert, Spain (Raggio et al., 2014, 2017; Pintado et al., 2010). As a consequence, this convergence leads to high photosynthetic efficiency rates at low temperatures for all study areas, regardless of the macroclimatic conditions of each habitat (Fig. 3, Fig. 5, Table 2; Weber et al., 2012). This supports the hypothesis that polar bryophytes do not show specific adaptations to polar conditions (Longton, 1988).

How *C. purpureus* is able to survive in contrasting habitats seems to be related to its ability to maximize its net photosynthesis at temperatures in which carbon loss by respiration is minimal. Populations from maritime Antarctica and the semi-arid desert show, respectively, that 16-21% and 15-37% of the gross photosynthesis correspond to respiration (Fig. 4). Given that 'full acclimation' has been defined as identical respiration rates occurring at two different temperatures (Larigauderie and Körner, 1995; Körner, 2003), we may consider that maritime Antarctica populations have 'full acclimation', while those from the semi-arid desert maintain a moderate acclimation (Fig. 4). When species are metabolically active in these regions, microclimatic conditions do not show abrupt changes (Convey et al., 2014). As a result, physiological processes are stably maintained throughout the year at moderate growth temperatures, thus facilitating the acclimation of respiration (Fig. 4; Xiong et. al, 2000; Lange and Green, 2005; Atkin et al., 2005, 2006a). In maritime Antarctica, such findings were previously pointed out by Xiong et al. (2000), who demonstrated a full acclimation of respiration in the vascular plants *Colobanthus quitensis* and *Deschampsia antarctica*. Nevertheless, specimens from continental Antarctica do not seem to be able to acclimate their respiration to temperature increase (Fig. 4), likely because they are subjected to higher temperature ranges when they are metabolically active (Atkin et al., 2005; Schroeter et al., 2017).

Thermal acclimation of respiration results in a reduction in the respiration sensitivity to temperature. Comparing the three habitats, the population of *C. purpureus*

shows a higher thermal acclimation and lower sensitivity in maritime Antarctica (Q_{10} = 1.68), moderate acclimation and intermediate sensitivity in the semi-arid desert (Q_{10} = 1.85), and no acclimation and higher sensitivity in continental Antarctica (Q_{10} = 1.95). At low temperatures (from 0 to 10ºC), the comparison of respiration sensitivity between both tundra biomes shows equal sensitivities (Q_{10} = 2.84), which supports that temperatures higher than 10ºC may harm populations from continental Antarctica. Previous studies found that Q_{10} of the Arctic plants exhibited substantially higher values than those from their temperate counterparts over a temperature range of 10-20ºC (Semikhatova et al., 1992). This trend seems to be related to the growth temperatures of the species in each habitat (Atkin et al., 2006b, Sancho et al., 2020).

As a consequence of an acclimation of the respiration, the optimal temperature for net photosynthesis increases due to the increase in gross photosynthesis (Green and Proctor, 2016), justifying that populations from continental Antarctica have lower optimums than those from maritime Antarctica and from the semi-arid desert. That trend in the optimum follows the mean macroclimatic temperature of each habitat (Fig. 1), implying different growth temperatures and, consequently, different acclimation strategies (Hicklenton and Oechel, 1976; Oechel, 1976; Kanda, 1979; Aro et al., 1987; Aro and Karunen, 1988; Xiong et al., 2000; Ino, 1990b; Pannewitz et al., 2006). Having low optimums, may be related to the fact that low temperatures promote the synthesis of more phospholipids and glycolipids as a strategy to regulate membrane permeability and fluidity (Aro et al., 1987).

Despite the optimal temperature described in this study fitting with the 5-16ºC for polar regions and 21-32 ºC for arid areas (Green and Proctor, 2016), there is high variability in the trait value among literature. For instance, the optimal temperature measured at 1000-1300 µmol photons m^{-2} s^{-1} PPFD for *C. purpureus* has been established between 7-10ºC (Pannewitz et al., 2005; Ino, 1990b), 15-20ºC (Ino, 1990a, 1994), and higher than 20ºC (Smith, 1999) in continental Antarctica; and between 20-30ºC in maritime Antarctica (Davey and Rothery, 1997; Perera-Castro et al., 2020). Such variability may highlight that bryophytes do not require low optimal temperatures to survive in Antarctica (Ino, 1990a; Perera-Castro et al., 2020). In fact, due to the cosmopolitan nature of *C. purpureus*, this species has a wide optimal temperature range for net photosynthesis according to geographic distribution, altitudinal preferences, and/or climatic conditions (Kappen et al., 1989; Sérgio et al., 2011). Furthermore, our

findings point that optimal temperature decreases when latitude increases in the Southern Hemisphere; however, more studies are needed to corroborate that trend.

Apart from the strategies of *C. purpureus* to be tolerant to heat and freezing, tolerance to radiation is also essential in habitats such as continental Antarctica. Lichens and mosses are capable of changing from shade-adapted forms to sun-adapted forms (Kappen et al., 1989; Pintado et al., 2005; Schroeter et al., 2012). Indeed, populations of *C. purpureus* from continental Antarctica have been described as a sun-adapted population (Ino, 1990a; Pannetwitz et al., 2005). In that habitat, lichens and bryophytes are mainly hydrated by meltwater during the summer, when mean PPFD reaches 536 μmols photons m^{-2} s^{-1} and mean temperature 3-5ºC (Ino, 1990b; Pannewitz et al., 2003a; Schroeter et al., 2017). Consequently, species from continental Antarctica have high respiration and low net photosynthesis, resulting in low photosynthetic efficiency (Fig. 3 and Table 2; Kappen et al., 1989; Schroeter et al., 2012). Promoting respiration may help plants to activate protection mechanisms such as (i) the reduction of reactive oxygen species (ROS) formation through the oxidation of excess cellular redox equivalents, and (ii) the synthesis of ascorbate used in cycles of xanthophyll and glutathione (Atkin et al., 2005). In addition, *C. purpureus* populations exposed to continuous radiation experience (i) partial chloroplast damage (Valanne, 1977; Aro and Valanne, 1979; Green et al., 2005), (ii) decreased Rubisco carboxylation activity (Valanne et al., 1978; Aro and Valanne, 1979), (iii) decreased chlorophyll content (Valanne, 1976b, Valanne et al., 1978; Aro and Valanne, 1979; Kappen et al., 1989; Post, 1990; Sala-Carvalho et al., 2022), (iv) increased concentration of carotenoids and anthocyanins (Smith, 1999; Lovelock and Robinson, 2002), and (v) increased thickness of the cell wall (Valanne et al., 1978).

The transition from shade- to sun-adapted forms seems to be related to the capability of *C. purpureus* to regenerate the chloroplast structure (Valanne, 1976a), accelerate CO_2 assimilation (Valanne, 1976a), and protect itself from ambient UV (Green et al., 2005). Ino (1990a) highlighted this transition from Japan to continental Antarctica, defining populations of this species as shade- and sun-adapted forms, respectively. Similarly, Davey and Rothery (1997) considered populations from maritime Antarctica as shade-adapted forms. Those classifications were based on the capacity of sun-adapted forms to maintain typically higher light compensation points (Pannetwitz et al., 2005; Schroeter et al., 2012). In concordance with that, the highest light compensation points at 10ºC occur in continental Antarctica (69-93 μmol photons m^{-2} s^{-1}, Pannetwitz et al.,

2005), followed by semi-arid desert (52 μmol photons m^{-2} s^{-1}, Green and Proctor, 2016; Weber et al., 2012), and finally by maritime Antarctica (35 μmol photons m^{-2} s^{-1}, see Fig. 2 and Table 2). This gradient is supported by the annual mean PPFD recorded in each area when lichens and bryophytes are metabolically active: 129-247 μmol photons m^{-2} s^{-1} at continental Antarctica (Schroeter et al., 2010, 2011; Raggio et al., 2016), 123 μmol photons m^{-2} s^{-1} in the Tabernas Desert (Spain, Raggio et al., 2017), and 56-12 μmol photons m^{-2} s^{-1} in maritime Antarctica (Schroeter et al., 2010; Raggio et al., 2016).

The ability of using low light to compensate carbon losses by respiration gives an advantageous photosynthetic performance to maritime Antarctica populations. In fact, this population has higher photosynthetic efficiency at all temperatures measured in comparison with the other two study areas. Furthermore, it also shows a high light-use efficiency from 0 to 25ºC (Lange, 2002; Pintado et al., 2005). Other functional traits such as the light saturation points calculated between 10-15ºC matches other studies of bryophytes in tundra biomes (Ueno et al., 2006). However, gross photosynthesis of *C. purpureus* in maritime Antarctica is much higher than that observed by Davey and Rothery (1997) likely due to area basis affecting the number and quality of active moss stems present in the cushion (Weber et al., 2012).

Thanks to cosmopolitanism, *C. purpureus* is able to adjust to the best physiological strategy in each habitat. The photosynthetic traits show high dissimilarity between tundra biomes, clearly isolating them from each other (Fig. 5), and provides an additional example of how different maritime and continental Antarctica habitats are for plant life. Contrarily, the population from the semi-arid desert is positioned among both (Fig. 5) due to its similarity in NP_{1300} with the population from continental Antarctica, and in respiration with that of maritime Antarctica (Fig. 3). These characteristics lead to intermediate rates of photosynthetic efficiency and gross photosynthesis (Fig. 5). It is particularly remarkable that specimens from the semi-arid desert do not show an abrupt decline of NP_{1300} at high temperatures in comparison to the two other populations (Fig. 3), which highlights the improved heat tolerance of this population.

5. Conclusions

The diverse climate conditions to which cosmopolitan species are subjected determine their physiological response range. Functional strategies such as the thermal acclimation of respiration, the photosynthetic efficiency modulation, the optimum temperature adjustment for net photosynthesis, and the ability to switch between shade- and sun-adapted forms seem to be crucial in determining the tolerance and adaptation patterns of the cosmopolitan species. Populations of *C. purpureus* from continental Antarctica and the Succulent Karoo Desert are high-radiation and heat tolerant, respectively. Nevertheless, maritime Antarctica is the least stressful habitat, and, thus, the most suitable for this species. Hence, photosynthetic traits of populations of *C. purpureus* from maritime and continental Antarctica are strongly different, while the population from the Succulent Karoo Desert shares photosynthetic traits with both Antarctic regions. The comparison of the eco-physiological response patterns of cosmopolitan species along a latitudinal gradient opens up new work perspectives addressing the potential spectrum of species' responses under climate change scenarios.

Chapter 2:

Variations in growth form and substrate switching as an adaptive response in drylands: a case study in the lichen genus *Xanthoparmelia*

Abstract

Phenotypic plasticity in lichens include variations in growth form as a response strategy to local environmental conditions. Hence, the taxonomical value of certain morphological traits used in species identification remains unclear, leading to ambiguous species boundaries. In order to highlight the adaptation strategies of lichens in drylands, the genetic diversity of both bionts, and the eco-physiological performance of the closely-related species *Xanthoparmelia pulla* and *X. pokornyi* were analysed. In the semi-arid region of the southeast of Spain, those species differ in growth form and substrate colonization, being foliose and rock-inhabiting in coastal populations, and sub-fruticose and soil-inhabiting in the inland desert, respectively. Our findings show that these species are highly similar to one another according to the sequencing of the markers nrITS, *β-tubulin,* and *MCM7* of the mycobiont. Therefore, variations in growth form may be a strategy to better adapt to the local environmental conditions. Furthermore, the species studied show similar photobiont community composition and low specificity between partner(s), which leads to physiological convergence. Nevertheless, there is a high genetic diversity of the lichen-associated algal communities on the coastal populations, as well as a potential complementary eco-physiological response between OTU1 and OTU2. Moreover, the physiological nuances found point out that populations from the desert are better acclimated to low temperatures. The noticeable convergence in all of the studied approaches highlights that variations in growth form and/or substrate switching may promote lichen's expansion into different habitats in drylands.

Keywords Species delimitation, growth form, functional convergence, substrate switching, photobiont, photosynthesis, drylands, Illumina meta-barcoding

1. **Introduction**

In drylands, lichens –together with bryophytes and cyanobacteria– constitute one of the most conspicuous autotrophic components of the biocrust (Belnap, 2003). Lichens are the result of a mutualistic relationship between a fungus (the so-called mycobiont) and a population of one or more photosynthetic partners (photobiont/s). This symbiosis dominates *ca.* 8% of the planet surface (Ahmadjian, 1995), but in drylands, they show a notable dominance on the landscape, occupying *ca.* 30% of the interplant spaces (Rodríguez-Caballero et al., 2017).

The thalli of lichens have been traditionally characterized by morphological traits and the chemical compounds produced by the mycobiont (Clauzade and Roux, 1985; Smith et al., 2009). However, a single lichen species under different environmental pressures may show differences in these traits, which lead to ambiguous species boundaries (e.g. Velmala et al., 2009; Pino-Bodas et al., 2011; Leavitt et al., 2011a; 2011b; Pérez-Ortega et al., 2012).

Because a given genotype may produce different phenotypes in response to distinct environmental pressures (ʻphenotypic plasticityʼ; Nicotra et al., 2010), morphological traits resulting from these pressures might be linked to functional success. Most plastic traits of plants are related to the capability to maximize the efficiency in the use of resources (Sultan, 2000). In the case of lichens, the most evident phenotypic trait that may be subjected to plasticity is the body-plan architecture or ʻgrowth formʼ (Grube and Hawksworth, 2007).

A single lichen species may have two different growth forms as a response to distinct abiotic pressures (Ertz et al., 2018; Osyczka et al., 2018). For instance, *Sticta filix* is a foliose species in dry and sunny habitats, and shrublike in wet and shady sites (James and Henssen, 1976); *Circinaria elmorei* varies between fruticose and crustose growth forms according to the microhabitat conditions (Kunkel, 1980), while *Aspicilia californica* switches from shrubby to crustose when it overgrows small pebbles (Sanders, 1999). Other common morphs in lichens include sessile or vagrant forms such as those reported in *Cetraria aculeata* (Pérez-Ortega et al., 2012; Printzen et al., 2013) that occur in windswept steppes and deserts, where the same species can form morphotypes attached to rock surfaces, or free ʻtumbleweed-likeʼ forms.

The substrate preferences are determined by the species' requirements and their physiological tolerance (Brodo, 1973). For example, Tretiach et al. (1995) found that populations of *Parmelia pastillifera* could be epilithic or epiphytic in two

microclimatically different habitats. In the same way, *Cladonia rangiferina* and *C. mitis* exchange saxicolous, terricolous or epiphytic forms (Tolpysheva and Timofeeva, 2008). Changes in habitat and/or substrates lead to differences in the eco-physiological performance patterns due to, for instance, the lichen dependence on hydration sources. For instance, populations of *Diploschistes diacapsis* from south-exposed slopes in drylands showed higher photosynthetic performance but shorter metabolic activity duration than the north-exposed ones (Pintado et al., 2005).

Photobiont/s identity also determines the eco-physiological patterns due to their role as primary producers. In spite of having found a predominant photobiont on the vast majority of species (Paul et al., 2018), a single mycobiont may be associated with multiple photobiont/s linages (e.g. James and Henssen, 1976; Sadowska-Des et al., 2014; Ertz et al., 2018) in order to maximize the physiological performance (Casano et al., 2011) and as a result of local environmental adaptation (e.g. Fernández-Mendoza et al., 2011; Werth and Sork, 2014; Yahr et al., 2006; Dal Grande et al., 2018).

The genus *Xanthoparmelia* (*Parmeliaceae*) has attracted much attention due to its high species diversity and broad morphological and chemical heterogeneity (e.g., Leavitt et al., 2011a, 2011b, 2018). It is typically characterized by species with foliose growth form that are often found occurring on soil and siliceous rocks from arid and subarid regions (Blanco et al., 2004). Within *Xanthoparmelia* genus, *Xanthoparmelia 'pulla* group' (Blanco et al., 2004; Amo de Paz et al., 2012; Leavitt et al., 2018) is a monophyletic group with complex systematics due to the significant discordance between the classifications based on morphology/chemistry and molecular phylogenetics (Leavitt et al., 2011a, 2011b; Amo de Paz et al., 2012). A key example of this conflict is represented by the species *Xanthoparmelia pulla* (Ach.) O. Blanco, A. Crespo, Elix, D. Hawksw. & Lumbsch and *X. pokornyi* (Körb.) O. Blanco, A. Crespo, Elix, D. Hawksw. & Lumbsch (Fig. 1), whose discrimination has been highly controversial for decades. Initially, *X. pokornyi* was described as a variety of *X. pulla* (Poelt, 1969; Gutiérrez and Casares, 1994) but they were later split into two different species due to little anatomical differences in the thalli (Esslinger, 1977; Amo de Paz et al, 2012). Chemically, Esslinger (1977) concluded that *X. pulla* was able to synthesize divaricatic acid, while *X. pokornyi* did not. However, its presence was later confirmed in *X. pokornyi* (Culberson et al., 1977). Despite both species having been described as foliose (Esslinger, 1977, Amo de Paz et al., 2012), there are some morphological differences between them. The species *X. pulla* has foliose growth form, adpressed thallus to the substrate, and numerous apothecia,

while the species *X. pokornyi* has foliose sub-fruticose growth form, thalli very loosely attached to the substrate, and uncommon apothecia (Nimis and Martellos, 2021). However, the substrate is clearly the divergent factor between them, being *X. pokornyi* primarily terricolous and *X. pulla* saxicolous (Esslinger, 1977, Nimis and Martellos, 2021).

The present study focuses on the species *X. pokorny* and *X. pulla* in order to evaluate whether their variation in growth form is caused by phenotypic plasticity, rather than by different genetic background. Hence, we first examined species boundaries of the mycobiont, analysing the markers nrITS, *β-tubulin,* and *MCM7*. Due to the fact that variation in growth form may be considered a functional trait to maximize the species fitness, we performed an eco-physiological analysis. Finally, we also examined the lichen-associated algal communities of both species using a meta-barcoding approach due to their role as primary producers. This allows us to answer the following questions: (i) are the differences in physiological performance due to host different photobiont/s?, (ii) to what extent are differences in photobiont community composition linked to host genetic identity, environmental factors and physiological performance?. Addressing the limits of phenotypical plasticity in lichens allow us to better understand their adaptation to drylands, where functional traits such as growth form and photobiont identity seem to be crucial for the organism's success.

2. Methods

2.1. Study site and sample collection

Lichen populations were collected from six slopes in the southeast of Spain (Almería); more specifically, three were located in the coastal habitat of Cabo de Gata (30S WF 85454 75865) and three in the Tabernas desert (30S WF 50209 96362) (Fig. 1). The study site is considered the most arid region of Europe. The Tabernas Desert consists of gypsum-calcareous mudstones and calcaric sandstones, with a mean annual precipitation of 235 mm (mainly falling in winter) and air temperature of 17.8°C (Chamizo et al., 2012). Similarly, Cabo de Gata consists in thin, and saturated in carbonates soils with moderate rock fragment content, with a mean annual rainfall of 200 mm and air temperature of 18°C (Chamizo et al., 2012).

North-facing slopes were selected in order to reduce the heterogeneity in samples growing conditions (Pintado et al., 1997, 2005). The minimum distance between populations was 1 km in a total area of *ca.* 200 m^2. The samples were collected at a

minimum distance of 1 m to avoid the collection of clonal material. For the eco-physiological analysis, 4 samples of each population were collected (12 samples of each habitat). For the photobiont sequencing, 28 samples of each population were collected (84 samples of each habitat). Finally, for the mycobiont sequencing, 8 samples of each population were collected for sequencing the markers *MCM7*, *β-tubulin* (24 samples in each habitat), while 28 samples of each population were collected for sequencing the nrITS (84 samples of each habitat).

In this study, all specimens found of *X. pulla* were saxicolous and foliose (Nimis and Martellos, 2021), and all of *X. pokornyi* were terricolous and sub-fruticose (Blanco et al., 2004; Rizzi and Giordano, 2012) (Fig. 1). Upon collection, thalli were air dried and then stored frozen at -20 °C until the experiments were carried out.
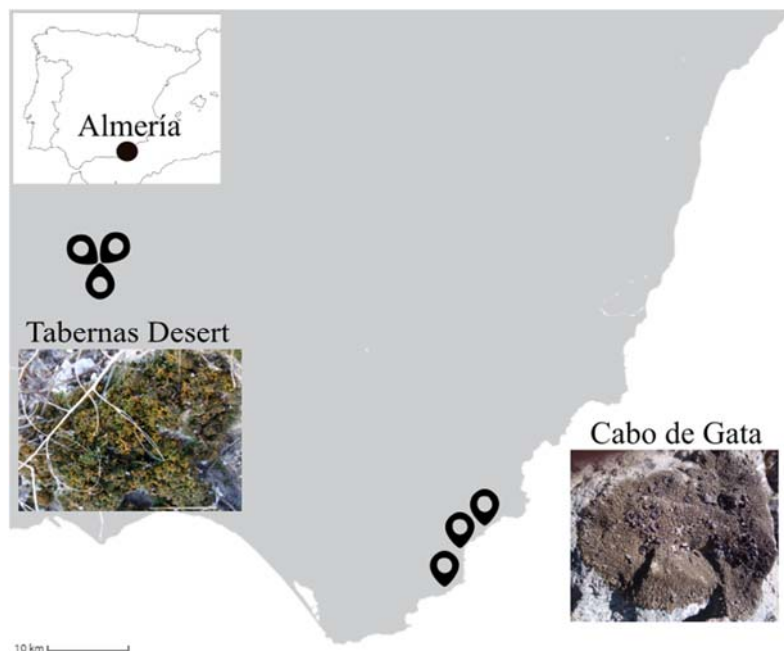
Fig. 1 Sampling sites of *X. pokornyi* (terricolous and sub-fruticose) and *X. pulla* (saxicolous and foliose) populations. Each icon represents one population.

2.2. CO$_2$ exchange

During the three days prior to the start of the measurements, samples were reactivated in a chamber at 12 °C, under a 12h in darkness followed by 12h of photoperiod (at a photosynthetically active photon flux density (PPFD) of 100 μmol photons m^{-2} s^{-1}). Thalli were kept moist by spraying with mineral water once a day. Substrate remnants of the terricolous samples were then removed in order to prevent them from interfering with

the measurements. It was not possible to remove the rock attached to the saxicolous specimens.

Before starting the CO_2 exchange measurements, the state of health of Photosystem II was checked using a Mini-PAM chlorophyll *a* fluorescence system (Walz, Germany). This system allows to monitor the maximal photochemical efficiency of photosystem II, which is remarkably constant when the photobiont/s are under optimal physiological conditions (0.63 - 0.76; Jensen, 2002). Therefore, all specimens which this value was lower than 0.63 were excluded from further analysis, in order to guarantee an optimal and homogeneous initial physiological status for all samples.

Gas exchange measurements were conducted using a portable Gas Exchange System (GFS-3000, Walz Mess und Regeltechnik, Effeltrich, Germany) that allows to control light, temperature, relative humidity (60-70%) and air flow (750 µmol min^{-1}). Two experiments were carried out: (i) desiccation response curves and (ii) light response curves.

To carry out the desiccation response curves, the samples were first hydrated to saturation by spraying them with mineral water and weighed to determine the maximum water content (MWC; Table S1). Thereafter they were introduced in the Gas Exchange System at 15 °C and 400µmol photonsm^{-2} s^{-1} PPFD, which are standard conditions for these type of experiments in sun-adapted lichens from mid-latitudes (Pintado et al., 2005; Pérez-Ortega et al., 2012; Raggio et al., 2018). During the dehydration process, net photosynthetic rate was automatically recorded every 3 minutes, while the water content was gravimetrically measured every 15 minutes. The water content when the sample reach to the maximum net photosynthetic rate (NP$_{400}$) was also recorded (OWC; Table S1). This experiment generated 24 desiccation response curves calculated on area basis.

The presence of the rock during the CO_2 exchange experiments could lead to potential bias in the calculus of MWC and OWC due to their capability to retain water. In order to solve that issue, the bare rock was subjected to the same hydration process explained before. Firstly, the lichen thallus was removed of the rock. Secondly, each rock was hydrated to saturation by spraying them with mineral water. Finally, they were weighed to determine their water content. The water content retained by the bare rock was then subtracted from the total water content of each sample. On average the bare rocks retained 10.16% of the total water content measured.

For the light response curves, specimens were hydrated to their OWC by spraying them with mineral water. We measured the light curves as the response of net CO_2

exchange to different PPFD (0, 25, 50, 100, 200, 400, 800, 1200, 1500 μmol photons m^{-2} s^{-1}) at several temperatures (5, 10, 15°C). The temperatures selected are the most common temperature ranges of temperature in these habitats when biocrust lichens are metabolically active (Pintado et al., 2010; Raggio et al., 2014, 2018). Dark respiration at the optimal water content (DRopt) was measured at 0 μmol photons m^{-2} s^{-1} and maximal net photosynthetic rate (NP$_{1500}$) at 1500 μmol photons m^{-2} s^{-1}, the highest PPFD measured. This experiment generated 72 light response curves calculated on area basis.

Both response curves were calculated on surface-area basis, independently of the growth form of each species. This method is widely accepted in comparative studies in lichens (e.g. Green and Lange, 1995; Lange et al., 1997; Büdel et al., 2014; Raggio et al., 2014), and studies with foliose and/or saxicolous specimens in which substrate and lichen are indivisible due to the partially penetration of the thallus to the rock (Chen et al., 2000).

Desiccation and light response curves were fitted to the best model using the CurveExpert Professional v.2.6.5. (Table S2), and subsequently, the physiological parameters detailed in Table S1 and S3 were calculated. A one-way ANOVA (p ≤ 0.05) was carried out for each sample and parameter measured in the desiccation and light response curves. Each physiological parameter was established as the dependent variable, and the habitat as an independent. Normality and homoscedasticity were checked using the Shapiro-Wilks test and the Bartlett test, respectively. If data did not accomplish the assumptions, Kruskal Wallis was performed.

2.3. Molecular studies of the mycobiont

2.3.1. DNA extraction, PCR and sequencing of the mycobiont

A piece of each thallus was frozen in liquid nitrogen and pulverized using crystal rods. Total DNA was extracted from the pulverized thalli remnants using DNeasy Plant Mini Kit (QIAGEN) according to the manufacter's protocol. The three most variable molecular mycobiont markers found in Leavitt et al. (2011a) for the *Xanthoparmelia* '*pulla* group' were selected for amplification: i) the nuclear ribosomal Internal Transcribed Spacer (nrITS), which is also the locus used generally for barcoding fungi (Schoch et al., 2012); and two nuclear protein-coding loci: ii) the *β-tubulin* and iii) the mini-chromosome maintenance complex component 7 (*MCM7*). The *MCM7* has been shown to offer a high molecular intra-population resolution in many lichen-forming fungi (Sadowska-Deś et al., 2014). PCR amplifications were carried out in microtubes containing 12.5μl AmpliTools Fast Master Mix (Biotools), 1.5μl of each primer at 10

µM, 5 µl of template DNA, and 4.5 µl of Ultrapure Water (Invitrogen). Details of the primers and PCR settings used in this study can be found in Tables S4 and S5, respectively. Amplification products were visualized on a 1% agarose gels stained with SYBR Safe DNA (Life Technologies Corporations, USA) and subsequently purified using the enzyme exoSAP-IT (GE Healthcare, UK). DNA strands were finally sequenced at Macrogen Europe (Frankfurt am Main). Electropherograms were checked, trimmed and assembled using Seqman v.4.03 (Dnastar Inc.). Detailed collection information and GenBank accession numbers are listed in Table S6.

2.3.2. Genetic diversity of the mycobiont

From the 48 samples collected for sequencing each marker, a total of 43 sequences were obtained for *β-tubulin*, and 44 for the nrITS and *MCM7*. The generated sequences of each marker were aligned using MAFFT v.7.308 (Katoh and Standley, 2013), with the parameters set to default. Ambiguously aligned positions were identified and removed. Subsequently, genetic diversity indices and haplotype networks were inferred for each marker, using DNAsp v. 6.12.03 (Rozas et al., 2017) and PopART v.1.7 (Leigh and Bryant, 2015), respectively.

2.3.3. Phylogenetic inference of the mycobiont

The 43-44 generated sequences of each marker (*β-tubulin*, *MCM7*, nrITS) were merged with two multi-locus datasets published in previous phylogenetic assessments of *Xanthoparmelia*: i) the nrITS and nrLSU data from Amo de Paz et al. (2012), and ii) the nrITS, *β-tubulin*, *MCM7*, nrLSU and mtSUU data from Leavitt et al. (2018). These data were downloaded and aligned independently with the software MAFFT v.7.308 (Katoh and Standley, 2013), with default parameters. Ambiguously aligned positions were identified and removed, and, then, concatenated. Sequences for several species in the *Xanthoparmelia* '*tegeta* group' were used as outgroups to root the corresponding phylogenetic tree. Sequences included in these two studies were downloaded from the GenBank database (http://www.ncbi.nlm.nih.gov/; Table S6).

The phylogenetic relationships of the combined datasets were inferred using both Maximum Likelihood and Bayesian Inference methods. In both methods, optimal substitution models for the six markers were inferred with PartitionFinder v.1.1.1 (Lanfear et al., 2012) considering a model with linked branch lengths and the Bayesian Information Criterion (BIC).

Maximum Likelihood was conducted with the online version of RAXML-HPC BLACKBOX v.8.2.12 (Stamatakis et al., 2014) on the CIPRES SCIENCE GATEWAY v.3.3 (Miller et al., 2010), assuming a GTRGAMMA model of evolution. Bootstrap nodal support (BS) was evaluated by calculating 1,000 bootstrap pseudoreplicates and only values equal or higher than 70% were regarded as significantly supported.

Bayesian Inference was conducted using MrBayes software with two parallel, simultaneous four-chain runs executed over 1×10^8 generations starting with a random tree, and sampling after every 1×10^4 steps. The first 25% of data were discarded as burn-in, and the 50% majority-rule consensus tree and corresponding posterior probabilities (PP) were calculated from the remaining trees. Average standard deviation of split frequencies (ASDSF) values below 0.005 and potential scale reduction factor (PSRF) values approaching 1.00 were considered as indicators of chain convergence. Nodes showing Bayesian posterior probabilities equal or higher than 0.95 were regarded as significantly supported. No molecular clock was assumed.

Both phylogenetic trees obtained in both methods were visualized in FigTree v.1.4 (Rambaut, 2018).

2.3.4. Species delimitation analysis of the mycobiont

From the 168 samples collected, a total of 162 sequences for the nrITS were obtained. These newly generated sequences were then aligned with all sequences included in the *Xanthoparmelia 'pulla'* groups from Amo de Paz et al. (2012) and Leavitt et al. (2018), as was previously explained. After that, two different species delimitation analyses based on single-locus datasets were performed.

The ABGD (Puillandre et al., 2012) is a distance-based approach which automatically detects a barcode gap that delimits candidate species based on non-overlapping values of intra- and interspecific genetic distances. It has been shown to be accurate in inferring species limits across diverse groups of the family *Parmeliaceae* (Leavitt et al., 2015). Runs were remotely carried out at http://wwwabi.snv.jussieu.fr/public/abgd/abgdweb.html, setting the prior intraspecific divergence ($P_{min} = 0.001$, $P_{max} = 0.01$), the number of steps (Steps = 10) and Nb bins = 20. Four analysis were performed with different values of relative gap width (X set to 0.1, 0.5, 1, and 1.5). The Kimura two parameters (K2P) model was chose to calculate genetic distances between individuals and the transition/transversion ratio (TS/TV). These values

were calculated for both above-mentioned alignments using MEGA 5.2 (Tamura et al., 2011), which resulted in a TS/TV values of 2.76.

The GMYC analysis (Fujisawa and Barraclough, 2013) combines a coalescent model of intraspecific branching with a Yule model for interspecific branching, which is then fitted to an inferred single-gene topology. GMYC requires an ultrametric tree computed in BEAST v.1.8.1. We used an uncorrelated relaxed clock and Yule tree prior. The other prior parameters were set to default. One run of 10 million generations each and sampled each 1000 steps. The first 25% of data were discarded as burn-in. Convergence was assessed by examining the likelihood plots through time using TRACER v1.7 (Rambaut et al., 2018). GMYC analysis was run using the '*splits*' package (Ezard et al., 2009) implemented for R software.

2.4. Molecular studies of the photobiont/s

2.4.1. Illumina metabarcoding of photobiont communities and bioinformatic analysis

To study the lichen-associated microalgal community, ITS2 was amplified and sequenced using Illumina MiSeq sequencing. The ITS2 region represents a good barcode locus for lichen-associated green algae (Coleman, 2009) because it provides good species-level resolution, high PCR reproducibility, and displays highly conserved secondary structure (see, for instance, Dal Grande et al., 2018).

To control for potential laboratory biases (Bálint et al., 2016), we sequenced two PCR replicates for each sample, randomized the replicates' order on the PCR plates, and used octamer-multiplexing labels following Gloor et al. (2010). The 25-µl PCR reactions contained 0.65 U TaKaRa ExTaq (Clontech Laboratories Inc., Palo Alto, CA, USA), 2.5-µl of buffer, 18.5-µl of water, 0.5-µl of bovine serum albumin (BSA; 10 mg ml -1), 2.0-µl of dNTP mixture (2.5mM each), 0.5 µl of total DNA (5 ng), and 0.5 µl (0.22-µM) of each primer. Details of the primers and PCR settings used in this study can be found in Tables S4 and S5. The end-labeled amplicons were solid phase reversible immobilization (SPRI)-purified, and concentration-normalized (using Qubit; Life Technologies, Darmstadt, Germany). Library preparation with the MetaFast protocol and paired-ended sequencing (2x300 bp) on an Illumina HiSeq (RapidRun mode) sequencer was performed by Fasteris (CH).

Quality filtering of raw reads was performed by removing all sequences shorter than 200 bp and with a quality score < 26 using the script

READS_QUALITY_LENGTH_DISTRIBUTION.PL (Bálint et al., 2014). We then assembled paired-reads with PANDAseq (Masella et al., 2012) with default settings and filtered primer artefacts using the script REMOVE_MULTIPRIMER.PY (Bálint et al., 2014). The reads were then reoriented in 5'-3' direction, and demultiplexed using FQGREP (https://github.com/indraniel/fqgrep). In order to extract the ITS2 region, we used the ITSX software (Bengtsson-Palme et al., 2013). OTU clustering was performed with SWARM v2 (Mahé et al., 2015) using two subsequent local clustering thresholds (d=1 followed by d=3; FROGS pipeline, Escudié et al., 2018). Chimeric OTUs were removed using the UCHIME method (Edgar et al., 2011) as implemented in VSEARCH v2 (Rognes et al., 2016). To taxonomically identify the OTUs, we performed BLASTn searches against the NCBI nucleotide '*Chlorophyta*' database followed by manual curation. We prioritized sequences obtained from pure cultured (SAG, UTEX) over environmental samples. We further compared the secondary structures of the ITS2 region of each OTU using the RNAfold WebServer with default settings in order to minimize potential oversplitting, i.e., different OTUs with identical ITS2 secondary structure.

Due to the lack of a mock community in our study, stringent filtering on the OTU table was applied to obtain reliable algal abundance estimates. First, we removed the highest number of reads found in the negative controls from the corresponding rows in the OTU table. We then merged the tables for the two PCR replicates keeping only those OTUs that were detected in both replicates. Finally, we retained OTUs with a total read abundance on a per-sample basis >0.005% and with a population abundance >50% in at least one population (Bokulich et al., 2013; Krohn et al., 2016).

To infer the phylogenetic position of the *Trebouxia* OTUs found in *Xanthoparmelia* populations we constructed a phylogenetic tree using the OTUs in this study and those representing the four major lineages of *Trebouxia* (Leavitt et al., 2015). Sequences were aligned using MAFFT on XSEDE v.7.308 (Katoh and Standley, 2013). We then constructed a maximum likelihood tree using RAXML-HPC BLACKBOX v.8.2.12 (Stamatakis et al., 2014) on the CIPRES SCIENCE GATEWAY v.3.3 (Miller et al., 2010) with a GTRGAMMA model. We visualized the phylogenetic tree using FigTree v.1.4.4 (Rambaut, 2018).

2.4.2. Statistical analysis of the lichen-associated algal communities

The OTU community composition was analysed with two-dimensional non-metric multidimensional scaling (NMDS) using Bray-Curtis distances and based on 1000 permutations. A percent of relative abundance was selected as a standardization method to perform the DeSeq analysis (Love et al., 2014).

The DeSeq analysis was performed to test whether there are significant differences in abundance levels between experimental groups using a negative binomial distribution.

Furthermore, for each habitat, three different factors were analyzed in order to determinate their influence on the lichen-associated algal communities: the climatic conditions, the physiological performance and the host genetic diversity.

As a proxy of the climate conditions, 19 bioclimatic variables were downloaded from Worldclim v2, at 30 arc-second resolution (http://www.worldclim.org). We reduced the variable's dimensionality using Principal Coordinates Analysis (PCoA) as implemented in the R package '*vegan*' (Oksanen et al., 2017). As climate proxy, we used the centroid coordinates of the first two PCoA axes scores of each population (Fig. S1). As a proxy of physiological performance, we selected the most explicatory parameters of the light response curves (NP_{1500} and DRopt), and we performed the analysis detailed previously (Fig. S2). For each habitat, Kendall correlation (p-value < 0.05) was performed between (i) OTU abundance and climatic conditions, and (ii) OTU abundance and physiological performance.

As a proxy of host genetic diversity, we considered the genetic variability found in the mycobiont nrITS region. VSEARCH v2 (Rognes et al., 2016) was used to cluster the 168 fungal sequences into OTUs using a similarity threshold of 99%. We, then, examined the specificity of mycobiont-photobiont interactions using a tripartite network analysis (Fig. S3). For this, we used the R packages '*igraph*' (Csardi et al., 2015) and '*bipartite*' (Dormann 2008). The resulting network represented the connection among the OTU diversity, the mycobiont haplotypes, and the habitat.

3. Results

3.1. CO₂ exchange

Desiccation response curves showed no statistically significant differences between habitats in any physiological parameter (Table S7; Fig. S4), maintaining similar averages for all of them (Table 1). The specimens' hydration to saturation showed *ca.* 1

mm precipitation equivalent in MWC (Lange et al., 1997, 2001). Moreover, after 27-35 minutes from the start of the desiccation response curve, specimens went into optimal conditions and remained there around 29-31% of the total curve duration. During that period of time, they achieved a net photosynthesis of 2.4-2.7 µmols CO_2 m^{-2} s^{-1} (NP$_{400}$), with an OWC of *ca.* 0.6 mm precipitation equivalent. The hydrated thalli lasted 95-114 minutes until being completely desiccated, with a total area below the response desiccation curve of 152-160 µmols CO_2 m^{-2} s^{-1} fixed (Table 1).

Table 1 Means and standard deviations (sd) of the photosynthetic parameters from the 12 fitted desiccation response curves for each habitat. Each curve was measured at PPFD of 400 µmol photons m^{-2} s^{-1} and temperature of 15 °C.

Photosynthetic parameter	Units	Habitat	Mean ± sd
NP$_{400}$	µmols CO_2 m^{-2} s^{-1}	Coast	2.73 ± 0.32
		Desert	2.42 ± 0.54
Area below the response desiccation curve		Coast	152 ± 44
		Desert	160 ± 61
Duration of the optimal conditions	minutes	Coast	31 ± 7
		Desert	29 ± 10
Starting of the optimal conditions	minutes	Coast	35 ± 13
		Desert	27 ± 9
Total duration of the desiccation curve		Coast	95 ± 25
		Desert	114 ± 39
MWC	mm	Coast	1.16 ± 0.34
		Desert	0.93 ± 0.14
OWC		Coast	0.62 ± 0.31
		Desert	0.56 ± 0.16

All physiological parameters obtained in the light response curves showed an increased with temperature raise, except the photosynthetic efficiency. The photosynthetic efficiency was higher at 10ºC for both habitats, and was higher in the desert habitat too for all temperatures measured (Table 2). This is linked to the lower DRopt rates found in the desert for all temperatures measured (Table 2).

At 5°C, DRopt, photosynthetic efficiency and LCP were significantly different (Table S8). The differences found in DRopt showed higher respiration on the coastal specimens, which in turn lead to lower photosynthetic efficiency. However, the DRopt were not different enough between habitats to lead to differences into GP. Samples from the desert compensated (LCP) at lower PPFD than the coast (Table 2, Fig. 2)

At 10°C, only NP_{1500} and photosynthetic efficiency were statistically significant (Table S8). The NP_{1500} of 3.42 µmols CO_2 m^{-2} s^{-1} measured on the desert specimens (Fig. 2), together with the lower DRopt, led to higher photosynthetic efficiency. Due to the coastal specimens had higher DRopt but lower NP_{1500} than the desert ones, and vice versa, the GP at 10ºC was similar between both habitats (Table 2).

At 15ºC, even though the values of the photosynthetic parameters were apparently different, they did not show any statistically significant differences between habitats (Table 2, Fig. 2).
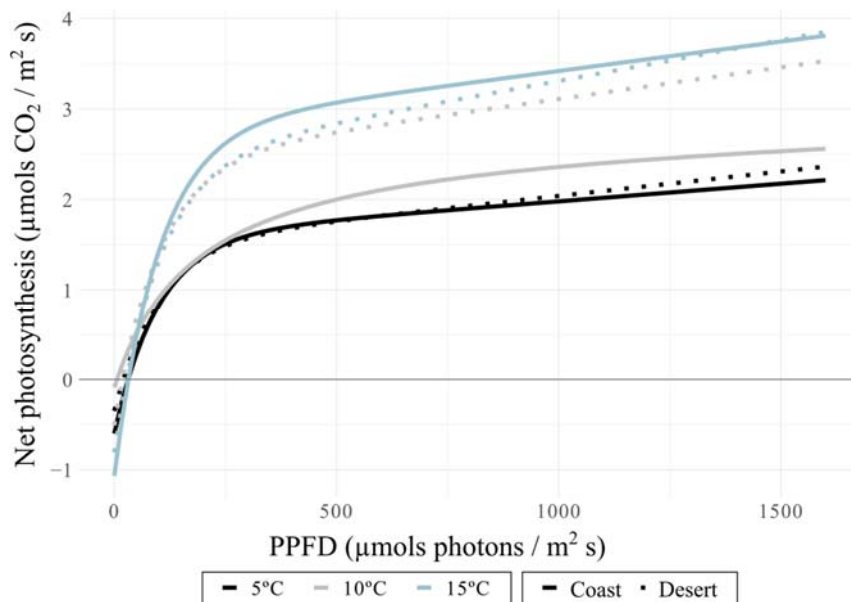
Fig. 2 Dependence of net photosynthesis to different light intensities at 5°C, 10°C, and 15°C, in Cabo de Gata and the Tabernas Desert. The R^2-adjust and standard deviation of each curves is detailed in Table S2.

Table 2 Means ± standard deviations of the photosynthetic parameters obtained from the fitted light response curves of the specimens from Cabo de Gata and the Tabernas Desert according to the temperature measured. The letters [a][b][c][d][e] and grey highlight indicate significant differences between habitats for p-value < 0.05.

Parameter	Units	5ºC		10ºC		15ºC	
		Coast	Desert	Coast	Desert	Coast	Desert
DRopt	$\mu mol\ CO_2\ m^{-2}\ s^{-1}$	-0.66 ± 0.39 [a]	-0.39 ± 0.09 [a]	-0.84 ± 0.53	-0.51 ± 0.21	-1.11 ± 0.64	-0.86 ± 0.27
NP_{1500}		2.15 ± 0.87	2.26 ± 0.56	2.51 ± 0.31 [d]	3.42 ± 0.79 [d]	3.73 ± 0.95	3.77 ± 0.74
GB		2.81 ± 1.22	2.66 ± 0.57	3.35 ± 0.64	3.93 ± 0.91	4.84 ± 1.49	4.63 ± 0.91
Photosynthetic efficiency	Adimensional	5.9 ± 1.4 [b]	6.1 ± 2.1 [b]	6.9 ± 3.5 [e]	7.7 ± 5 [e]	3.8 ± 2.7	4.9 ± 1.2
Φ	$mol\ CO_2\ mol^{-1}\ quanta$	0.0135 ± 0.0042	0.0125 ± 0.0027	0.0150 ± 0.0035	0.0142 ± 0.0037	0.0174 ± 0.0051	0.0167 ± 0.0040
LSP	$\mu mols\ photons\ m^{-2}\ s^{-1}$	709 ± 180	710 ± 155	810 ± 167	920 ± 124	981 ± 242	967 ± 161
LCP		48 ± 21 [c]	32 ± 10 [c]	56 ± 33	36 ± 11	63 ± 29	53 ± 16

3.2. Molecular studies of the mycobiont

3.2.1   Genetic diversity and haplotype networks of the mycobiont

We generated 44 sequences for both nrITS, and *MCM7*, and 43 sequences for *β-tubulin* with lengths of 503, 592, and 442 bp, respectively, after editing and trimming each alignment (Table S9 and S10). The genetic diversity estimators of each marker showed higher values of number of singleton variable sites, and number of polymorphic sites for nrITS. However, *β-tubulin* showed higher number of haplotypes, average number of nucleotide differences and nucleotide diversity. Finally, *MCM7* showed higher values for the parsimony informative sites and haplotype diversity (Table S9 and S10). On the other hand, the coastal habitat showed notably higher values for all genetic diversity estimators, with higher number of polymorphic mutations for *β-tubulin* and *MCM7* (Table 9 and 10).

The primers used for nrITS amplification allowed us to reveal the presence of two different introns in the small subunit ribosomal RNA (18S). They were found in both *Xanthoparmelia* species, without any correspondence to one or another.

The haplotype networks resulted in 10, 12 and 9 haplotypes for nrITS, *β-tubulin* and *MCM7*, respectively (Fig. 3; Table S9). In general, the vast majority of haplotypes were separated by only one mutation, whereas only a few haplotypes of nrITS and *β-tubulin* were differentiated by up to four mutations (Fig. 3b). For all three markers, both habitats shared at least one haplotype, which coincided with the predominant haplotype in every network (Fig. 3, Fig. S5).
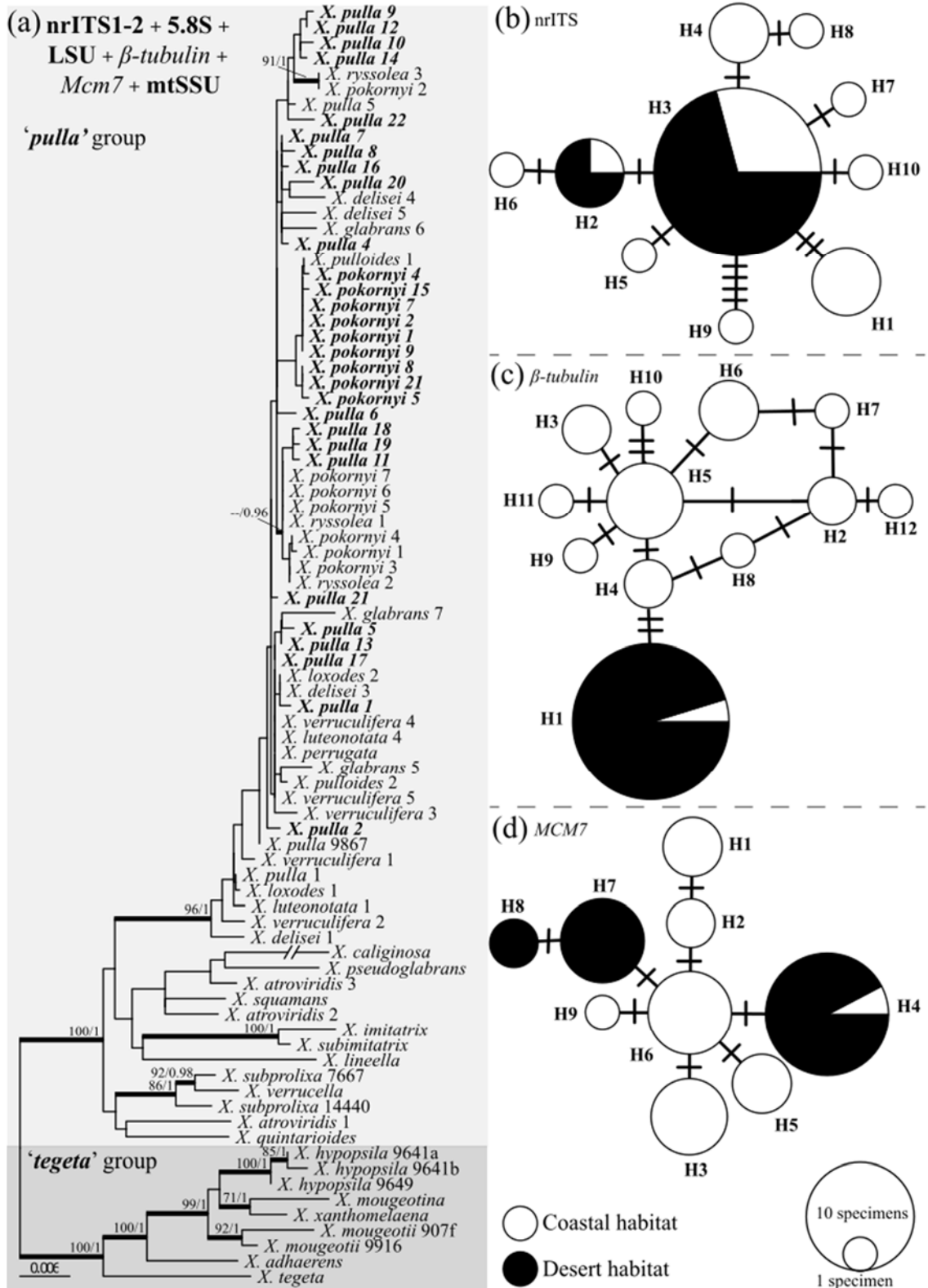
(a) **nrITS1-2 + 5.8S + LSU + *β-tubulin* + *Mcm7* + mtSSU**

'*pulla*' group

'*tegeta*' group

(b) nrITS

(c) *β-tubulin*

(d) *MCM7*

○ Coastal habitat
● Desert habitat

10 specimens

1 specimen

Fig. 3 *Left panel:* (a) Maximum Likelihood consensus tree showing phylogenetic relationships of *Xanthoparmelia 'pulla'* and *'tegeta* group' based on six markers (nrITS, LSU, *ß-tubulin*, *MCM7*, mtSSU). Branches and labels in bold indicate bootstrap statistical support values greater than 70%, and new sequences generated in this study, respectively. *Right panel:* Statistical parsimony networks for haplotypes of the (b) nrITS, (c) *ß-tubulin*, and (d) *MCM7*. The size of the circles in the networks is proportional to the numbers of individuals bearing the haplotype. Mutations are shown as hatch marks.

3.2.2   Phylogenetic inference of the mycobiont

Single-gene phylogenies revealed non-monophyletic relationships for *X. pulla* and *X. pokornyi* (Fig. S5).

The RAxML multi-locus phylogeny based on the six-locus dataset had a lnL value of -7364.2646 (Fig. 3). The *Xanthoparmelia* '*pulla*' and '*tegeta*' groups were resolved as monophyletic (BS=100%; PP=1). Within the former clade, the samples of both habitats were intermixed with sequences of several species, including other specimens assigned to our focal species, forming a well-supported subclade (BS=96%; PP=1). Phylogenetic relationships within this subclade were in general equivocal, with some haplotypes showing a closer relationship with the species *X. pulloides*, *X. delisei*, *X. glabrans*, *X. verruculifera*, *X. ryssolea*, *X. luteonotata*, *X. perrugata,* and *X. loxodes* rather than to the remaining inferred *X. pulla* and *X. pokornyi* haplotypes.

3.2.3   Species delimitation analysis of the mycobiont

The results of the ABGD analysis estimated eight groups for *Xanthoparmelia 'pulla'* group. According to this species solution, the first group included the specimens corresponding to *X. pulla, X. pokornyi, X. pulloides, X. delisei, X. glabrans, X. verruculifera, X. ryssolea, X. luteonotata, X. perrugata, X. loxodes* could comprise a single species. The second group included *X. subproxila* and *X. verrucella*. The third group *X. atroviridis* and *X. squamans*. The forth group included *X. imitatrix* and *X. subimitatrix*. Finally, each one of the other four groups left corresponded to *X. caliginosa, X. pseudoglabrans, X. quintarioides*, and *X. lineella*, respectively.

The results of the GMYC analysis estimated five clusters for *Xanthoparmelia 'pulla'* group (Coefficient interval: 4-8 species, LR test = 0.01). The first and the third

groups of GMYC included the same species than the first and the third groups in ABGD, respectively. The second group included *X. lineella* and *X. quintarioides*. The forth group included *X. imitatrix, X. subimitatrix, X. subproxila* and *X. verrucella*. Finally, the fifth group included *X. caliginosa* and *X. pseudoglabrans.*

3.3. Metabarcoding, phylogenetic placement, and diversity of *Xanthoparmelia-association* OTUs

A total of 18.766.486 paired-end Illumina MiSeq reads for the first replicate and 19.394.654 for the second one were generated. From these, we removed 12.07% and 11.67% respectively from the total number of reads during the quality filtering step. After demultiplexing, 8.203.955 and 8.710.057 were retained for each replicate, respectively. Once replicates were merged and the percent of representation of each OTU for the population was checked, only 12 OTUs were retained representing a total of 9.281.273 reads. Of these twelve OTUs, 8 OTUs belonged to the genus *Trebouxia* (average OTU length: 225 bp; Table S11). The other OTUs represented three genera commonly associated with free-living soil microalgae or found in association with terricolous lichens of the genus *Stereocaulon*, such as *Vulcanochloris sp*. (Vančuroá et al. 2015), and of the genus *Psora*, *Placidium* and *Claviscidium*, such as *Mymercia sp*. (Moya et al. 2018).

Of the 8 *Trebouxia* OTUs, only OTU37 and OTU31 were identified using Blastn at the species rank as *T. arboricola* and *T. asymmetrica*, respectively. After ensuring that their nrITS secondary structures were distinct from one another (Fig. S6), we checked their phylogenetic placement (Fig. S7). Except for two *Trebouxi*a OTUs belonging to the S clade ('*simplex/jamesii* group') (OTU40 and OTU61), all remaining ones belonged to the A clade ('*arboricola* group').

Algal OTU abundances varied depending on the habitat. Despite of OTU1 being the predominant alga in both habitats, its relative abundance was lower at the coastal sites due to the presence of OTU2 and OTU5, which represented 13.88% and 3.98% of the total algal community reads, respectively (Fig. 4 and Fig. 5). The DeSeq analysis pointed these three OTUs as the only ones with significant relative abundance differences between habitats (Fig. S8). The less common OTUs represented only 0.22% of the overall algal abundance in the desert and 0.08% on the coast.
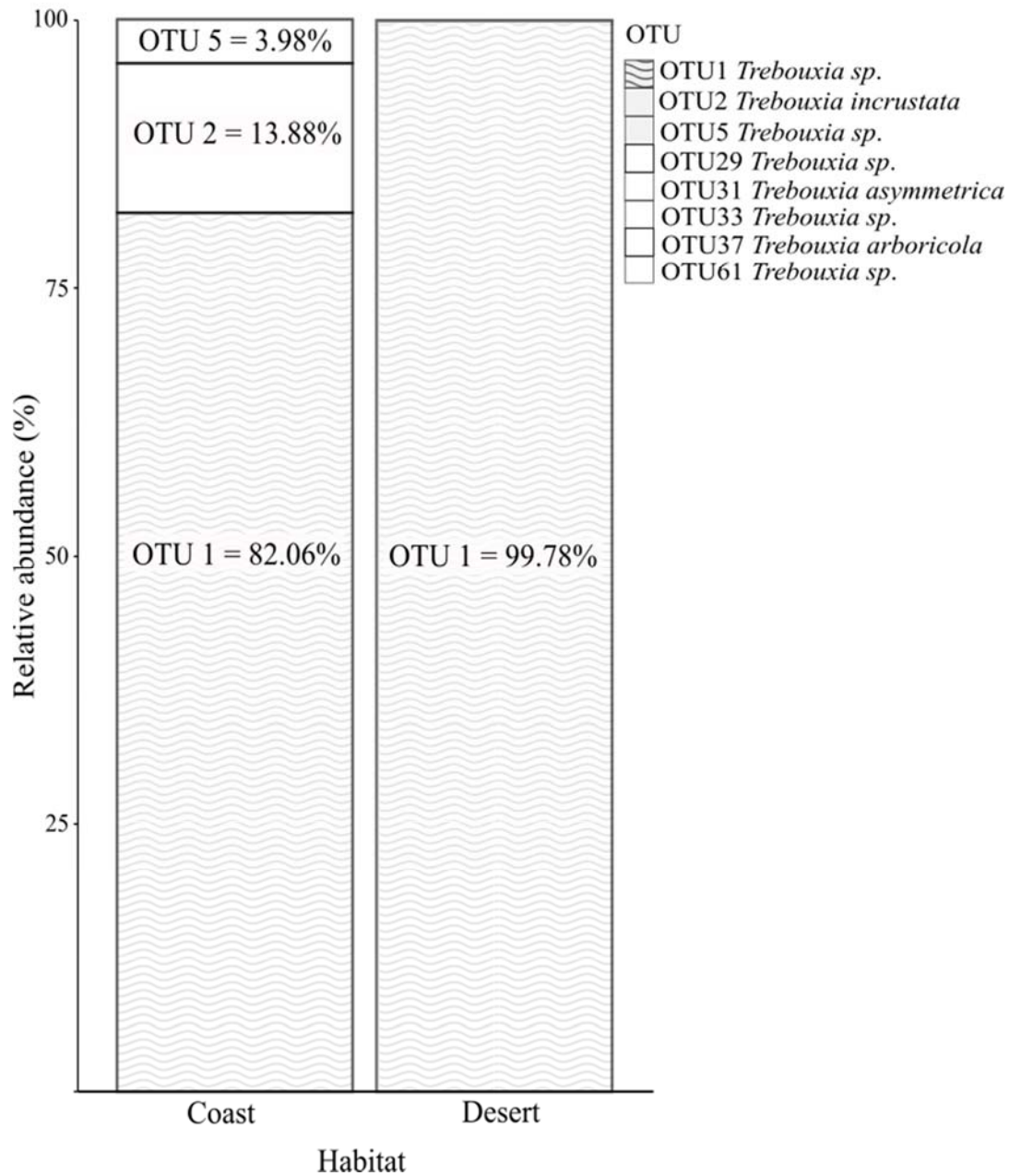
Fig. 4: Comparison of relative abundances within the *Trebouxia* OTU community in the Tabernas Desert and Cabo de Gata. The bar plot shows the most abundant OTUs for each habitat and their diversity The less frequent OTUs represented only 0.22 % of the total algal diversity in the desert and 0.08% in the coast.
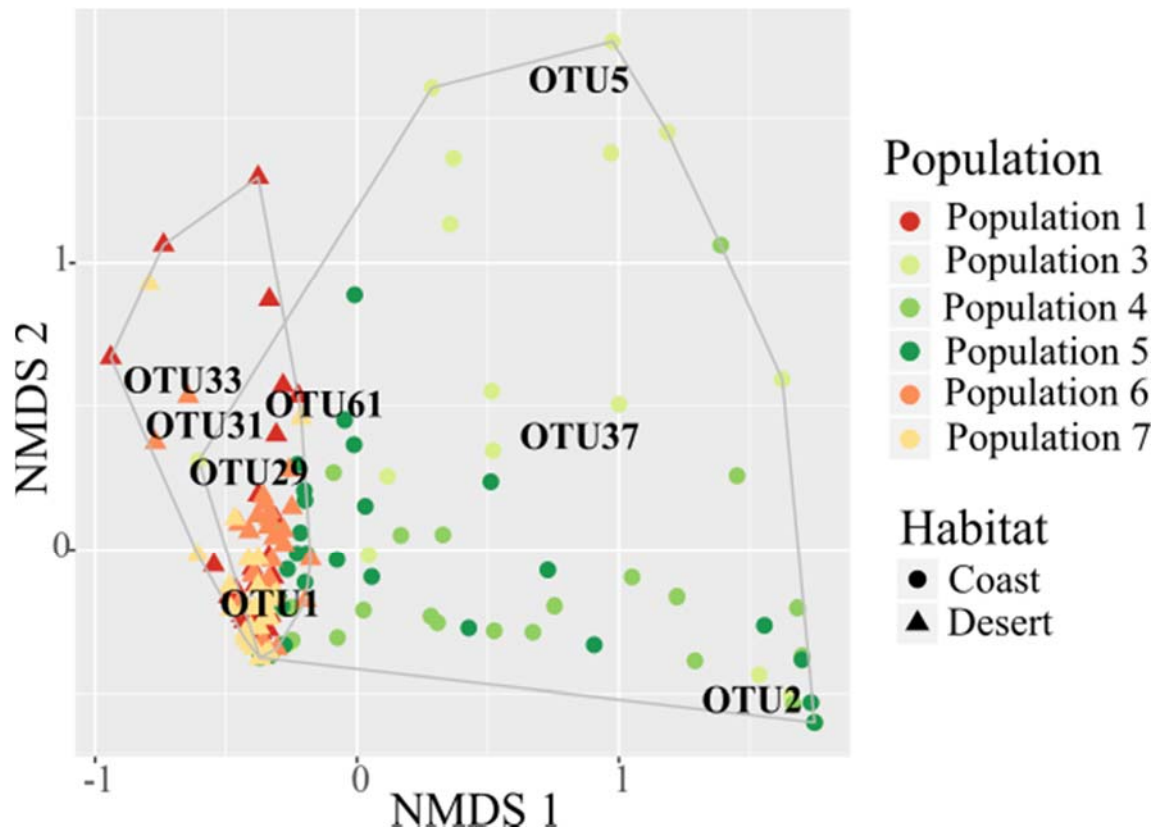
Fig. 5: Similarity of *Trebouxia* OTU community associated with the populations from Cabo de Gata and Tabernas Desert habitats. This is a non-metric multidimensional scaling (NMDS) ordination of *Trebouxia* OTUs based on their composition and abundances. A greater distance between two points (samples) indicates a lower similarity, whereas clustered points indicate samples with similar OTU composition and abundance. NMDS stress = 0.11.

Our findings indicated that several OTUs coexisted in the same lichen thallus. OTU1 is the only photobiont in 97.59% and 54.67% of the samples of the desert and the coast, respectively. In the rest of the cases there is at least one more photobiont (Table 3). The coexistence of two OTUs represented 1.27% in the desert and 10.67% on the coast of the total samples collected (Table 3).

Table 3: Predominant OTU found in specimens from Cabo de Gata and the Tabernas Desert. We considered that there was one predominant OTU per thallus when the OTU's abundance was greater than 90%; there was at least one additional photobiont when the primary photobiont was between 80-90%, and more than two photobionts when the predominant OTU was less than 80%. The number and proportion of OTUs found in each habitat are detailed in the table.

Nº of photobionts	OTU	Nº samples	OTU abundance in each habitat (%)	Total OTU abundance (%)
Saxicolous and foliose species from the coast				
Predominant OTU	OTU 1	41	54.67%	25.95%
	OTU5	17	22.67%	10.76%
At least one additional photobiont	OTU1 + (OTU5 or OTU2)	9	12.00%	5.70%
Two photobionts	OTU1 + (OTU5 or OTU2)	8	10.67%	5.06%
TOTAL			**100 %**	**52.53%**
Terricolous and sub-fruticose species from the desert				
Predominant OTU	OTU 1	81	97.59%	51.27%
At least one additional photobiont	OTU1 + (OTU 31 or OTU29)	2	2.41%	1.27%
TOTAL			**100 %**	**47.47%**

3.4.Predictors of the lichen-associated algal communities

Climatic conditions-. Climatic conditions on the coast were significantly correlated with OTU2. The negative relationship in the Kendall correlation analysis showed that the climate conditions on the coast decrease the abundance of OTU2 (Fig. 6). In the desert, correlation coefficients are close to zero, showing no-influence of climate on OTU abundance.

Host genetic diversity-. We found five fungal haplotypes in total. The coastal habitat included all fungal haplotypes while the desert only had three of them (f0, f1, and f4). No specific interaction was found between host genetic groups, algal OTUs and habitat (Fig. S3).

Physiological performance-. Physiological performance on the coast were significantly correlated with OTU2. The negative relationship in the Kendall correlation analysis suggested that an increase in OTU2 abundance reduces the physiological efficiency in specimens from the coastal sites. Contrary, and despite of OTU1 was not significant, the positive correlation found may point that OTU1 enhance the physiological performance of the specimens from the coast. No significant relationships were found between OTU abundance and physiological performance in the desert (Fig. 6).
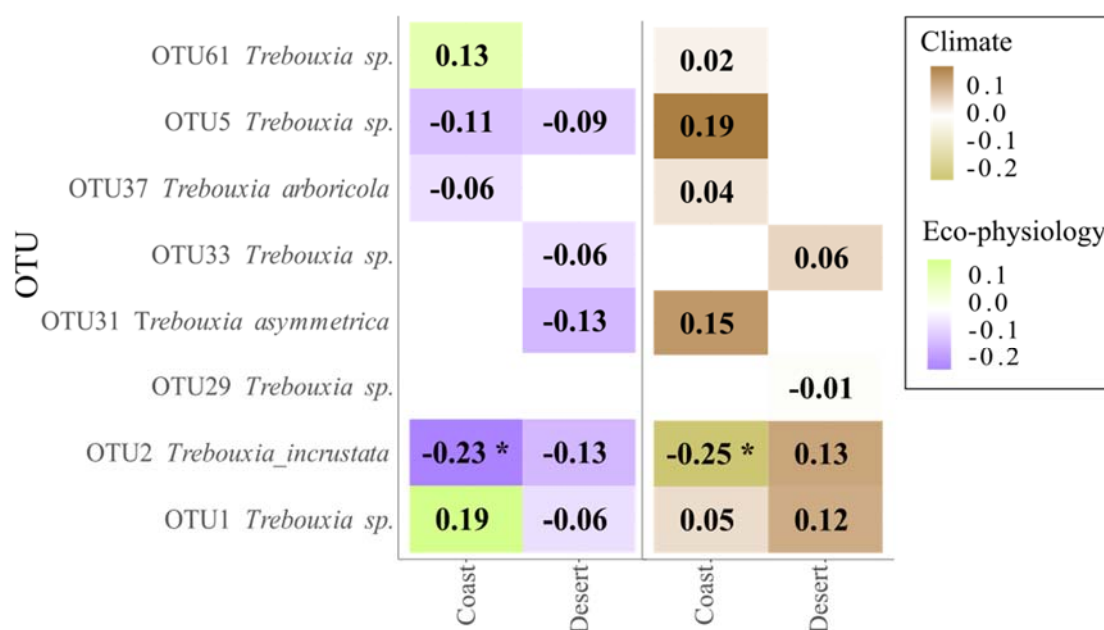

Fig. 6: Kendall rank correlation between the *Trebouxia* OTU abundances and the eco-physiological (purple/green gradient) and the climatic (brown gradient) predictors. The figure shows the correlation obtained, their direction and their statistically significance with a p-value < 0.05 (*).

4. Discussion

Possible overestimation of the number of species in the Xanthoparmelia *'pulla group'*

The species delimitation analysis and the multi-locus phylogenetic inference place in the same group all specimens of the *Xanthoparmelia 'pulla* group' identified as *X. pulla, X. pokornyi, X. pulloides, X. delisei, X. glabrans, X. verruculifera, X. ryssolea, X. luteonotata, X. perrugata, X. loxodes.* This finding suggests that *X. pokornyi* and *X. pulla* may be conspecific (Fig. 3), which support the hypothesis of Levitt et al. (2011b) about the potential overestimation of the number of species included in *Xanthoparmelia 'pulla* group'.

Furthermore, the absence of monophyletic groups and the high number of polytomies found in the phylogenetic inferences point out the remarkable genetic similarity of the mycobionts (Fig. 3, Fig. S5). Hence, *X. pokornyi* and *X. pulla* may not represent distinct evolutionary units, being a case in which the traditional methods for species identification may have tended to obscure the recognition of their natural lineages (Pino-Bodas et al., 2011; Printzen et al., 2013). Nevertheless, more experiments are needed to corroborate whether *X. pokornyi* and *X. pulla* belong to a unique species.

The high genetic diversity found in the coastal populations (Fig. 3 and 5) may be related to the species' potential for colonizing new habitats (Osyczka et al., 2014). In fact, this higher diversity may be the consequence of substrate switching, which would promote populations' isolation and, consequently, diversification (Brodo, 1973). Also, the presence of two different introns may be related to the findings of Gutiérrez et al. (2007), who analyzed species of *Parmeliacea* family in different countries. They concluded that the gain and loss of introns may be explained by the transition between different environments at high geographic scale.

Growth form and/or substrate switching lead to physiological convergence as a response to local environmental conditions.

Physiological convergence between species is supported by the low statistically significant differences found in the eco-physiological analysis (Table 2). However, they maintain different local adaptations to low temperatures (Lange and Green, 2005).

Quick recovery of CO_2 exchange has been found in species from drylands due to the frequent and severe drying (e.g. Kappen et al., 1979, Lange et al., 1990, 1996). The similarity of the desiccation response curves between habitats (Table 1) may point out that species are under similar dry-wet cycles. According to Schlensog et al. (2004), the

length and stability of the active period (95-114 minutes in our model species) are inversely related to the recovery speed (27-35 minutes in our species model, in concordance with Csintalan et al., 1998). This similarity in the desiccation curves leads to similar carbon fixation (Table 1).

Specimens from both habitats showed a typical saturation-type light response, which corresponds to 'sun-plant' characteristics (Lange, 2001; Fig. 2). They maintain similar LSP and LCP (Table 2), indicating that they are probably under the same solar radiation (Green et al., 2008). This is corroborated by the quantum yield of photosynthesis, exhibiting also similar efficiency in quanta absorption (Table 2; Pintado et al., 2005). Nevertheless, when temperatures get lower, the photosynthetic efficiency is more favorable for the desert specimens than for the coastal ones due to their reduction in the respiration rates (Table 2; Raggio et al., 2018). Additionally, the NP_{1500} found at 10°C is higher in the desert, making photosynthetic efficiency even more favourable for the specimens from this habitat (Fig. 2). A similar pattern was found in the terricolous lichen *Seirophora lacunosa* from the Tabernas Desert and *Ramalina bourgeana* from Cabo de Gata (Del Prado and Sancho, 2000). This pattern corresponds to an adaptation of the desert population to low temperatures (Lange et al., 1997, Lange, 2003; Pintado et al., 2010). In fact, species typical from arid and semi-arid deserts may maintain high net photosynthesis down to 2°C, while their optimal range is between 10 and 28°C (Lange, 2001). This is due to the fact that, when lichens are metabolically active, thallus temperatures are much lower than air temperatures because of the evaporative cooling and the low irradiance during - and briefly after - rainfall or early morning dew (Lange, 2001).

Hence, the photosynthetic convergence may be related to differences in growth form and/or substrate (Paoli et al., 2017). These factors highly affect water use efficiency (Rundel, 1978; Souza-Egipsy et al., 2000; Table 1), as occur in *Cetrariella delisei* which is able to colonize different substrates with no significant differences in water content (Inoue et al., 2014).

Microclimatic differences among habitats may be compensated by different substrate colonization (Pharo and Beattie, 2002). For instance, rock calcium content and atmospheric humidity seem to be the main drivers to explain the *Xanthoparmelia* species distribution (Rizzi and Giordani, 2012). According to that, the saxicolous specimens from the coast are subjected to higher relative humidity (Souza-Egipsy and Sancho, 2001), less evapotranspiration (Chamizo et al., 2015), and higher microclimatic temperature (Souza-

Egipsy and Sancho, 2001) than the desert ones. These particular local conditions explain, thus, (i) the higher photosynthetic efficiency in the desert specimens at all temperatures measured (Fig. 2 and Table 2), and (ii) the absence of habitat-specific responses at 15ºC, which is justified by the fact that temperatures beyond that threshold normally induce metabolic deactivation through desiccation in that semi-arid region (Fig. 2 and Table 2; Green et al., 2008; Raggio et al., 2014).

Similar photobiont community composition in both species, low host specificity between
bionts and complementarity eco-physiological responses of the coastal photobiont/s.

Photobiont diversity in both species was low and dominated by the same *Trebouxia* species (OTU1; Fig. 4). The vast majority of the thalli comprised a single algal OTU, which corroborates the hypothesis by Paul et al. (2018) that there is generally a single and predominant photobiont in each lichen thallus. The similarity of the photobiont composition between thalli with different morphology clearly excludes the role of the algal community in driving morphological differentiation in the lichen thallus. Furthermore, due to the high number of mycobionts sharing a common green algae partner, the role of the photobiont identity as a functional trait to explain differences between species along aridity gradients seems to not be enough by itself (Matos et al., 2015).

The little differences in photobiont community composition found between both species are attributed to the presence of two additional photobionts in the coastal samples (OTU2 and OTU5, Table 3). The abundance of OTU2 seems to be limited by the environmental conditions of the coast (Fig. 6). However, no climatic effects were found neither for the most predominant OTU in both habitats (OTU1) nor for the desert habitat (Fig. 6). We may then hypothesize that the mycobiont associates with OTU1 because it may be the widest spread algae in this habitat. Interestingly, OTU2 displayed lower physiological efficiency than OTU1 in the coastal sites (Fig. 6). This complementarity eco-physiological response is in accordance with the reports by Casano et al. (2011). However, more replicates are necessary to confirm these initial findings and understand how the variation in OTU1 and OTU2 composition affect the physiological responses.

The low specificity found in the mycobiont-photobiont interactions fits well to the general pattern proposed by Leavitt et al. (2015) for the genus *Xanthoparmelia*. Moreover, Leavitt et al. (2015) also suggested that photobiont plurality is more common in taxa with lower specificity, which is in agreement with our findings (Table 3). This

absence of specificity could be a successful advantage for the mycobiont, possibly facilitating its dispersal over a broader range of habitats (Muggia et al., 2014).

5. Conclusions

The high genetic similarity found in the mycobionts of *Xanthoparmelia pulla* and *X. pokornyi* suggests that these species may not represent distinct evolutionary units. Hence, variations in growth form allows these lichens to better adapt to the local environmental conditions in drylands. Furthermore, the low specificity between the symbionts, and the homogeneity in the predominant photobionts indicates that variation in growth form and/or substrate switching are crucial for explaining the physiological convergence found between species. Nevertheless, the desert populations showed a bit lower genetic diversity of the overall photobiont community, and better acclimation to low temperatures than the coastal ones. Moreover, specimens from the coast show a limitation in the abundance of OTU2 caused by the climate conditions of this region, and an apparent complementary eco-physiological response between the photobionts OTU1 and OTU2.

Chapter 3:

Climate change leads to higher NPP at the end of the century in the Antarctic Tundra: Response patterns through the lens of lichens

Abstract

Poikilohydric autotrophs are the main colonizers of the permanent ice-free areas in the Antarctic tundra biome. Global climate warming and the small human footprint in this ecosystem make it especially vulnerable to abrupt changes. Elucidating the effects of climate change on the Antarctic ecosystem is challenging because it mainly comprises poikilohydric species, which are greatly influenced by microtopographic factors. In the present study, we investigated the potential effects of climate change on the metabolic activity and net primary productivity (NPP) in the wide-spread lichen species *Usnea aurantiaco-atra* (Jacq.) Bory. Long-term monitoring of chlorophyll *a* fluorescence in the field was combined with photosynthetic performance measurements in laboratory experiments in order to establish daily response patterns under biotic and abiotic factors at micro- and macroscale. Our findings suggest that macroclimate is a poor predictor of NPP, thereby indicating that microclimate is the main driver due to the strong effects of microtopographic factors on cryptogams. Metabolic activity is also crucial for estimating the NPP, which is highly dependent on the type, distribution, and duration of the hydration sources available throughout the year. Under RCP 4.5 and RCP 8.5, metabolic activity will increase slightly compared with that at present due to the increased precipitation events predicted in MIROC5. Temperature is highlighted as the main driver for NPP projections, and thus climate warming will lead to an average increase in NPP of 167–171% at the end of the century. However, small changes in other drivers such as light and relative humidity may strongly modify the metabolic activity patterns of poikilohydric autotrophs, and thus their NPP. Species with similar physiological response ranges to the species investigated in the present study are expected to behave in a similar manner provided that liquid water is available.

Key words Net primary productivity (NPP), metabolic activity, macroclimate, microclimate, Model for Interdisciplinary Research on Climate 5 (MIROC5), poikilohydric autotrophs

1. Introduction

Since the second half of the 20th century, the Antarctic Peninsula has experienced among the fastest rates of regional warming throughout the world (Vaughan et al., 2003). In particular, temperatures have increased by 0.54 °C per decade since the 1950s, with initial warming by 0.32 °C per decade until 1997, followed by cooling at 0.47 °C per decade until 2014 (Turner et al., 2016; Oliva et al., 2017; Gonzalez and Fortuny, 2018). Therefore, there is a great concern about the implications of climate change for this biome and the vulnerability of the species that inhabit the area (Turner et al., 2005; Thomas et al., 2009; Sancho et al., 2017). Furthermore, the relative simplicity of this ecosystem (Convey, 2013) makes maritime Antarctica one of the most suitable areas for elucidating the potential effects of climate change.

The Antarctic terrestrial vegetation is assembled in extensive tufts over 0.3% of the permanent ice-free surface (Convey et al., 2020). The main components are lichens, which comprise 65% of the total species identified (Casanovas et al., 2015). The successful survival of this group is facilitated by their poikilohydric nature because their hydration status tends to be in equilibrium with the environment, where they are metabolically active when hydrated and dormant when dry. Dormancy constitutes an abiotic stress avoidance strategy that ensures the survival of these species (Green et al., 2018). This response trait (any trait that varies in response to changes in environmental conditions according to Violle et al., 2007) is widespread in various organisms, such as mosses, nematodes, tardigrades, rotifers, and collembolans (Convey et al., 2020).

Despite the large amount of fresh water present in Antarctica, it is biologically unavailable because it is in the form of ice. Therefore, the different available hydration sources and their regimes in Antarctica restrict the presence of poikilohydric autotrophs to habitats where water is useable (Pannewitz et al., 2003b). Liquid water is supplied in the forms of rainfall and meltwater (mostly during the austral summer; Kappen et al., 1995; Schlensog et al., 2013), but also from snowfall, permanent snow, and ice banks (Robinson et al., 2003), which might only be available during a few days or even weeks per year (Kennedy, 1993). Thus, refuges such as rock crevices or drainage basins are considered essential for providing protection against harsh conditions, including dehydration (Sadowsky et al., 2016), thereby highlighting the important effects of microclimate on terrestrial biota (Sancho et al., 2016).

Understanding the spatial and temporal variations in the Antarctic terrestrial ecosystem (Chown and Convey, 2007) requires investigations of the metabolic response

traits of poikilohydric autotrophs at different scales. At the spatial scale, Guglielmin et al. (2012) concluded that the effect of the air temperature on the soil surface temperature changes seasonally in maritime Antarctica. During the winter, its effect is drastically reduced because of the protection provided by snow cover. However, this cover melts during the summer and the air temperature has a greater impact on the soil surface temperature. Schroeter et al. (2010) observed that in spite of the 16 °C difference in mean air temperature between maritime and continental Antarctica, lichens were metabolically active at almost identical microclimatic temperatures (*ca.* 2 °C), thereby indicating convergence at a microclimatic scale. At the temporal scale, the opportunistic responses of poikilohydric autotrophs to transient periods of favorable microclimatic conditions have been demonstrated in several biomes, thereby highlighting the need for investigations at high temporal resolution (Insarov and Schroeter, 2002).

The activation of metabolism in poikilohydric autotrophs initiates processes such as photosynthesis that do not occur in a dormant state. Therefore, the duration of metabolic activity is essential for modeling the productivity of cryptogams (Schroeter et al., 2000). In maritime Antarctica, net primary productivity (NPP) is restricted to the four to six warmer months of the year (Block et al., 2009) when temperature and radiation are sufficiently high to allow the release of liquid water and promote carbon gain.

In the present study, we evaluated how the main abiotic factors in maritime Antarctica might modulate the metabolic activity and NPP in lichens in order to predict the effects of climate change. Assessing that is important for obtaining a better understanding of changes in the global carbon cycle because the contribution of poikilohydric autotrophs to the global NPP is estimated about 3.9 Pg C year^{-1} (7% of the NPP by terrestrial vegetation)(Elbert et al., 2012; Porada et al., 2013, 2014), from which 20% comes from biomes similar to maritime Antarctica, such as polar deserts and alpine tundra.

Hence, a long-term microclimate, macroclimate, and metabolic activity monitoring was conducted for *Usnea aurantiaco-atra* (Jacq.) Bory, which is one of the most common lichens in maritime Antarctica (Øvstedal and Smith, 2001). Modeling was performed to evaluate the effects of different regional (micro- and macroclimate) and temporal (intra- and interannual fluctuations) scales. In this study, we determined: (i) the interaction between photosynthetically active radiation (PAR), temperature, relative humidity (RH), and precipitation on the metabolic activity and NPP of lichens; (ii) the vulnerability of lichens to the climate change scenarios predicted by the

Intergovernmental Panel on Climate Change (IPCC); (iii) whether NPP could be predicted using macroclimate rather than microclimate; and (iv) whether NPP is overestimated if metabolic activity is not included in the models.

We hypothesized that NPP of lichens would increase under climate change scenarios due to global warming. This hypothesis was also suggested in previous studies, such as those by Smith (1999), Xiong et al. (2000), and Singh et al. (2018), based on experimental observations that the current temperature and PAR in maritime Antarctica do not allow many cryptogams to achieve their maximal net photosynthesis. The environmental conditions that these species experience are widely known as 'suboptimal conditions'.

2. Methods

2.1. Research site

The research site is located near the Juan Carlos I Spanish Antarctic Station in an ice-free area of South Bay, Livingston Island, South Shetland Islands, maritime Antarctica (62°39′46″S, 60°23′20′W). Most of Livingston Island is of volcanic origin but the study area comprises sedimentary rocks, with a sequence of shale and turbiditic deposits. Due to its location at the northernmost tip of the Antarctic Peninsula, the region is exposed to mild or cold air masses (Gonzalez and Fortuny, 2018). The effects of the sea and almost continuous cloud cover lead to small daily and annual temperature oscillations in maritime Antarctica (Bargagli, 2005). The temperature often remains close to the freezing point even during the winter (AEMET, 2019). The radiation also exhibits strong seasonal variations (AEMET, 2019).

2.2. Gas exchange analysis

Photosynthesis data for *U. aurantiaco-atra* were obtained from laboratory measurements by Kappen (1985) using an infrared gas analyzer (Binos, Firma Leybold Heraeus, Hanau). This system provides accurate interpretations of the effects of changing environmental conditions on gas exchange processes (Midgley et al., 1997). The system comprises temperature and humidity controlled Plexiglas cuvette, with fan-operated air circulation, and flow meters to maintain a constant airstream of $0.5\,l\,h^{-1}$ (Kappen, 1983). The response of the net photosynthesis (mg CO_2 gDW^{-1} h^{-1}) to incident light was determined at five light intensities (0, 50, 130, 290 and 470 µmol photons m^{-2} s^{-1}) and six different temperatures (−5, 0, 5, 10, 15, and 20 °C) at an air CO_2 content of 350 ppm.

86

Due to the minimum photosynthetic threshold detectable by the infrared gas analyzer, photosynthetic rates under -6 °C were set to zero. Previous field measurements of 0.008 mg CO_2 gDW^{-1} h^{-1} at -10 °C in Antarctica support this assumption (Kappen, 1989; Schroeter et al., 1995).

2.3.   Metabolic activity monitoring

We obtained long-term photosystem II activity measurements using a PAM monitoring system (MoniDA, Gademann Instruments, Germany). MoniDA is a non-invasive and automatic system that measures chlorophyll *a* fluorescence and reports it to a database via satellite or local networks (Murchie and Lawson, 2013; Raggio et al., 2016).

The MoniDA central unit recorded data from two probes placed close to the samples, which were on a rock colonized with lichens near Juan Carlos I Spanish Antarctic Station. Each probe contained a single optical fiber for fluorescence measurements, as well as microclimatic sensors for measuring PAR (μmol photons m^{-2} s^{-1}) and temperature (°C). The sensors were located *ca.* 3 mm from the *U. aurantiaco-atra* thalli, and metabolic activity and microclimatic data were recorded simultaneously at hourly intervals from January 2009 to December 2014. The activity or inactivity of the photosynthetic systems was determined using a saturation pulse method (Schreiber et al., 1986). Basal fluorescence (F) was measured by irradiating the samples with a low intensity-modulated light (0.025 μmol photons m^{-2} s^{-1}), which was sufficiently low to not induce electron transport through photosystem II but sufficiently high to obtain a minimum chlorophyll fluorescence value. The samples were then subjected to a saturating pulse of actinic light (for about 1 s at 4000 μmol photons m^{-2} s^{-1}) to induce a maximum fluorescence value (Fm′) and shut down the photosystem II reaction centers. The light absorbed by photosystem II (the effective photosynthetic yield of photosystem II or yield) was calculated as (Fm′ - F) / Fm′ (Schreiber and Bilger, 1993; Maxwell and Johnson, 2000; Fracheboud, 2004). Yield values of zero indicated inactivity of photosystem II, and thus the samples were considered to be metabolically inactive, whereas yields greater than zero indicated the activity of photosystem II (Raggio et al., 2014). The metabolic activity (%) was calculated on a daily basis as the number of records when the yield was greater than zero divided by the total number of records.

The harsh environmental conditions in Antarctica resulted in several gaps in our dataset, and thus, made it necessary to check and validate the measurements. As a

consequence, the measurement period used for this study was a 41-month period comprising valid data from January 2009 to July 2011, and from February 2014 to December 2014. The total dataset included 58.010 hourly records, which correspond to one of the longest field dataset for Antarctica.

2.4. Climate data

2.4.1. Macroclimate

Macroclimatic data at hourly intervals were obtained from the Spanish Meteorological Agency (AEMET; https://antartida.aemet.es/). The automatic weather station (Campbell CR 1000) was located in an open area about 500 m from the study area (AEMET, 2019).

Mean air temperature (°C), solar radiation (W m^{-2}), precipitation (mm), and relative humidity (%) data were downloaded for two different time periods at hourly intervals: (i) from 2000 to 2009 corresponding to the same time period as the Historical scenario, and (ii) from 2009 to 2014 corresponding to the same time period as the long-term chlorophyll *a* fluorescence measurements.

According to the conversion method described by Sager and Mc Farlane (1997), solar radiation in W m^{-2} was transformed into PAR in μmol photons m^{-2} s^{-1} assuming that 50% of the total incident solar energy was PAR (Papaioannou et al., 1993).

2.4.2. Global climate model

Model for Interdisciplinary Research on Climate 5 (MIROC5; Watanabe et al., 2010) is a coupled general circulation model (CGCM) developed for the fifth phase of the Coupled Model Intercomparison Project (CMIP5) used in the IPCC Fifth Assessment Report (AR5). The projections were generated using climate forcing data derived from the first ensemble member (r1i1p1). Data are publicly available from the Earth System Grid Federation website (https://esgf-node.llnl.gov/projects/cmip5/). Near surface mean air temperature (K), mean surface downwelling shortwave radiation in the air (W m^{-2}), precipitation (mm), and near-surface relative humidity (%) data were all downloaded with daily resolution (the maximum resolution available). Climate change scenarios were designed to operate at decade scales in order to increase their robustness (Flato et al., 2013).

Two representative concentration pathways (RCP 4.5 and RCP 8.5; Collins et al., 2013) were selected for the middle (years 2040 to 2049) and end of the century (years

2090 to 2099). RCP 4.5 describes a global scenario where carbon emissions increase and stabilize at 538 ppm CO_2 before the year 2100, temperature increases by 1.1 °C to 2.6 °C, and radiative forcing reaches 4.5 W m^{-2}. RCP 8.5 is the most aggressive global scenario and it is characterized by greenhouse gas emissions increasing to 936 ppm by the year 2100, temperature increasing by 2.6 °C to 4.8 °C, and radiative forcing of 8.5 W m^{-2}. The Historical scenario from 2000 to 2009 was also considered in order to compare the climate change simulations with the real macroclimatic conditions.

2.4.3. Statistical scaling

In order to correct the bias related to climate change scenarios (Historical scenario, RCP 4.5, and RCP 8.5), the delta change method was applied to the following predictors: PAR, relative humidity, and temperature (Maraun, 2016; Fang et al., 2015). Therefore, the 'deltas' (anomalies) were calculated as the differences between the simulated Historical scenario and the real macroclimatic conditions from 2000 to 2009 for each variable and on a daily basis. Absolute differences were used for temperatures and relative changes for precipitation (Navarro-Racines et al., 2020). The delta changes were then subtracted from the RCPs and the Historical scenario.

Downscaling of the climate change scenarios to microclimate was then also performed using the delta change method for PAR and temperature at daily intervals (Navarro-Racines et al., 2020; Hülber et al., 2016). The delta changes were calculated as the differences between the real macroclimatic conditions from 2009 to 2014 and the microclimatic measurements in the same time period, which were then subtracted from the climate change scenarios.

The precipitation rates obtained from simulated climate change scenarios are still controversial, which is one of the main weaknesses of these models (Turner et al., 2007). Therefore, in order to reduce the dependence of the model on precipitation rates and analyze how metabolic activation changed under different hydration sources, precipitation was represented as a categorical factor with three levels: 'rainfall', 'snowfall', and 'non-precipitation events'. 'Rainfall' was defined as records of precipitation occurring at temperatures at or above 0 °C. 'Snowfall' was defined as records of precipitation occurring at temperatures below 0 °C (Marks et al., 2013). 'Non-precipitation events' were defined as periods when no precipitation occurred but the species was active. These categorical factors allowed us to test how different forms of

precipitation were distributed throughout the year but without altering the total annual precipitation, and the roles of rainfall and snowfall as metabolic activation triggers.

2.5.   Generalized additive model (GAM)

GAM was used to model nonlinear trends in the time series, such as seasonal or within year variation. We performed three sequential GAM analyses to investigate how macro- and microclimatic patterns might affect the relationship between metabolic activity and NPP. The GAMs were implemented using the *mgcv* package in R (Wood, 2019). A cubic spline smoothing function was used for each predictor and for the tensor product of the interaction effects between predictors. In both cases, the *k*-dimensions were optimized by cross validation. Stepwise model selection was used to select the predictors to retain in the model according to the best deviance reduction (Akaike information criterion). GAM multi-dimensional smoothing effects plots were visualized using *mgcViz* (Fasiolo et al., 2020). A p-value < 0.05 was considered as the minimum level of significance.

The first GAM (GAM 1; Fig. S1) modeled the response pattern of the net photosynthesis relative to temperature and PAR under laboratory conditions. This response pattern was used to estimate the NPP on the long-term monitoring dataset from 2009 to 2014. NPP was estimated at two different geographic scales (micro- and macroclimate). Moreover, the effect of metabolic activity as a biotic driver was evaluated at each geographic scale. To evaluate it, two different situations were modeled: (i) considering only the periods of time when the lichen was metabolically active, and (ii) assuming that the lichen was always active. The long-term monitoring dataset at hourly intervals was divided into four different datasets for the analysis (Table 1). The response variable for each dataset was the net photosynthetic rate. The smoothing terms were temperature (k = 9), and PAR (k = 9). The tensor product was the two-way interaction between temperature and PAR (k = 27).

Table 1 Summary of the datasets used to model the daily net primary productivity (NPP) of *U. aurantiaco-atra* at Livingston Island (maritime Antarctica) from 2009 to 2014.

Datasets	Climatic conditions	Metabolic activity	Output matrix
Dataset 1	Microclimate	Included	Microclimatic PAR and temperature, metabolic activity and the associated net photosynthetic rate.
Dataset 2	Microclimate	It was assumed that lichens were always active	Microclimatic PAR and temperature, and the associated net photosynthetic rate.
Dataset 3	Macroclimate	Included	Macroclimatic PAR and temperature, metabolic activity and the associated net photosynthetic rate.
Dataset 4	Macroclimate	It was assumed that lichens were always active	Macroclimatic PAR and temperature, and the associated net photosynthetic rate.

A second GAM (GAM 2) was performed in order: (i) to determine how the main macroclimatic factors influenced the daily metabolic activity pattern from 2009 to 2014, and (ii) to predict the metabolic activity for RCP 4.5 and RCP 8.5 in the middle and at the end of the century. The response variable was metabolic activity. The smoothing terms were macroclimatic temperature (k = 9), macroclimatic PAR (k = 9), macroclimatic relative humidity (k = 9), and precipitation (k = 3, using 'fs' as a penalized smoothing basis). The tensor product was the three-way interaction between temperature, PAR, and relative humidity according to each precipitation category ('rainfall', 'snowfall', and 'non-precipitation events', k = 124).

A third GAM was required (GAM 3) due to the temporal mismatch between the long-term monitoring data from 2009 to 2014 (at hourly intervals) and the RCP simulations (at daily intervals). This model allowed us: (i) to determine how the main

microclimatic drivers and metabolic activity influenced the daily NPP; and (ii) to predict the NPP based on RCP 4.5 and RCP 8.5. In the analysis, the microclimatic temperature, microclimatic PAR, and metabolic activity were averaged, and the NPP was summed. The response variable was daily NPP. The smoothing terms were the microclimatic temperature (k = 9), microclimatic PAR (k = 9), and metabolic activity (k = 9). The tensor product was the three-way interaction between temperature, PAR, and metabolic activity (k = 103).

3.   RESULTS

3.1.   Climate conditions from 2009 to 2014

The microclimatic and macroclimatic data are presented in Table 2. On average, the microclimatic temperature was 0.9 °C higher than the air temperature (Table 2; Fig. S2a). Among the total microclimatic and macroclimatic temperature records, 7.3% and 10.3% were lower than -6 °C, respectively. Complete darkness occurred in 57% of the total microclimatic PAR records (Table 2). The average annual mean microclimatic PAR was 155 µmol photons m^{-2} s^{-1} lower than the average macroclimatic PAR (Table 2 and Fig. S2b). This difference was higher from November to March when it reached 240 µmol photons m^{-2} s^{-1}.

The mean annual precipitation was 373 mm, with larger amounts in the summer months (Fig. S2d).

Table 2 Summary of the microclimatic and macroclimatic conditions measured from 2009 to 2014 at Livingston Island (maritime Antarctica). The 25%, 50% and 75% quantiles are represented as $Q_{25\%}$, $Q_{50\%}$ and $Q_{75\%}$, respectively.

	MICROCLIMATE		MACROCLIMATE		
	Temperature (ºC)	PAR (μmol photons m^{-2} s^{-1})	Temperature (ºC)	PAR (μmol photons m^{-2} s^{-1})	RH (%)
Mean ± Standard deviation	-0.3 ± 3.9	30 ± 106	-1.2 ± 3.6	185 ± 339	82 ± 10
Minimum	-14.9	0	-17.4	0	32
$Q_{25\%}$	-2.9	0	-3.2	6	75
$Q_{50\%}$	-0.2	0	-0.6	16	84
$Q_{75\%}$	2.4	15	1.3	212	91
Maximum	23.4	2065	9.4	2961	100

3.2. NPP from 2009 to 2014

The NPP estimates based on microclimate and considering when the lichen was metabolically active ('Dataset 1' in Table 1) exhibited a similar annual pattern for the four years monitored from 2009 to 2014 (Fig. 1).

The mean daily NPP (± standard deviation) was 0.25 ± 0.09 mg CO_2 gDW^{-1} day^{-1}. The mean NPP during the warmest months from November to March was 0.7 ± 0.2 CO_2 gDW^{-1} day^{-1}, and -0.08 ± 0.07 mg CO_2 gDW^{-1} day^{-1} during the coldest months from April to October (Fig. 1).

The mean monthly NPP was positive during the warmest months and negative during the coldest months (Fig. 1), thereby indicating carbon gain and loss, respectively. The highest NPP occurred in February 2014 (42.7 mg CO_2 gDW^{-1} $month^{-1}$) and the lowest in July 2014 (-15 mg CO_2 gDW^{-1} $month^{-1}$) (Fig. 1).

The mean annual NPP over the 42-month period was 92.2 mg CO_2 gDW^{-1} $year^{-1}$. The mean NPP was 366.3 mg CO_2 gDW^{-1} in the warmest months and -61.1 CO_2 gDW^{-1} in the coldest months.
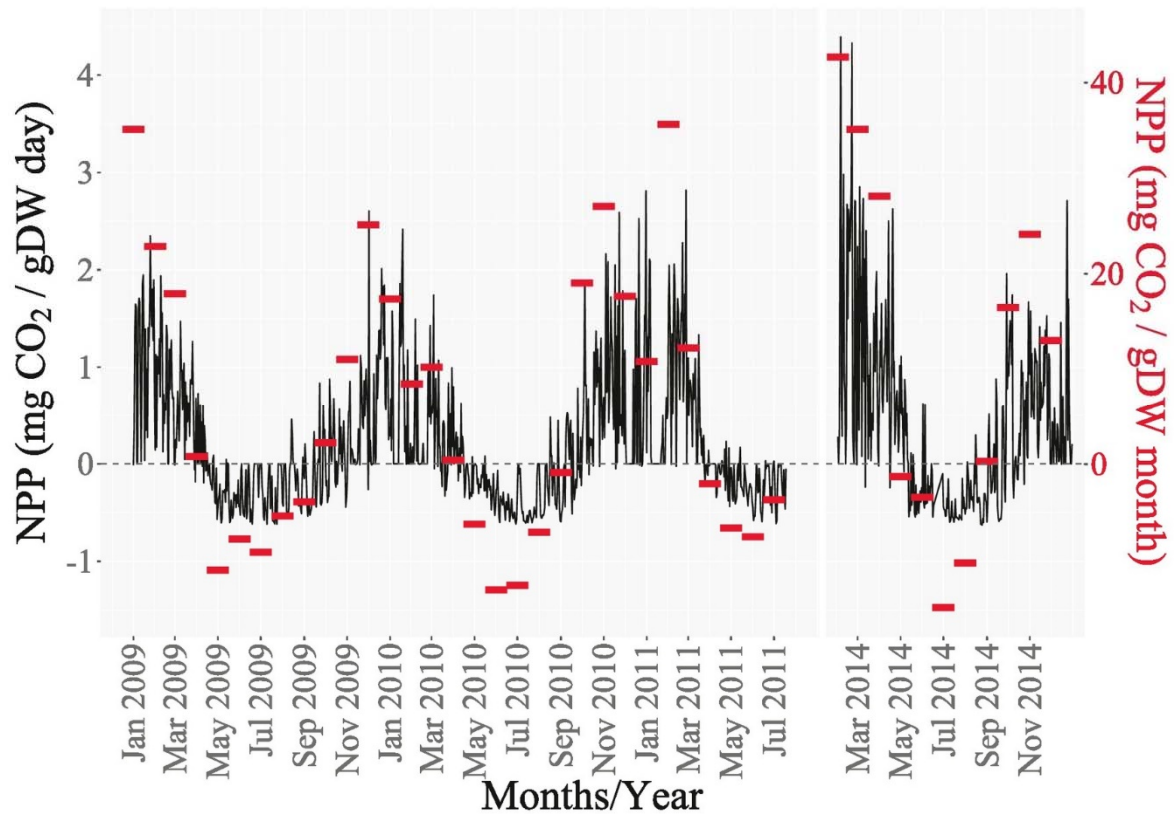
Fig. 1 Net primary productivity (NPP) from 2009 to 2014 of *U. aurantiaco-atra* at maritime Antarctica at daily (black lines) and monthly (red horizontal lines) intervals. The NPP estimations were based on microclimate and considering only the periods when the species was metabolically active. Negative values represent carbon losses and positive values represent carbon gains.

Compared with the NPP modeling results based on microclimate and metabolic activity as main drivers ('Dataset 1' in Table 1), the other three datasets employed to estimate the NPP ('Dataset 2', 'Dataset 3', and 'Dataset 4' in Table 1) obtained the following overestimates (Fig. 2): (i) the NPP estimates based on microclimate and assuming that the species was always metabolically active were overestimated by 3.8 times, reaching 356.2 mg CO_2 gDW^{-1} $year^{-1}$; (ii) the NPP estimates based on macroclimate and including the metabolic activity were overestimated by 4.4 times, reaching 409 mg CO_2 gDW^{-1} $year^{-1}$; and (iii) the NPP estimates based on macroclimate and assuming that the species was always metabolically active were overestimated 9.8 times, reaching 906.6 mg CO_2 gDW^{-1} $year^{-1}$.

Comparison of NPP estimates obtained at micro- and macroscale showed that the monthly NPP values based on macroclimate were positive for all months throughout the

year, whereas those based on microclimate were negative from May to October (Fig. 2). The NPP estimates were higher when the model was based on macroclimatic data.
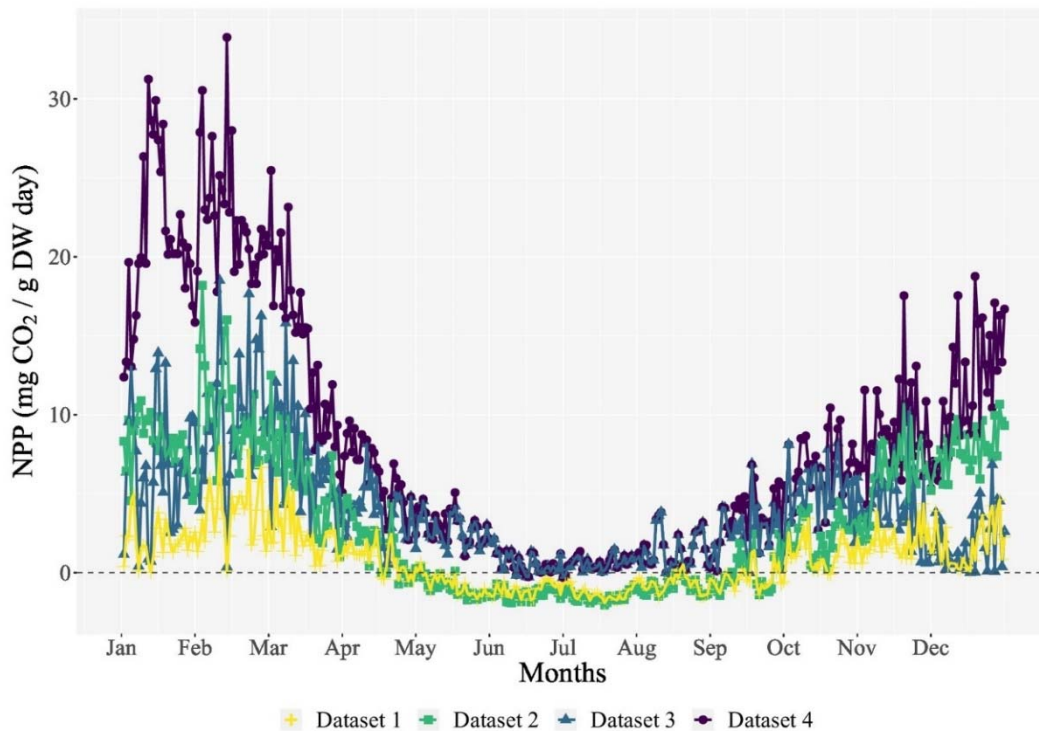
Fig. 2 Daily net primary productivity (NPP) of *U. aurantiaco-atra* at maritime Antarctica as the mean from 2009 to 2014. The NPP estimations were based on microclimate and considering only the periods when the species was metabolically active ('Dataset 1'); on microclimate but assuming that the species was always active ('Dataset 2'); on macroclimate and considering only the periods when the species was metabolically active ('Dataset 3'); and on macroclimate but assuming that the species was always active ('Dataset 4'). Negative values represent carbon losses and positive values represent carbon gains.

The response pattern of the NPP was analyzed with GAM 3, where the model had an R^2 value of 0.89 and it explained 90% of the total deviance. The significant variables according to GAM 3 are shown in Table 3. The graphic output of the model shown in Fig. 3 illustrates how the NPP changed according to both the abiotic factors and metabolic activity. The most important results in Fig. 3 are as follows: (i) temperature was a crucial driver when the species was metabolically active for long periods of time; and (ii) during shorter metabolic activity periods, higher PAR values and lower temperatures were required to maximize the NPP (Fig. 3 and Table 3).

Table 3: Significance of the smoothing terms obtained from the generalized additive model (GAM 3), in which the effect of microclimate and metabolic activity on the daily net primary productivity (NPP) of *U. aurantiaco-atra* at Livingston Island (maritime Antarctica) from 2009 to 2014 is evaluated. The edf corresponds to the estimated degrees of freedom. P-value < 0.05 is considered as the minimum level of significance.

Smoothing terms	edf	F-test	p-value
s(PAR)	6.93	0.27	0.969
s(Temperature)	6.23	25.7	< 2e-16
s(Metabolic activity)	1	0.69	0.407
s(PAR, Metabolic activity, Temperature)	87.8	29.1	< 2e-16
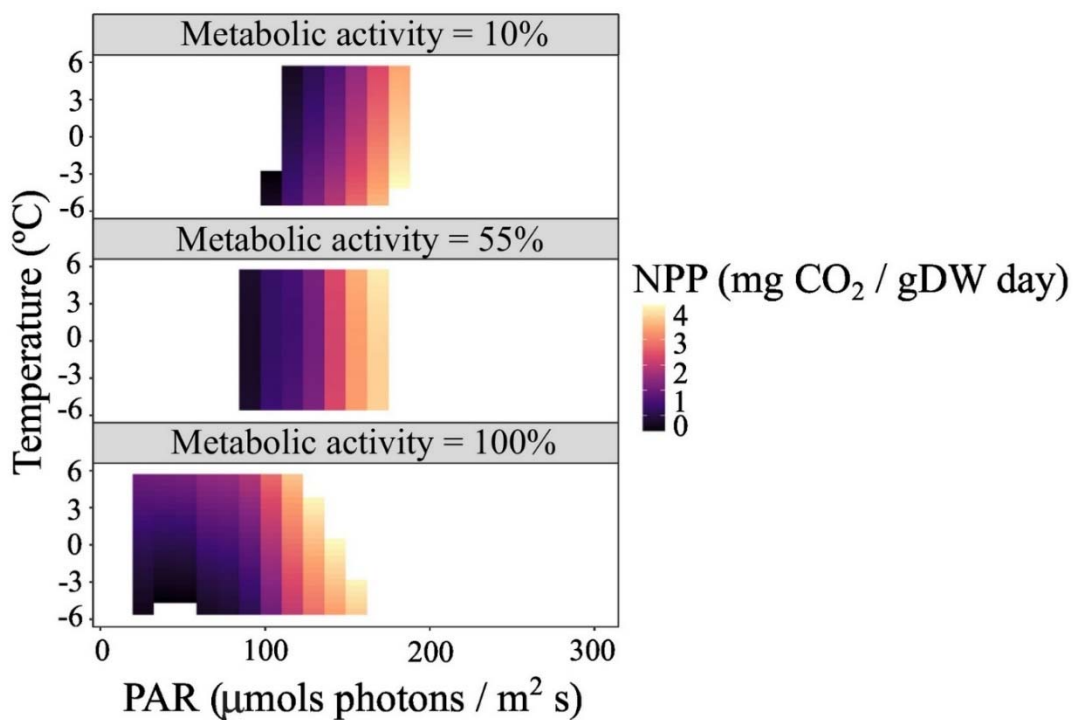
Fig. 3 Four-way interaction between daily microclimate (temperature and PAR), metabolic activity, and net primary productivity (NPP) from 2009 to 2014 of *U. aurantiaco-atra* at maritime Antarctica. The four-way interaction is visualized as a contour plot of three-way interactions between daily microclimate (temperature and PAR), and NPP at one different metabolic activity level (10, 55, and 100%). The colour gradient corresponds to the response variable, in which high NPP is shown in light orange and low NPP in black.

3.3.   Metabolic activity from 2009 to 2014

The long-term measurements of chlorophyll *a* fluorescence obtained in the field indicated that the mean annual metabolic activity (± standard deviation) was $67.4 \pm 26.4\%$ from 2009 to 2014. The mean metabolic activity (± standard deviation) was $48.8 \pm 34.4\%$ in the warmest months and $80.1 \pm 20.9\%$ in the coldest months (Fig. S3).

Rainfall and snowfall caused metabolic activation in 4.3% and 0.28% of the total records, respectively. The other records where rainfall or snowfall were not recorded but the species was metabolically active ('non-precipitation events') comprised 95.4% of the total records.

The metabolic activity response pattern was analyzed with GAM 2, where the model had an R^2 value of 0.58 and it explained 60% of the total deviance. The significant variables according to GAM 2 are shown in Table 4. The graphic output from the model presented in Fig. 4 shows how the metabolic activity changed according to the abiotic factors. The most important results in Fig. 4 are as follows: (i) the hydration sources ('rainfall', 'snowfall', and 'non-precipitation events') had different effects on the metabolic activity pattern; (ii) the high relative humidity when it was raining and low relative humidity when it was snowing led to metabolic activity with a longer duration; (iii) when non-precipitation events were recorded but the species was metabolically active, small changes in any driver led to greater changes in the duration of metabolic activity; and (iv) temperature was the main driver related to the metabolic activity response pattern (Fig. 4 and Table 4).

Table 4: Significance of the smoothing terms obtained from the generalized additive model (GAM 2), in which the effect of macroclimate on the daily metabolic activity of *U. aurantiaco-atra* at Livingston Island (maritime Antarctica) from 2009 to 2014 is evaluated. The edf corresponds to the estimated degrees of freedom. P-value < 0.05 is considered as the minimum level of significance.

Smoothing terms	edf	F-test	p-value
s(PAR)	1.00	2.49	0.11
s(Temperature)	6.24	2.49	0.02
s(RH)	2.35	0.73	0.51
s(Precipitation)	0.00	0.00	0.37
te(Temperature, PAR, RH): Non precipitation events	34.96	3.86	0.00
te(Temperature, PAR, RH): Rainfall	11.22	2.39	0.00
te(Temperature, PAR, RH): Snowfall	8.49	1.33	0.21
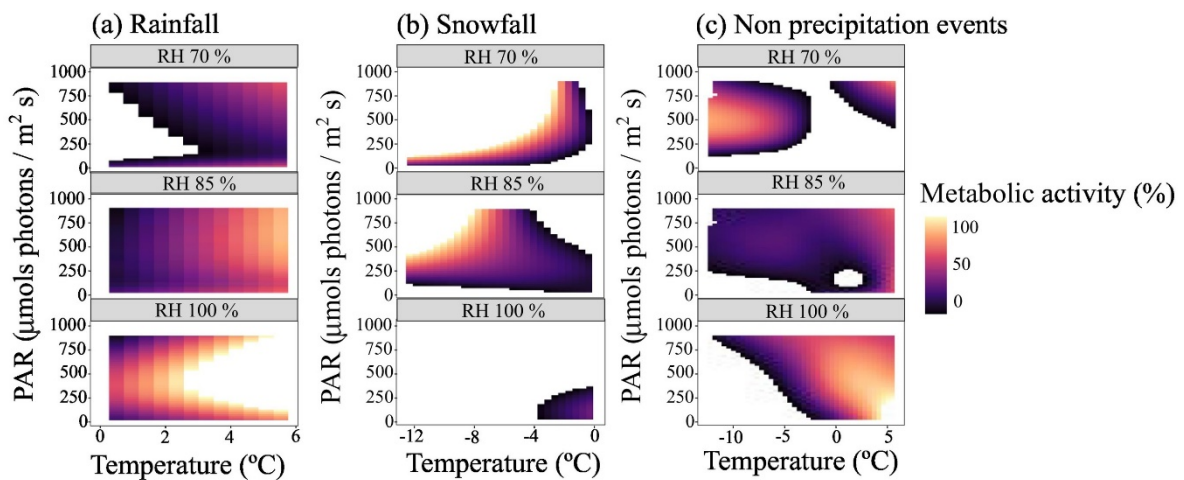
Fig. 4 Four-way interaction between daily macroclimate (temperature, PAR, and relative humidity (RH)) and metabolic activity according to the hydration source (rainfall, snowfall, and non-precipitation events) of *U. aurantiaco-atra* at maritime Antarctica. The four-way interaction is visualized as a contour plot of three-way interactions between daily macroclimate (temperature and PAR), and metabolic activity at one different relative humidity level (70, 85, and 100%). The colour gradient corresponds to the response variable, in which high metabolic activity is shown in red and no metabolic activity in black.

3.4. Metabolic activity and NPP predictions under climate change scenarios

The mean metabolic activity patterns were similar according to the RCPs and field measurements (Fig. 5), with high and relatively stable metabolic activity from May to October, and low rates from November to April. The metabolic activity was predicted to increase slightly under both RCP scenarios (RCP 4.5 and RCP 8.5), especially at the end of the century. The mean metabolic activity was predicted to increase from 67.4% at present to 71.9/70.4% under RCP 4.5 and to 71.3/72.9% under RCP 8.5 for the middle/end of the century, respectively. In the warmest months (from November to March), the metabolic activity was predicted to increase from 48.8% at present to 56.9/57.3% and 56.9/60% under RCP 4.5 and RCP 8.5 for the middle/end of the century, respectively.
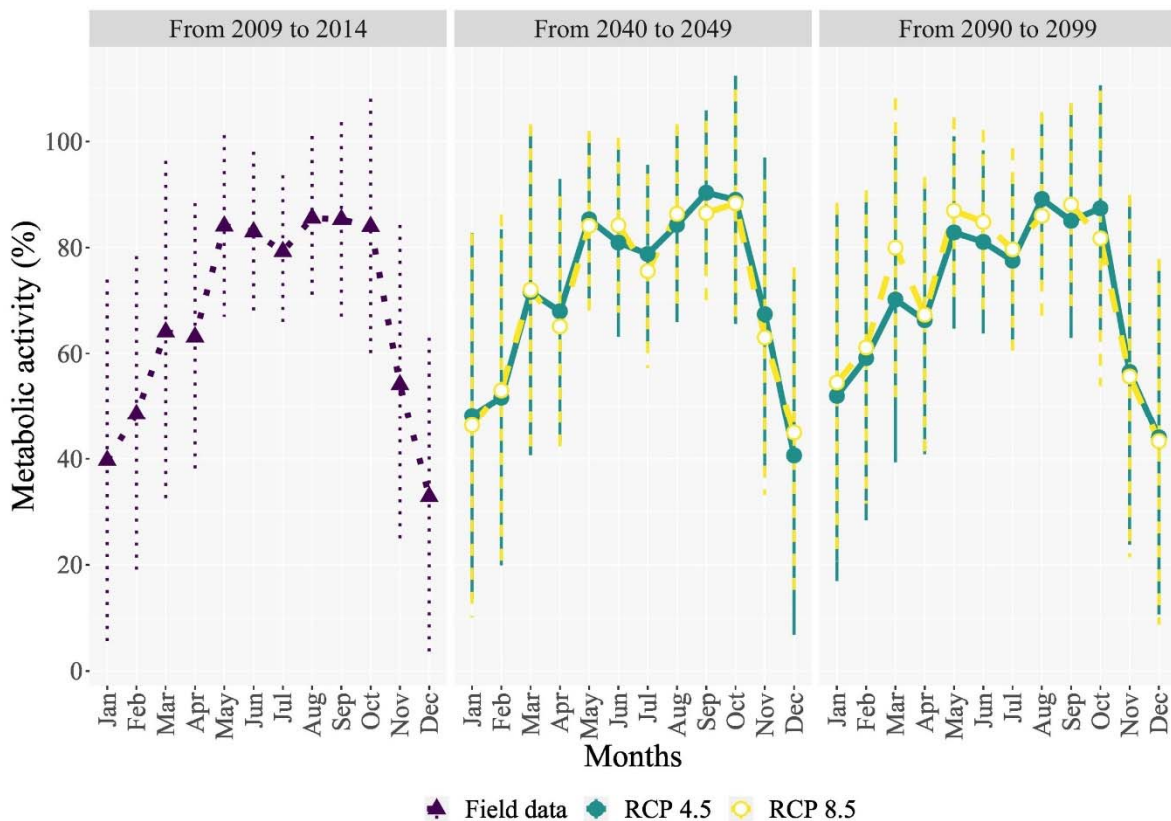
Fig. 5 Monthly mean of metabolic activity of *U. aurantiaco-atra* at maritime Antarctica for three different periods of time. The metabolic activity from 2009 to 2014 corresponds to the field measurements. The metabolic activity in the middle (2040 to 2049) and in the end (2090 to 2099) of the century corresponds to the projected values for the RCP 4.5 and RCP 8.5 scenarios. Vertical lines represent the standard error values.

The mean NPP was predicted to increase under both RCPs in the middle and at the end of the century (Fig. 6). In the middle of the century, NPP was predicted to increase by 167% (154 mg CO_2 gDW^{-1} $year^{-1}$) under RCP 4.5 and by 153% (141 mg CO_2 gDW^{-1} $year^{-1}$) under RCP 8.5. At the end of the century, the NPP was predicted to stabilize under RCP 4.5 and to increase by 189% (174 mg CO_2 gDW^{-1} $year^{-1}$) under RCP 8.5. The current five months of negative NPP were predicted to decrease to four months under both RCPs by the middle of the century and to three months under RCP 8.5 by the end of the century.
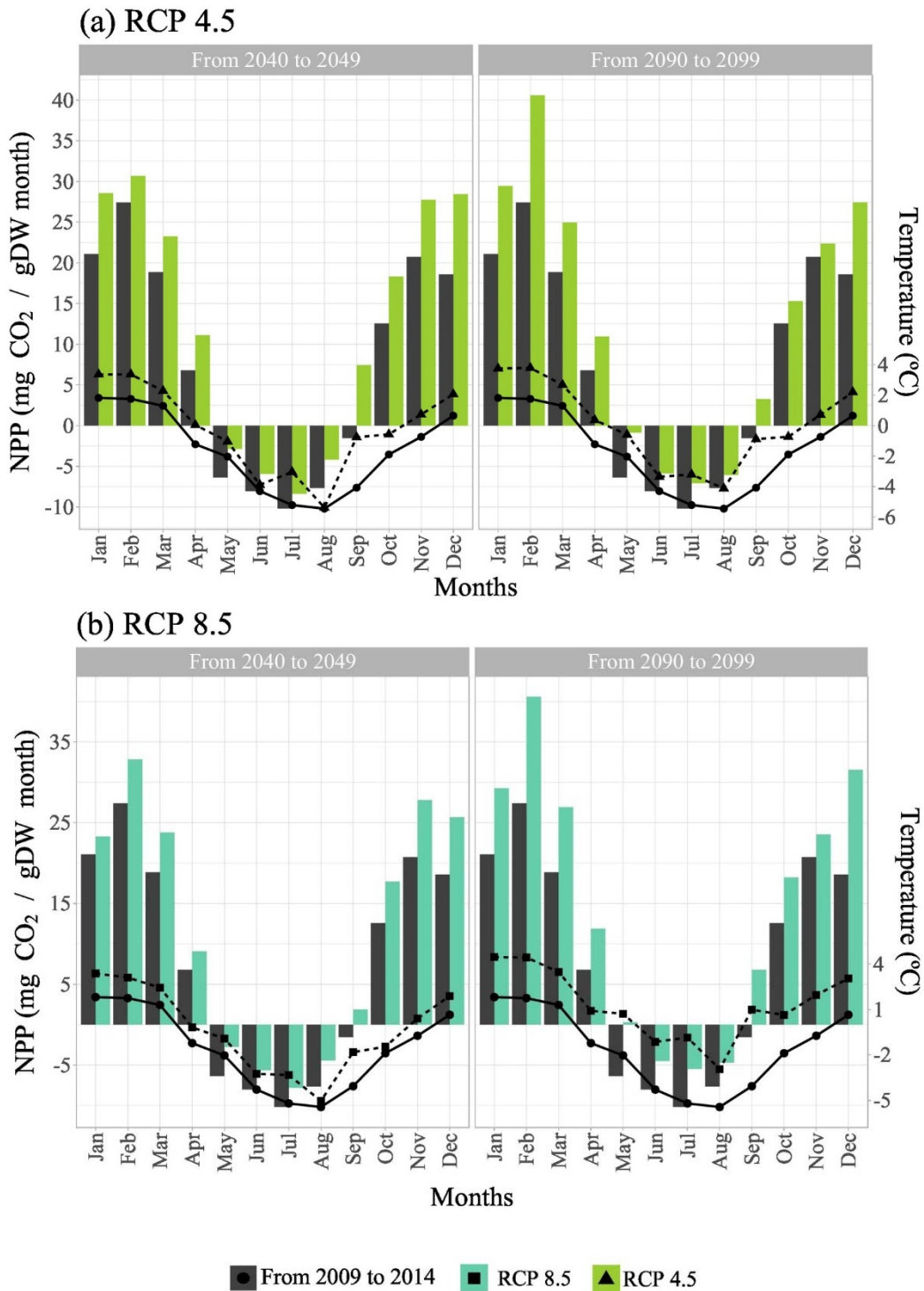
Fig. 6 Projection of the monthly net primary productivity (NPP) at the middle and the end of the century for (a) RCP 4.5 and (b) RCP 8.5 of *U. aurantiaco-atra* at maritime Antarctica. Black bars represent the NPP from 2009 to 2014. Negative values represent carbon losses and positive values represent carbon gains. The black lines are the monthly mean of macroclimatic temperature for the present time and for the RCPs.

4. Discussion

4.1. Baseline for predictions under climate change: suboptimal conditions and spatial resolution in dormant species

Modeling the effect of climate change on the physiological performance of poikilohydric autotrophs is a complex problem because they are highly dependent on the microtopographic factors and are normally subjected to suboptimal environmental conditions.

The mismatch between the spatial scale of the models and organisms needs to be adjusted (Potter et al., 2013). The macroclimate-based NPP model showed that even when metabolic activity was included as a biotic driver, the NPP was overestimated by 4.4 times (Fig. 2) probably due to the macroclimatic PAR was six times greater than the microclimatic PAR. In fact, our findings showed that the NPP was higher when PAR was higher (Fig. 3). Quantifying the error incurred when modeling the NPP using micro- or macroclimate highlights the importance of the micro-topographic conditions, which are highly heterogeneous and might diverge strongly from the surrounding macroclimate (Schroeter et al., 2017; Holmes and Dingle, 1965). Therefore, models established based on macroclimate are poor predictors of the NPP. Determining the effects of geographic scales on both the metabolic activity and NPP can allow a baseline to elucidate the potential effects of climate change on the global carbon cycle in tundra biomes such as maritime Antarctica.

The ability of cryptogams to entry into dormant status is determined by the climatic conditions. The benefits of dormancy include allowing species to increase their resistance to freezing and water shortage, as well as avoiding the need to cope with high PAR and temperature (Green et al., 2007). In general, microclimatic temperatures when lichens are metabolically active in maritime Antarctica range from 1.1 °C to 4 °C (Schroeter et al., 2010; Schlensog et al., 2013; Raggio et al., 2016; Schroeter et al., 2017), which is around 10 °C lower than the optimal temperature for net photosynthesis measured under laboratory conditions (Kappen, 1985; Harrisson et al., 1986, 1989; Harrisson and Rothery, 1988; Kappen and Redon, 1987; Kappen et al., 1988; Schroeter et al., 1995; Laguna-Defior et al., 2016). Our findings demonstrated that the duration of metabolic activity was a crucial biotic driver to model the NPP in dormant species, where the NPP was overestimated by 3.8 times when metabolic activity was not considered in the predictive models (Fig. 2).

4.2. Longer duration of metabolic activity during the summer under climate change

The response patterns of lichens to climate trends are highly dependent on their physiological tolerance range. In particular, their characteristic poikilohydry means that the capacity for survival is associated with the hydration sources available in a niche.

We found that metabolic activity patterns changed according to the available hydration sources, which varied throughout the seasons. Rainfall mainly occurs during the Antarctic summer and high relative humidity appeared to be essential for delaying the dehydration process, thereby maximizing the metabolic activity (Fig. 4a). By contrast, snowfall led to high metabolic activity when the relative humidity was low (Fig. 4b). The effect of snowfall was not statistically significant (Table 4) but both rainfall and snowfall events appeared to trigger metabolic activation of the study species (Fig. 4). The metabolic activity detected when no precipitation events were recorded may have been due to the extension of metabolic activity after rainfall and snowfall events (Schroeter et al., 2010) because the species could remain wet for several hours under low temperatures and high humidity in maritime Antarctica (Barták et al., 2005). In these conditions, hydration could be extended for up to 20 hours (Kappen and Schroeter, 1997).

The occurrences of metabolic activity when no precipitation events were recorded may also have been due to a wide variety of potential hydration sources, such as meltwater and snow cover. Small changes in any driver led to large changes in the duration of metabolic activity and temperature was the most important driver (Fig. 4c). Similar to rainfall events, high relative humidity led to high metabolic activity at temperatures above 0 °C (Fig. 4c). This effect can be explained by meltwater in the early summer, which has been established as another hydration source that is available for short periods of time to morphotypes attached tightly to rocks (Kappen, 2000; Barták et al., 2005). When temperatures dropped below 0 °C, high metabolic activity was dependent on PAR and it only occurred when the relative humidity was low (Fig. 4c). This pattern was suggested previously by Kappen et al. (1995) who concluded that lichens covered by snow layers could be metabolically active during the colder months. Some radiation may penetrate through the snow layer to melt the ice crystals closest to the lichen thalli and activate them (Kappen et al., 1995).

Relative humidity plays an indirect role in Antarctica (Fig. 4, Table 4) by prolonging the duration of metabolic activity rather than promoting metabolic activation (Green and Proctor, 2016). Hydration by humid air appears to be a slow process, and thus complete hydration of the lichen thalli may take a long time (Lange et al., 1988).

However, it has been demonstrated that epiphytic species such as *Usnea dasopoga* may exhibit full reactivation under humid conditions (*ca.* 50 min; Phinney et al., 2018).

The seasonal metabolic activity patterns are not expected to change greatly by the end of the century. The metabolic activity response pattern highlights (i) the effects of precipitation events, which are concentrated in the summer and spring seasons (AEMET, 2019; Vignon et al., 2021), and (ii) the freezing temperatures and low water availability which do not imply a dormant state of metabolic inactivity during the Antarctic winter (Fig. 5; Robinson et al., 2003). Metabolic activity may increase from 67.4% to 70.4% and 72.9% at the end of the century under RCP 4.5 and RCP 8.5, respectively (Fig. 5). We hypothesize that the pronounced predicted increase during the warmest months is related to increases in the amount of the precipitation events and changes in the hydrological regimes (Lee et al., 2017; Vignon et al., 2021). However, the high metabolic activity found under the RCPs may be also explained by: (i) the accumulation of snow predicted at the end of the century in Antarctica providing protection to the species (Ye and Mather, 1997); and (ii) the ice melt predicted for coastal regions (Lee et al., 2017).

Therefore, under climate change conditions, lichens in tundra biomes with similar physiological tolerance ranges to the model species will exhibit increased periods of metabolic activity provided that liquid water is available. Furthermore, understanding how the response patterns of lichens are modulated by different hydration sources is crucial for assessing the potential effects of climate change on the survival of cryptogams due to the passive dependence of poikilohydric autotroph species on surrounding water.

4.3. Higher NPP under RCP 4.5 and RCP 8.5 due to climate warming

Under climate change scenarios, the projected increase in temperature will lead to increases in NPP of 167% and 189% under RCP 4.5 and RCP 8.5 at the end of the century, respectively (Fig. 6). These increases are supported by the significant effect of microclimatic temperature on NPP (Table 4), which we found was greater at high metabolic activity levels (Fig. 3). Therefore, extending the duration of metabolic activity will lead to higher NPP values at temperatures above 0 °C. However, the maximum NPP will be reached only if PAR is around 100–200 μmol photons $m^{-2}\,s^{-1}$, which corresponds to the mean PAR value when poikilohydric autotrophs are metabolically active in maritime Antarctica (Schroeter et al., 2017). NPP appears to be modulated by the ability of species to compensate for carbon loses at low PAR values, which is related to

adaptation to the suboptimal conditions present in Antarctica (e.g., Kappen and Redon, 1987; Schroeter et al., 1995; Pannewitz et al., 2006).

The mean microclimatic temperature of -0.3 °C and PAR of 30 μmol photons m^{-2} s^{-1} found on Livingston Island are markedly lower than the conditions needed to maximize NPP. The temperature at which *U. aurantiaco-atra* achieves its maximum net photosynthesis has been established as *ca.* 12.7 °C (Laguna-Defior et al., 2016). The NPP exceeded two times the mean NPP on 22.5% of the days from 2009 to 2014, which high-lights that exceptional microclimatic conditions lead to an extra carbon gain. This opportunistic behavior in response to optimal transient periods is considered a strategy for maximizing the NPP and it may be related to rapid metabolic reactivation of the species (Kappen, 1985). Higher NPP values were predicted under climate change scenarios but the opportunistic response is unpredictable due to the low temporal resolution of RCPs, which are designed to operate at decade scales.

Therefore, according to our models, the effects of climate change on the NPP will be highly positive due to global warming. The synergy among abiotic conditions appears to be highly dependent on the species and its habitat (Colesie et al., 2018). However, the response to the CO_2 concentration has been investigated rarely in Antarctic cryptogams. Previous studies in other biomes showed that the tolerance of lichens to high CO_2 concentrations is dependent on the species (e.g., Lange et al., 1999; Lange, 2002), thereby demonstrating the need to produce better models for understanding the NPP response patterns of tundra biome species to climate change.

Changes in the NPP might affect the Antarctic landscape structure and community composition. Thus, the current biomes in the sub-Antarctic area such as Navarino Island (Southern Chile) could provide a good control model for the expected changes because they have similar macroclimatic conditions to those projected by RCPs for maritime Antarctica at the end of the century. Previous studies of the same model species showed that the annual metabolic activity was lower on Navarino Island than maritime Antarctica (only 42.9%; Laguna-Defior, 2016) but the photosynthetic performance was similar in both areas (Laguna-Defior, 2016). It has also been suggested that climate change will lead to an expansion of the ice-free areas by about 25% (Lee et al., 2017), thereby providing more niches for colonization and increasing the connectivity between terrestrial vegetation patches. These changes could lead to biotic homogenization at a regional scale (Lee et al., 2017) and favor the best adapted species, but also lead to the extinction of less competitive species. New species might invade the ice-free areas, including colonization

by mosses (Walther et al., 2002) or by invasive species such as *Poa annua* (Molina-Montenegro et al., 2016). Moreover, the two higher plants that are present in Antarctica (*Colobanthus quitensis* and *Deschampsia antarctica*) might undergo rapid expansion in terms of both their extent and number (Smith, 2001). The invasion by *P. annua* might be explained by its high productivity, which is greater than that of the native *D. antarctic*a (Green et al., 2007). In fact, the NPP of the native vascular plants in maritime Antarctica (Edwards and Smith, 1988) has been estimated as higher than those of bryophytes (e.g., Baker, 1972; Collins and Callaghan, 1980; Davis, 1981; Ino, 1983b; Davey and Rothery, 1997) and lichens (Hooker, 1980; Smith, 1984; Kappen, 1985, 1988; Schroeter et al., 1995; Schroeter, 1997).

5.   Conclusions

Predicting how climate change will impact the terrestrial vegetation in Antarctica is challenging because the predominant terrestrial vegetation is symbiotic, poikilohydric, and strongly influenced by microtopographic factors. Therefore, considering drivers such as microclimate and metabolic activity is essential to avoid overestimating the NPP, thereby allowing a baseline to be established for elucidating the potential effects of climate change in tundra biomes such as maritime Antarctica. Under climate change conditions, metabolic activity is predicted to increase due to the greater availability of water sources, as well as, the NPP due to climate warming. Therefore, species with similar physiological ranges to the species investigated are expected to maintain similar behavior at the end of the century.

Discussion

Acclimation of bryophytes and lichens to local environmental conditions of extreme regions is linked to their ability to be physiologically plastic. Despite bryophytes and lichens being clearly different from each other, their poikilohydric nature allows them to maintain similar physiological strategies in order to maximize their fitness.

In drylands, *Ceratodon purpureus* and *Xanthoparmelia* populations seem to be able to thermally acclimate their respiration within a temperature range of 5-15ºC. In fact, respiration represents 15-32% (Chapter 1) and 19-21% (Chapter 2) of the total gross photosynthesis, respectively. This agrees with the results obtained by Lange and Green (2005), who found that lichens from steppes even reach full acclimation. Accordingly, net photosynthesis and respiration values are also similar when comparing the *Xanthoparmelia* populations (Chapter 2) and the moss stems of *C. purpureus* (Weber et al., 2012). Nevertheless, the comparison of these lichen thalli with the entire moss turfs - rather than with moss stems - shows dissimilarity in the photosynthetic parameters as Weber et al. (2012) pointed out, demonstrating that the methodology used in CO_2 experiments highly influences the results obtained.

The carbon balance is the difference between carbon gains of net photosynthesis and carbon losses of respiration. In the context of that balance, *C. purpureus* is photosynthetically most efficient at 5ºC (Chapter 1), while *Xanthoparmelia* populations perform best at 10ºC (Chapter 2). Despite that, all of them have similar optimal temperatures for net photosynthesis *ca.* 20ºC (unpublished data; Weber et al., 2012). This highlights similar altitudinal preferences, climatic conditions and/or geographic distribution among species (Kappen et al., 1989; Sérgio et al., 2011). Hence, differences in photosynthetic efficiency seem to be species-specific and may be driven by the temperatures at which net photosynthesis and respiration occur under field conditions (Raggio et al., 2014). In fact, each species may be metabolically active at different times according, for instance, to their ability to uptake and retain water or to the micro-topographic factors (Pintado et al., 1997). Therefore, the trade-off between carbon gain and duration of metabolic activity seems to be crucial to explain the physiological strategy of species. Other studies in the Tabernas Desert showed similar optimal temperatures for *Teloschistes lacunosus* and *Ramalina bourgeana* (del Prado and Sancho, 2000), *Diploschistes diacapsis* (Pintado et al., 2005), and *Squamarina cartilaginea, Toninia albilabra, Psora decipiens* and *Didymodon rigidulus* (Raggio et al.,

2014). The photosynthetic efficiency for some of these species was also similar, being maximum at 5ºC and 10ºC (Raggio et al., 2014, 2018).

The light compensation points between *C. purpureus* and the *Xanthoparmelia* desert population also show convergent trends. This functional trait highlights that both species, together with *Didymodon rigidulus, Psora decipiens,* and shade-adapted populations of *Diploschistes diacapsis*, all thrive under similar light radiation conditions in the desert due to all of them having similar compensation points (Raggio et al., 2018; Pintado et al., 2005). In fact, Weber et al. (2012) described that the moss *C. purpureus* from the Succulent Karoo Desert is located in protected areas under shrubs, where impact by trampling is low and moisture conditions are more favourable. Similarly, *Xanthoparmelia* populations are also distributed in the Tabernas Desert as Weber et al. (2012) mentioned for *C. purpureus* in the Succulent Karoo Desert. Hence, *Xanthoparmelia* specimens from the inland desert and the coastal habitats could modify their growth form and/or substrate preferences as a strategy to maximize their fitness in their respective habitats (Chapter 2).

Xanthoparmelia populations from the inland desert and the coastal region are mainly differentiated from one another by the respiration rates at low temperatures, being lower those from the desert than those from the coast (Chapter 2). This is explained by the species ability to be physiologically plastic rather than by the presence of different photobiont partner/s. Our findings showed homogeneity in the photobiont community among both *Xanthoparmelia* species and low specificity of mycobionts towards photobiont/s partner/s. (Chapter 2). Despite that, there is a slightly higher photobiont diversity and potential complementary eco-physiological response between OTU1 and OTU2 in the coastal specimens (Chapter 2). Differences in the photobiont/s community may be the result of environmental filtering (Dal Grande et al., 2017a) or habitat conditions (Domaschke et al., 2012), which would constrain the potential symbionts available within each region.

In continental Antarctica, populations of *C. purpureus* show no thermal acclimation to respiration (Chapter 1) like other lichens and bryophytes do (e.g. Hicklenton and Oechel, 1976; Wagner et al., 2013b, Colesie et al., 2018). CO_2 exchange measurements in continental Antarctica show the optimal temperature for net photosynthesis to be *ca.* 10ºC for species growing in moist habitats. This is the case with the endemic lichens *Xanthoria mawsonii* (Pannewitz, et al., 2006), the endemic moss *Schistidium antarctici* (Kappen et al., 1989) and

the cosmopolitan moss *C. purpureus* itself (Ino, 1990a, 1990b; Pannewitz et al., 2005). Living in this habitat leads species to be continuously active during the growing season and survive under high light radiation (Kappen et al., 1989; Schroeter and Scheidegger, 1995; Pannewitz et al., 2005, 2006). Hence, species have developed protective mechanisms in order to avoid the photodamage. For instance, several studies demonstrated that photoinhibition occurs during high light periods in the daytime but recovery is complete overnight (Lovelock et al., 1995a, 1995b; Green et al., 2000; Lud et al., 2002, 2003; Schroeter et al., 2012). The strategy of species is, thus, to maximize the carbon gain at high radiation levels (Kappen et al., 1989; Green et al., 2005; Pannewitz, et al., 2006; Schroeter et al., 2012). In accordance with that, the strategies acquired to survive in continental Antarctica seem to be species-specific and closely related to habitat preferences (e.g. Ino, 1990a; Kappen and Breuer, 1991; Tarnawski et al., 1992; Smith, 1999).

In maritime Antarctica, the physiological responses of *C. purpureus* and *U. aurantiaco-atra* populations may differ because of their geographical distribution, being cosmopolitan and endemic, respectively. Contrary to the physiological convergence of *C. purpureus* and *Xanthoparmelia* populations from the semi-arid desert, *C. purpureus* and *U. aurantiaco-atra* from maritime Antarctica show divergent results. According to our findings, the less harsh climatic conditions makes maritime Antarctica the most suitable habitat for lichens and bryophytes' success (Chapter 3). Hence, we may hypothesize that species such as *C. purpureus* are able to perform efficiently in all climatic conditions of maritime Antarctica due to their cosmopolitan nature. However, species restricted to a narrower distribution such as *U. aurantiaco-atra* (Laguna-Defior et al., 2016; Walker, 1985) may only be able to perform under small windows of favorable conditions. Hence, maritime Antarctica would be characterized by species-specific responses, rather than by physiological convergence between species caused by abiotic stresses. Previous studies have shown that net photosynthesis is highly variable in species from maritime Antarctica, being those values of bryophytes higher than in lichens (e.g. Convey, 1994; Davey and Rothery, 1997; Kappen, 2000; Perera-Castro et al., 2021). However, the comparison of CO_2 exchange rates of lichens and bryophytes of maritime Antarctica becomes challenging because the vast majority of studies are expressed on a weight basis and measured under different laboratory conditions.

The comparison between maritime and continental Antarctica show that species in both areas are metabolically active at similar microclimatic temperatures *ca.* 2ºC (Schroeter et al., 2011). Nevertheless, climatic conditions in maritime Antarctica keep species from being subjected to hard stresses, which allows for higher net photosynthesis, and lower respiration rates in cosmopolitan species such as *C. purpureus* (Chapter 1) and *Bryum pseudotriquetrum* (Pannewitz et al., 2005; Perera-Castro et al., 2021).

The effect of micro- and macroclimate conditions on the physiological performance of lichens and bryophytes has been widely studied (e.g. Schroeter et al., 2010, 2017; Pintado et al., 2010; Schlensog et al., 2013; Raggio et al., 2016). Focusing on the most relevant factors described in previous studies, our model point out the mean temperature as the main driver for explaining changes on both metabolic activity and net primary productivity (NPP) of *U. aurantiaco-atra* in maritime Antarctica (Chapter 3). Our findings suggest that macroclimate is a poor predictor of NPP likely due to the strong effects of micro-topographic factors on cryptogams.

Metabolic activity is highly dependent on the type, distribution, and duration of the hydration sources available throughout the year (Chapter 3). High metabolic activity in maritime Antarctica is led by (i) rainfall events and high relative humidity, or (ii) snowfall events and low relative humidity (Chapter 3). The metabolic activity detected when no precipitation events were recorded may have been due to the extension of metabolic activity duration after rainfall and snowfall events (Schroeter et al., 2010), or to the presence of other hydration sources such as meltwater and snow cover. Lichens and bryophytes from this region may be metabolically active all day, while those from semi-arid deserts are restricted to night and early morning due to the high temperatures present during daylight (Lange and Bertsch, 1965; Maphangwa et al., 2012; Raggio et al., 2014). Hence, the role of temperature on the timing and duration of metabolic activity is crucial, and clearly affects the daily carbon balance (Chapter 3). During short metabolic activity periods, higher PAR and lower temperatures are required to maximize NPP (Chapter 3). This highlights the importance of modulating the light compensation point according to the environmental conditions. In regions such as maritime Antarctica, it is crucial to compensate at lower PAR values than other regions like semi-arid deserts in order to maximize NPP due to the usually low radiation present (Schroeter et al., 2017).

Studying the physiological plasticity of species may be help to predict the potential effects of climate change (e.g. Baldauf et al., 2020). Due to the low resolution of the IPCC scenarios and the importance of micro-topographic factors on cryptogams, the first step to model the physiological response patterns of lichens and bryophytes under climate change scenarios is quantifying the bias between modelling macro- and microclimate (Chapter 3). This bias includes a NPP overestimation by 4.4 times when the modelling is based on macroclimate. Furthermore, the opportunistic behaviour of lichens and bryophytes and their poikilohydric nature make NPP prediction challenging. Despite these constraints, our findings show that as long as water is provided, the lichen *U. aurantiaco-atra* may slightly increase the duration of its metabolic activity and greatly enhance NPP at the end of the century (Chapter 3). Including our prediction as one of the multiple plausible future scenarios for this species is supported by (i) the studies by Laguna-Defior (2016) between Navarino (Chile) and Livingston Island (maritime Antarctica), and (ii) the robustness of using several years as a baseline for the prediction. Nevertheless, better models are needed for understanding the potential effects of climate change on these organisms, by including other factors such as thickness of snow cover, CO_2 concentration, and water content of the lichen thalli among others. Also, field measurements of metabolic activity and photosynthesis under various climatic conditions are required as a control to verify the trends obtained in the modelling.

Conclusions

1. Our findings demonstrate that *Ceratodon purpureus* always performs better at low temperatures and it is able to thermally acclimate its respiration according to the local environmental conditions.

2. The optimal temperature for net photosynthesis in populations of *C. purpureus* is in agreement with the mean macroclimatic temperature for each habitat. In the Southern Hemisphere, this optimal temperature decreases as latitude increases.

3. Photosynthetic traits of populations of *C. purpureus* from maritime and continental Antarctica are strongly different, while the population from the Succulent Karoo Desert shares traits with both Antarctic regions.

4. The lichen species *Xanthoparmelia pulla* and *X. pokornyi* show high genetic similarity between their mycobionts, which questions their identity as two different species.

5. The physiological convergence found between *X. pulla* and *X. pokornyi* highlights that phenotypic plasticity and/or substrate switching are strategies that maximize the lichens' fitness to the local environmental conditions.

6. Mycobionts of these two *Xanthoparmelia* taxa have similar photobiont community composition and low specificity towards photobiont partners. Nevertheless, the lichen-associated algal communities of the coastal population have higher genetic diversity compared with the specimens from the inland desert.

7. Microclimate and metabolic activity are essential drivers to avoid overestimations of cryptogams' net primary productivity (NPP) in maritime Antarctica. Despite macroclimate being a poor predictor of NPP, modelling NPP at different geographic scales allows to establish a baseline to elucidate the potential effects of climate change in poikilohydric autotrophs.

8. Mean temperature is the main driver in explaining changes on both metabolic activity and NPP in regions such as maritime Antarctica.

9. Metabolic activity is highly dependent on the type, distribution, and duration of the hydration sources available throughout the year in maritime Antarctica. The extension of the duration of metabolic activity is linked to high relative humidity for rainfall, and low relative humidity for snowfall.

10. Under climate change scenarios, the lichen *U. aurantiaco-atra* may exhibit increased periods of metabolic activity and also NPP by the end of the century.

References

AEMET, 2019, Informe Antártico del año 2019. Available at: https://antartida.aemet.es/index.php?pag=informes&bol=9.

Agam, N., Berliner, P.R., 2006. Dew formation and water vapour adsorption in semi-arid environments - a review. J. Arid Environ. 65, 572-590.

Ahmadjian, V., 1995. Lichens are more important than you think. BioScience 45(3), 124.

Amo de Paz, G., Cubas, P., Crespo, A., Elix, J.A., Lumbsch, H.T., 2012. Transoceanic dispersal and subsequent diversification on separate continents shaped diversity of the *Xanthoparmelia* '*pulla* group' (Ascomycota). PloS One 7(6), e39683.

Arnold, P.A., Nicotra, A.B., Kruuk, L.E.B., 2019. Sparse evidence for selection on phenotypic plasticity in response to temperature. Philos. Trans. R. Soc. B. 374, 20180185.

Aro, E.-M., Valanne, N., 1979. Effect of continuous light on CO_2 fixation and chloroplast structure of the mosses *Pleurozium schreberi* and *Ceratodon purpureus*. Physiol. Plant. 45, 460-466.

Aro, E.-M., 1982. A Comparison of the chlorophyll-protein composition and chloroplast ultrastructure in two bryophytes and two higher plants. Z. Pjlanzenphysiol. Bd. 108(2), 97-105.

Aro, E.-M., Somersalo, S., Karunen, P., 1987. Membrane lipids in *Ceratodon purpureus* protonemata grown at high and low temperatures. Physiol. Plant. 69, 65-72.

Aro, E.-M., Karunen, P., 1988. Effects of hardening and freezing stress on membrane lipids and CO_2 fixation of *Ceratodon purpureus* protonemata. Physiol. Plant. 74: 45-52.

Ascaso, C., Souza-Egipsy, V., Sancho, L.G., 2003. Locating water in the dehydrated thallus of lichens from extreme microhabitats (Antarctica). Biblioth. Lichenol. 85, 215-223.

Asplund, J., Wardle, D.A., 2017. How lichens impact on terrestrial community and ecosystem properties. Biol. Rev. Camb. Philos. Soc. 92(3), 1720-1738.

Atkin, O.K., Tjoelker, M.G., 2003. Thermal acclimation and the dynamic response of plant respiration to temperature. Trends. Plant. Sci. 8(7), 343-351.

Atkin, O.K., Bruhn, D., Hurry, V.M., Tjoelker, M.G., 2005. The hot and the cold: unravelling the variable response of plant respiration to temperature. Funct. Plant Biol. 32(2), 87-105.

Atkin, O., Scheurwater, I., Pons, T., 2006a. High thermal acclimation potential of both photosynthesis and respiration in two lowland *Plantago* species in contrast to an alpine congeneric. Glob. Chang. Biol. 12(3), 500-515.

Atkin, O., Bruhn, D., Tjoelker, M.G., 2006b. Response of plant respiration to changes in temperature: mechanisms and consequences of variations in Q_{10} values and acclimation. In: Lambers, H., Ribas-Carbo, M. (Eds.), Plant respiration: From cell to ecosystem. Springer, Dordrecht, pp 95-135.

Baker, J.H., 1972. The rate of production and decomposition of *Chorisodontium aciphyllum* (Hook. f. Wils.) Broth. Br. Antarct. Surv. Bulletin 27, pp 123-129.

Baldauf, S., Porada, P., Raggio, J., Maestre, F.T., Tietjen, B., 2020. Relative humidity predominantly determines long-term biocrust-forming lichen cover in drylands under climate change. J. Ecol. 109, 1370-1385.

Bálint, M., Schmidt, P.A., Sharma, R., Thines, M., Schmitt, I., 2014. An Illumina meta-barcoding pipeline for fungi. Ecol. Evol. 4, 2642-2653.

Bálint, M., Bahram, M., Eren, A.M., Faust, K., Fuhrman, J.A., Lindahl, B., O'Hara, R.B., Öpik, M., Sogin, M.L., Unterseher, M., Tedersoo, L., 2016. Millions of reads, thousands of taxa: microbial community structure and associations analyzed via marker genes. FEMS Microbiol. Rev. 40, 686-700.

Bargagli, R., 2005. Antarctica: geomorphology and climate trends. In: Bargagli, R. (Ed.), Antarctic Ecosystems: Environmental contamination, climate change, and human impact. Springer, Berlin, pp 1-40.

Barták, M., Gloser, J., Hájek, J., 2005. Visualized photosynthetic characteristics of the lichen *Xanthoria elegans* related to daily courses of light, temperature and hydration: a field study from Galindez Island, maritime Antarctica. Lichenologist 37(5), 433-443.

Barták, M., 2014. Lichen photosynthesis scaling from the cellular to the organism level. In: Hohmann-Marriott M.F. (Ed.), The structural basis of biological energy generation. Springer, Netherlands, pp 379-400.

Bastin, J.F., Berrahmouni, N., Grainger, A., Maniatis, D., Mollicone, D., Moore, R., Patriarca, C., Picard, N., Sparrow, B., Abraham, E.M., Aloui, K., Atesoglu, A., Attore, F., Bassüllü, Ç., Bey, A., Garzuglia, M., García-Montero, L.G., Groot, N., Guerin, G., Laestadius, L., … Castro, R., 2017. The extent of forest in dryland biomes. Science 356(6338), 635-638.

Belnap, J., 2003. The world at your feet: desert Biological Soil Crusts. Front. Ecol. Environ. 1, 181-189.

Beltrán-Sanz, N., Raggio, J., Gonzalez, S., Dal Grande, F., Prost, S., Green, A., Pintado, A., Sancho, L.G., (2022). Climate change leads to higher NPP at the end of the century in the Antarctic Tundra: Response patterns through the lens of lichens. Sci. Total Environ. 835, 155495.

Bengtsson-Palme, J., Ryberg, M., Hartmann, M., Branco, S., Wang, Z., Godhe, A., Wit, P.D., Sánchez-García, M., Ebersberger, I., Sousa, F., Amend, A.S., Jumpponen, A., Unterseher, M., Kristiansson, E., Abarenkov, K., Bertrand, Y.J., Sanli, K., Eriksson, K.M., Vik, U., Veldre, V., Nilsson, R.H., 2013. Improved software detection and extraction of ITS1 and ITS2 from ribosomal ITS sequences of fungi and other eukaryotes for analysis of environmental sequencing data. Methods Ecol. Evol. 4(10), 914-919.

Biersma, E.M., Convey, P., Wyber, R., Robinson, S.A., Dowton, M., van de Vijver, B., Linse, K., Griffiths, H., Jackson, J.A., 2020. Latitudinal biogeographic structuring in the globally distributed moss *Ceratodon purpureus*. Front. Plant. Sci. 11, 502359.

Bjerke, J.W., Bokhorst, S., Callaghan, T.V., Zielke, M., Phoenix, G.K., 2013. Rapid photosynthetic recovery of a snow-covered feather moss and *Peltigera* lichen during sub-Arctic midwinter warming. Plant. Ecol. Divers. 6(3-4), 383-392.

Blanco, O., Crespo, A., Elix, J., Hawksworth, D., Lumbsch, H.T., 2004. A molecular phylogeny and a new classification of parmelioid lichens containing *Xanthoparmelia*-type lichenan (Ascomycota: Lecanorales). Taxon 53, 959-975.

Block, W., Smith, R.I.L., Kennedy, A.D., 2009. Strategies of survival and resource exploitation in the Antarctic fellfield ecosystem. Biol. Rev. Camb. Philos. Soc. 84(3), 449-484.

Bokulich, N.A., Subramanian, S., Faith, J.J., Gevers, D., Gordon, J.I., Knight, R., Mills, D.A., Caporaso, J.G., 2013. Quality-filtering vastly improves diversity estimates from Illumina amplicon sequencing. Nat. methods 10, 57-59.

Bölter, M., Beyer, L., Stonehouse, B., 2002. Antarctic coastal landscapes: characteristics, ecology and research. In: Beyer, L., Bölter, M. (Eds.), Geo-ecology of Antarctic ice-free coastal landscapes. Springer, Berlin, pp 5-15.

Brodo, I.M., 1973. Substrate ecology. In: Ahmadjian, V., Hale, M.E. (Eds), The lichens. Academic Press, New York, pp 401-441.

Brostoff, W., Sharifi, M., Rundel, P., 2005. Photosynthesis of cryptobiotic soil crusts in a seasonally inundated system of pans and dunes in the western Mojave Desert, CA: Field studies. Flora 200, 592-600.

Büdel, B., Colesie, C., Green, T.G.A., Grube, M., Lázaro, R., Loewen-Schneider, K., Maier, S., Peer, T., Pintado, A., Raggio, J., Ruprecht, U., Sancho, L.G., Schroeter, B., Türk, R., Weber, B., Wedin, M., Westberg, M., Williams, L., Zheng, L. 2014. Improved appreciation of the functioning and importance of Biological Soil Crusts in Europe: The Soil Crust International Project (SCIN). Biodivers. Conserv. 23(7), 1639-1658.

Cantón, Y., Solé-Benet, A., Lázaro, R., 2003. Soil-geomorphology relations in gypsiferous materials of the Tabernas Desert (Almería, SE Spain). Geoderma 115, 193-222.

Cao, S., Zhang, J., Zheng, H., Liu, C., Zhou, Q., 2015. Photosynthetic performance in Antarctic lichens with different growth forms reflect the diversity of lichenized algal adaptation to microhabitats. Pol. Polar Res. 36, 175-188.

Casano, L., Campo, E.M., García-Breijo, F., Reig-Armiñana, J., Gasulla, F., Hoyo, A.D., Guéra, A., Barreno, E., 2011. Two *Trebouxia* algae with different physiological performances are ever-present in lichen thalli of *Ramalina farinacea*. Coexistence versus competition? Environ Microbiol 13(3), 806-818.

Casanovas, P., Lynch, H.J., Fagan, W.F., 2013. Multi-scale patterns of moss and lichen richness on the Antarctic Peninsula. Ecography 36, 209-219.

Casanovas, P., Black, M., Fretwell, P., Convey, P., 2015. Mapping lichen distribution on the Antarctic Peninsula using remote sensing, lichen spectra and photographic documentation by citizen scientists. Polar Res. 34, 1-8.

Chamizo, S., Cantón, Y., Lázaro, R., Solé-Benet, A., Domingo, F., 2012. Crust composition and disturbance drive infiltration through Biological Soil Crusts in semi-arid ecosystems. Ecosystems 15, 148-161.

Chamizo, S., Cantón, Y., Rodríguez-Caballero, E., Domingo, F., 2015. Biocrusts positively affect the soil water balance in semi-arid ecosystems. Ecohydrology 9, 1208-1221.

Chapin, F.S., Woodwell, G.M., Randerson, J.T., Rastetter, E.B., Lovett, G.M., Baldocchi, D.D., Clark, D.A., Harmon, M.E., Schimel, D.S., Valentini, R., Wirth, C., Aber, J.D., Cole, J.J., Goulden, M.L., Harden, J.W., Heimann, M., Howarth, R.W., Matson, P.A., McGuire, A.D., … Schulze, E.-D., 2006. Reconciling carbon-cycling concepts, terminology and methods. Ecosystems 9, 1041-1050.

Chen, J., Blume, H., Beyer, L., 2000. Weathering of rocks induced by lichen colonization - a review. Catena 39, 121-146.

Cheng, T., Xu, C., Lei, L., Li, C., Zhang, Y., Zhou, S., 2016. Barcoding the kingdom Plantae: new PCR primers for ITS regions of plants with improved universality and specificity. Mol. Ecol. Resour. 16 138-149.

Chown, S.L., Convey, P., 2007. Spatial and temporal variability across life's hierarchies in the terrestrial Antarctic. Philos. Trans. R. Soc. Lond. Ser. B Biol. Sci. 362(1488), 2307-2331.

Chwedorzewska, K., 2009. Terrestrial Antarctic ecosystems in the changing world: An overview. Pol. Polar Res. 30(3), 263-276.

Clarke, A., Murphy, E., Meredith, M., King, J., Peck, L., Barnes, D., Smith, R., 2007. Climate change and the marine ecosystem of the western Antarctic Peninsula. Phil. Trans. R. Soc. B. 362, 149-166.

Clarke, L., Ayre, D., Robinson, S., 2009. Genetic structure of East Antarctic populations of the moss *Ceratodon purpureus*. Antarct. Sci. 21(1), 51-58.

Clauzad, G., Roux, C., 1985. Likenoj de okcidenta Eŭropo: Ilustrita determinlibro. Bull. Soc. Bot. Cent. Ouestt 7, 1-893.

Coleman, A.W., 2009. Is there a molecular key to the level of 'biological species' in eukaryotes? A DNA guide. Mol. Phylogenet. Evol. 50, 197-203.

Colesie, C., Williams, L., Büdel, B., 2017. Water relations in the soil crust lichen *Psora decipiens* are optimized via anatomical variability. Lichenologist 49(5), 483-492.

Colesie, C., Büdel, B., Hurry, V., Green, T.G.A., 2018. Can Antarctic lichens acclimatize to changes in temperature? Glob. Chang. Biol. 24(3), 1123-1135.

Collins, N.J., 1973. Productivity of selected bryophytes in the maritime Antarctica. In: Bliss, L.C., Wiegolaski, F.E. (Eds.), Proceedings of the conference on primary production and production processes, tundra Biome. IBP Tundra Biome Steering Committee, Edmontom, pp 177-183.

Collins, N.J., 1977. The growth of mosses in two contrasting communities in the maritime Antarctic: Measurement and prediction of net annual production. In: Llano G.A. (Ed.), Adaptations within Antarctic ecosystems. Smithsonian Institution Press, Washington, pp 921-933.

Collins, N.J., Callaghan, T.V., 1980. Predicted patterns of photosynthetic production in maritime Antarctic mosses. Ann. Bot. 45, 601-620.

Collins, M., Knutti, R., Arblaster, J., Dufresne, J.-L., Fichefet, T., Friedlingstein, P., Gao, X., Gutowski, W.J., Johns, T., Krinner, G., Shongwe, M., Tebaldi, C., Weaver, A.J., Wehner, M., 2013. Long-term climate change: projections, commitments and

irreversibility. In: Stocker, T.F., Qin, D., Plattner, G.-K., Tignor, M., Allen, S.K., Boschung, J., Nauels, A., Xia, Y., Bex, V., Midgley, P.M. (Eds.), Climate Change 2013: The Physical Science Basis. Contribution of Working Group I to the Fifth Assessment Report of the Intergovernmental Panel on Climate Change. Cambridge University Press, Cambridge, pp 1029-1136.

Convey, P., 1994. Photosynthesis and dark respiration in Antarctic mosses - an initial comparative study. Polar Biol. 14, 65-69.

Convey, P., 2001. Terrestrial ecosystem responses to climate changes in the Antarctic. In: Walther, G.R., Burga, C.A., Edwards, P.J. (Eds.), 'Fingerprints' of climate change. Springer, Boston, pp 17-42.

Convey, P., 2005. Antarctic terrestrial ecosystems: responses to environmental change. Polarforschung 75, 101-111.

Convey, P., 2013. Antarctic Ecosystems. In: Levin, S.A. (Ed.), Encyclopaedia of biodiversity. Elsevier, San Diego, pp 179-188.

Convey, P., Chown, S.L., Clarke, A., Barnes, D.K.A., Bokhorst, S., Cummings, V., Ducklow, H.W., Frati, F., Green, T.G.A., Gordon, S., Griffiths, H.J., Howard-Williams, C., Huiskes, A.H.L., Laybourn-Parry, J., Lyons, W.B., McMinn, A., Morley, S.A., Peck, L.S., Quesada, A., Robinson, S.A., Schiaparelli, S., Wall, D.H., 2014. The spatial structure of Antarctic biodiversity. Ecol. Monogr. 84, 203-244.

Convey, P., Biersma, E.M., Casanova-Katny, A., Maturana, C.S., 2020. Chapter 10 - refuges of Antarctic diversity. In: Oliva, M., Ruiz-Fernández, J. (Eds.), Past Antarctica. paleo-climatology and climate change. Academic Press, pp 181-200.

Cove, D.J., Knight, C.D., Lamparter, T., 1997. Mosses as model systems. Trends. Plant. Sci. 2, 99-10.

Cove, D.J., Bezanilla, M., Harries, P., Quatrano, R., 2006. Mosses as model systems for the study of metabolism and development. Annu. Rev. Plant. Biol. 57, 497-520.

Culberson, C.F, Culberson, W.L., Esslinger, T.L., 1977. Chemosyndromic variation in the *Parmelia 'pulla* group'. Bryologist 80(1), 125-135.

Csardi, N.T.G., 2015. Igraph: Network analysis and visualization. R package version 1.2.4.1.

Csintalan, Z., Takács, Z., Proctor, M.C.F., Lichtenthaler, H.K., Tuba, Z., 1998. Desiccation and dehydration response of desiccation tolerant moss and lichen species from a temperate semi-desert grassland. J Hattori Bot. Lab. 84, 71-80.

Dal Grande, F., Rolshausen, G., Divakar, P.K., Crespo, A., Otte, J., Schleuning, M., Schmitt, I., 2017a. Environment and host identity structure communities of green algal symbionts in lichens. New Phytol. 217(1), 277-289.

Dal Grande, F., Sharma, R., Meiser, A., Rolshausen, G., Büdel, B., Mishra, B., Thines, M., Otte, J., Pfenninger, M., Schmitt, I., 2017b. Adaptive differentiation coincides with local bioclimatic conditions along an elevational cline in populations of a lichen-forming fungus. BMC Evol. Biol. 17(1), 93.

Dal Grande, F., Rolshausen, G., Divakar, P., Crespo, A., Otte, J., Schleuning, M., Schmitt, I., 2018. Environment and host identity structure communities of green algal symbionts in lichens. New Phytol. 217, 277-289.

Davey, M.C., Pickup, J., Block, W., 1992. Temperature variation and its biological significance in fellfield habitats on a maritime Antarctic island. Antarct. Sci. 4(4), 383-388.

Davey, M.C. 1997a. Effects of continuous and repeated dehydration on carbon fixation by bryophytes from the maritime Antarctic. Oecologia 110, 25-31.

Davey, M.C., 1997b. Effects of short-term dehydration and rehydration on photosynthesis and respiration by Antarctic bryophytes. Environ. Exp. Bot. 37(2-3), 187-198.

Davey, M.C., Rothery, P., 1997. Interspecific variation in respiratory and photosynthetic parameters in Antarctic bryophytes. New Phytol. 137(2), 231-240.

Davis, R.C., 1981. Structure and function of two Antarctic terrestrial moss communities. Ecol. Monogr. 51(2), 125-143.

Davis, R.C., 1983. Prediction of net primary production in two Antarctic mosses by two models of net CO_2 fixation. Br. Antarct. Surv. 59, 47-61.

Del Prado, R., Sancho, L.G., 2000. Water relations and photosynthetic performance of fruticose lichens from the semi-arid southeast of Spain. Flora 195(1), 51-60.

Delgado-Baquerizo, M., Maestre, F.T., Escolar, C., Gallardo, A., Ochoa, V., Gozalo, B., Prado-Comesaña, A., 2014. Direct and indirect impacts of climate change on microbial and biocrust communities alter the resistance of the nitrogen cycle in a semi-arid grassland. J. Ecol. 102(6), 1592-1605.

Domaschke, S., Fernández-Mendoza, F., García, M.A., Martín, M.P., Printzen, C., 2012. Low genetic diversity in Antarctic populations of the lichen-forming ascomycete *Cetraria aculeata* and its photobiont. Polar Res. 31, 17353.

Dormann, C.F., Gruber, B., Fruend, J., 2008. Introducing the bipartite package: Analyzing ecological networks. Trends Ecol. Evol. 8, 8-11.

Duveneck, M.J., Thompson, J.R., 2017. Climate change imposes phenological trade-offs on forest net primary productivity. JGR Biogeosciences 122(9), 2298-2313.

Edgar, R.C., Haas, B.J., Clemente, J.C., Quince, C., Knight, R., 2011. UCHIME improves sensitivity and speed of chimera detection. Bioinformatics 2, 2194-2200.

Edwards, J.A., Smith, R.I.L., 1988. Photosynthesis and respiration of *Colobanthus quitensis* and *Deschampsia antarctica* from maritime Antarctic. Br. Antarct. Surv. Bulletin 81, pp 43-63.

Elbert, W., Weber, B., Burrows, S., Steinkamp, J., Büdel, B., Andreae, M.O., Pöschl, U., 2012. Contribution of cryptogamic covers to the global cycles of carbon and nitrogen. Nat. Geosci. 5, 459-462.

Ertz, D., Guzow-Krzemińska, B., Thor, G., Łubek, A., Kukwa, M., 2018. Photobiont switching causes changes in the reproduction strategy and phenotypic dimorphism in the Arthoniomycetes. Sci. Rep. 8(1), 4952.

Escudié, F., Auer, L., Bernard, M., Mariadassou, M., Cauquil, L., Vidal, K., Maman, S., Hernandez-Raquet, G., Combes, S., Pascal, G., 2018. FROGS: Find, Rapidly, OTUs with Galaxy Solution. Bioinformatics 34, 1287-1294.

Esslinger, T.L., 1977. A chemosystematic revision of the brown Parmeliae. J. Hattori Bot. Lab. 42, 1-211.

Ezard, T., Fujisawa, T., Barraclough, T.G., 2009. Splits: Species' limits by threshold statistics. R package version. R Foundation for Statistical Computing. http://R-Forge.R-project.org/projects/splits/

Fang, G.H., Yang, J., Chen, Y.N., Zammit, C., 2015. Comparing bias correction methods in downscaling meteorological variables for a hydrologic impact study in an arid area in China. Hydrol. Earth Syst. Sci. 196, 2547-2559.

Fasiolo, M., Nedellec, R., Goude, Y., Wood, S.N., 2020. Visualisations for Generalized Additive Models. Retrieved from. https://cran.r-project.org/web/packages/mgcViz/mgcViz.pdf.

Feng, W., Zhang, Y., Wu, B., Qin, S., Lai, Z., 2014. Influence of environmental factors on carbon dioxide exchange in Biological Soil Crusts in desert areas. Arid. Land Res. Manag. 28, 186-196.

Fernández-Mendoza, F., Domaschke, S., García, M.A., Jordan, P., Martín, M.P., Printzen, C., 2011. Population structure of mycobionts and photobionts of the widespread lichen Cetraria aculeata. Mol. Ecol. 20(6), 1208-1232.

Ferrenberg, S., Reed, S.C., Belnap, J., 2015. Climate change and physical disturbance cause similar community shifts in Biological Soil Crusts. Proc. Natl. Acad. Sci. U.S.A. 112(39), 12116-12121.

Flato, G., Marotzke, J., Abiodun, B., Braconnot, P., Chou, S.C., Collins, W., CoX, P., Driouech, F., Emori, S., Eyring, V., Forest, C., Gleckler, P., Guilyardi, E., Jakob, C., Kattsow, V., Reason, C., Rummukainen, M., 2013. Evaluation of climate models. In: Stocker, T.F., Qin, D., Plattner, G.-K., Tignor, M., Allen, S.K., Boschung, J., Nauels, A., Xia, Y., Bex, V., Midgley, P.M. (Eds.), Climate Change 2013: The Physical Science Basis. Contribution of Working Group I to the Fifth Assessment Report of the Intergovernmental Panel on Climate Change. Cambridge University Press, Cambridge, pp 741-866.

Fracheboud, Y., 2004. Using chlorophyll fluorescence to study photosynthesis. Institute of Plant Science ETH. Universitatstrass CH-8092 Zurich.

Fujisawa, T., Barraclough, T.G., 2013. Delimiting species using single-locus data and the Generalized Mixed Yule Coalescent approach: a revised method and evaluation on simulated data sets. Syst. Biol. 62(5), 707-724.

Gardes, M., Bruns, T.D., 1993. ITS primers with enhanced specificity for basidiomycetes - application to the identification of mycorrhizae and rusts. Mol. Ecol. 2(2), 113-118.

Giordani, P., Brunialti, G., Bacaro, G., Nascimbene, J., 2012. Functional traits of epiphytic lichens as potential indicators of environmental conditions in forest ecosystems. Ecol. Indic. 18, 413-420.

Giordani, P., Incerti, G., Rizzi, G., Rellini, I., Nimis, P., Modenesi, P., Güsewell, S., 2014. Functional traits of cryptogams in Mediterranean ecosystems are driven by water, light and substrate interactions. J. Veg. Sci. 25(3), 778-792.

Gloor, G.B., Hummelen, R., Macklaim, J.M., Dickson, R.J., Fernandes, A.D., MacPhee, R., Reid, G., 2010. Microbiome profiling by Illumina sequencing of combinatorial sequence-tagged PCR products. PloS One 5, e15406.

Gonzalez, S., Fortuny, D., 2018. How robust are the temperature trends on the Antarctic Peninsula? Antarct. Sci. 30(5), 322-328.

Green T.G.A., Lange O.L., 1995. Photosynthesis in poikilohydric plants: A comparison of lichens and bryophytes. In: Schulze, E.D., Caldwell, M.M. (Eds.), Ecophysiology of photosynthesis. Springer Study Edition, Berlin, pp 319-341.

Green, T.G.A., Büdel, B., Meyer, A., Zellner, H., Lange, O.L., 1997. Temperate rainforest lichens in New Zealand: light response of photosynthesis. N.Z. J. Bot. 35, 493-504.

Green, T.G.A., Schroeter, B., Seppelt, R.D., 2000. Effect of temperature, light and ambient UV on the photosynthesis of the moss *Bryum argenteum* Hedw. in continental Antarctica. In: Davison, W., Howard-Williams, C., Broady, P., (Eds.), Antarctic ecosystems: models of wider ecological understanding. Caxton Press, Christchurch, 165-170.

Green, T.G.A., Kulle, D., Pannewitz, S., Sancho, L.G., Schroeter, B., 2005. UV-A protection in mosses growing in continental Antarctica. Polar Biol. 28, 822-827.

Green, T.G.A., Schroeter, B., Sancho, L.G., 2007. Plant life in Antarctica. In: Pugnaire, F., Valladares, F. (Eds.), Functional plant ecology. CRC-Press, Boca Raton, pp 389-433.

Green, T.G.A., Nash, T., Lange, O.L., 2008. Physiological ecology of carbon dioxide exchange. In: Nash, T. (Ed.), Lichen biology. Cambridge University Press, Cambridge, pp 152-181.

Green, T.G.A., Sancho, L.G., Pintado, A., 2011. Ecophysiology of desiccation/rehydration cycles in mosses and lichens. In: Luttge, U., Beck, E., Bartels, D. (Eds.), Plant desiccation tolerance. Springer-Verlag, Heidelberg, pp 89-120.

Green, T.G.A., Proctor, M.C.F., 2016. Physiology of photosynthetic organisms within Biological Soil Crusts: Their adaptation, flexibility, and plasticity. In: Weber, B., Büdel, B., Belnap, J. (Eds.), Biological Soil Crusts: An organizing principle in drylands. Springer, Cham, pp 347-381.

Green, T.G.A., Pintado, A., Raggio, J., Sancho, L.G., 2018. The lifestyle of lichens in soil crusts. Lichenologist 50(3), 397-410.

Grote, E.E., Belnap, J., Housman, D.C., Sparks, J.P., 2010. Carbon exchange in Biological Soil Crusts communities under differential temperatures and soil water contents: Implications for global change. Glob. Chang. Biol. 16(10), 2763-2774.

Grube, M., Hawksworth, D.L., 2007. Trouble with lichen: the re-evaluation and re-interpretation of thallus form and fruit body types in the molecular era. Mycol. Res. 111(Pt9), 1116-1132.

Grube, M., Berg, G., Andrésson, O.S., Vilhelmsson, O., Dyer, P.S., Miao, V.P.W., Mia, V.W.P., 2013. Lichen genomics: prospects and progress. In: Martin, F. (Ed.), The ecological genomics of fungi. Wiley Blackwell, New Jersey, pp 191-212.

Guglielmin, M., Worland, M.R., Cannone, N., 2012. Spatial and temporal variability of ground surface temperature and active layer thickness at the margin of maritime Antarctica, Signy Island. Geomorphology 155-156, 20-33.

Gutiérrez, L., Casares, M., 1994. Flora liquénica de los yesos miocénicos de la provincia de Almería (España). Candollea 49, 343-358.

Gutiérrez, G., Blanco, O., Divakar, P.K., Lumbsch, H.T., Crespo, A., 2007. Patterns of group I intron presence in nuclear SSU rDNA of the lichen family *Parmeliaceae*. J. Mol. Evol. 64(2), 181-195.

Guzow-Krzemińska, B., 2006. Photobiont flexibility in the lichen *Protoparmeliopsis muralis* as revealed by ITS rDNA analyses. Lichenologist 38, 469-476.

Harrisson, P., Walton, D., Rothery, P., 1986. The effects of temperature and moisture on dark respiration in the foliose lichen *Umbilicaria antarctica*. New Phytol. 103, 443-455.

Harrisson, P.M., Rothery, P., 1988. Net CO_2 exchange in relation to thallus moisture and temperature in two fruticose lichens *Usnea antarctica* and *Usnea aurantiaco-atra* from the maritime Antarctic. Polarforschung 58(2-3), 171-179.

Harrisson, P., Walton, D., Rothery, P., 1989. The effects of temperature and moisture on CO2 uptake and total resistance to water loss in the Antarctic foliose lichen *Umbilicaria antarctica*. New Phytol. 111(4), 673-682.

He, X., He, K. S., Hyvönen, J., 2016. Will bryophytes survive in a warming world? Perspect. Plant Ecol. Evol. Syst. 19, 49-60.

Hicklenton, P.R., Oechel, W.C. 1976. Physiological aspects of the ecology of *Dicranum fuscescens* in the subarctic. I. Acclimation and acclimation potential of CO2 exchange in relation to habitat, light, and temperature. Canad. J. Bot. 54(10), 1104-1119.

Hodkinson, B.P., Lendemer, J.C., 2013. Next-generation sequencing reveals sterile crustose lichen phylogeny. Mycosphere 4(6), 1028-1039.

Hoffman, G.R., Gates, D.M., 1970. An energy budget approach to the study of water loss in cryptogams. J. Torrey Bot. Soc. 97(6), 361-366.

Holmes, R.M., Dingle, A.N., 1965. The relationship between the macro- and microclimate. Agric. Meteorol. 2(2), 127-133.

Hooker, T.N., 1980. Growth and production of *Usnea antarctica* and *U. fasciata* on Signy Island, South Orkney Islands. Br. Antarct. Surv. Bulletin. 50, pp 35-49.

Hülber, K., Wessely, J., Gattringer, A., Moser, D., Kuttner, M., Essl, F., Leitner, M., Winkler, M., Ertl, S., Willner, W., Kleinbauer, I., Sauberer, N., Mang, T., Zimmermann, N.E., Dullinger, S., 2016. Uncertainty in predicting range dynamics of endemic alpine plants under climate warming. Glob. Chang. Biol. 22(7), 2608-2619.

Ino, Y., 1983a. Estimation of primary production in moss community on East Ongul Island, Antarctica. Geography, 30-38.

Ino, Y., 1983b. Photosynthesis and primary production in moss community at Syowa Station, Antarctica. Jap J Ecol, 33: 427-433.

Ino, Y., 1990a. Comparison of net photosynthesis and dark respiration of Antarctic mosses measured in the Antarctic and in Japan. Proc. NIPR. Symp. Polar. Biol. 3, 245-253.

Ino, Y., 1990b. Field measurement of net photosynthesis of mosses at Langhovde East Antarctica. Ecol. Res. 5, 195-205.

Ino, Y., 1994. Field measurement of the photosynthesis of mosses with a portable CO_2 porometer at Langhovde, East Antarctica. Antarct. Rec. 38(2), 178-184.

Inoue, T., Kudoh, S., Uchida, M., Tanabe, Y., Inoue, M., Kanda, H., 2014. Effects of substrate differences on water availability for Arctic lichens during the snow-free summers in the High Arctic glacier foreland. Polar Sci. 8, 397-412.

Insarov, G., Schroeter, B., 2002. Lichen monitoring and climate change. In: Nimis, P.L., Scheidegger, C., Wolseley, P.A. (Eds.), Monitoring with lichens. Springer, Dordrecht, pp 183-201.

James, P.W., Henssen, A., 1976. The morphological and taxonomic significance of cephalodia. In: Brown, D.H., Hawksworth, D.L., Bailey, R.H. (Eds.), Lichenology: Progress and problems. Academic Press, London, pp 27-77.

Jensen, M., 2002. Measurement of chlorophyll fluorescence in lichens. In: Kranner, I.C., Beckett, R.P., Varma, A.K. (Eds.), Protocols in lichenology. Springer, Berlin, pp 135-151.

Jules, E.S., Shaw, A.J., 1994. Adaptation to metal-contaminated soils in populations of the moss, *Ceratodon purpureus*: vegetative growth and reproductive expression. Am. J. Bot. 81, 791-797.

Kanda, H., 1979. Regenerative development in culture of Antarctic plants *Ceratodon purpureus* (Dew.) Brid. Mem. Natl. Inst. Pol. Res. Spec. Issue. 11, 58-69.

Kappen, L., Lange, O.L., Schulze, E.-D., Evenari, M., Buschbom, U., 1979. Eco-physiological investigations on lichens of the Negev desert. VI. Annual course of photosynthetic production of *Ramalina maciformis* (Del). Bory. Flora 168, 85-108.

Kappen, L., 1983. Ecology and physiology of the Antarctic fruticose lichen *Usnea sulphurea* (Koenig) Th. Fries. Polar Biol. 1, 249-255.

Kappen, L., 1985. Water relations and net photosynthesis of *Usnea.* A comparison between *Usnea fasciata* (maritime Antarctic) and *Usnea sulphurea* (continental Antarctic). Lichen Physiology and Cell Biology, 41-56.

Kappen, L., Redon, J., 1987. Photosynthesis and water relations of three maritime Antarctic lichen species. Flora 179(3), 215-229.

Kappen, L., 1988. Eco-physiological relationships in different climatic regions. In: Galun, M. (Ed.), Handbook of lichenology. CRC-Press, Florida, pp 37-100.

Kappen, L., Meyer, M., Bölter, M., 1988. Photosynthetic production of the lichen *Ramalina terebrata* Hook. f. et Tayl., in the maritime Antarctic. Polarforschung, 58(213), 181-188.

Kappen, L., 1989. Field measurements of carbon dioxide exchange of the Antarctic lichen *Usnea sphacelata* in the frozen state. Antarct. Sci. 1(1), 31-34.

Kappen, L., Smith, R.I.L., Meyer, M., 1989. Carbon dioxide exchange of two ecodemes of *Schistidium antarctici* in continental Antarctica. Polar. Biol. 9, 415-422.

Kappen, L., Breuer, M. 1991. Ecological and physiological investigations in continental Antarctic cryptogams. II. Moisture relations and photosynthesis of lichens near Casey Station, Wilkes Land. Antarct. Sci. 3(3), 273-278.

Kappen, L., Sommerkorn, M., Schroeter, B., 1995. Carbon acquisition and water relations of lichens in polar regions — potentials and limitations. Lichenologist 27(6), 531-545.

Kappen, L., Schroeter, B., 1997. Activity of lichens under the influence of snow and ice. Polar Biol. 10, 163-168.

Kappen, L., 2000. Some aspects of the great success of lichens in Antarctica. Antarct. Sci. 12(3), 314-324.

Kappen, L., Valladares, F., 2007. Opportunistic growth and desiccation tolerance, the ecological success of the poikilohydrous strategy. In: Pugnaire, F.I., Valladares, F. (Eds.), Functional plant ecology. CRC Press/Taylor & Francis, Boca Raton, pp 7-65.

Katoh, K., Standley, D.M., 2013. MAFFT multiple sequence alignment software version 7: improvements in performance and usability. Mol. Biol. Evol. 30(4), 772-780.

Kennedy, A.D., 1993. Water as a limiting factor in the Antarctic terrestrial environment: a bio-geographical synthesis. Arct. Alp. Res. 25(4), 308-315.

Kennedy, A.D., 1995. Antarctic terrestrial ecosystem response to global environmental change. Annu. Rev. Ecol. Evol. Syst. 26, 683-704.

Kidron, G.J., Lázaro, R., 2020. Are coastal deserts necessarily dew deserts? An example from the Tabernas Desert. J. Hydrol. Hydromech. 68, 19-27.

Kirschbaum, M., 1995. The temperature dependence of soil organic matter decomposition, and the effect of global warming on soil organic C storage. Soil Biol. Biochem. 27(6), 753-760.

Koch, N.M., Matos, P., Branquinho, C., Pinho, P., Lucheta, F., Martins, S., Vargas, V., 2019. Selecting lichen functional traits as ecological indicators of the effects of urban environment. Sci. Total Environ. 654, 705-713.

Körner, C., 2003. Alpine plant life. Springer, Berlin Heidelberg New York.

Krohn, A., Stevens, B., Robbins-Pianka, A., Belus, M., Allan, G.J., Gehring, C., 2016. Optimization of 16S amplicon analysis using mock communities: implications for estimating community diversity. PeerJ Prepr. 4, e2196v3.

Kunkel, G., 1980. Microhabitat and structural variation in the *Aspicilia desertorum* group (lichenized Ascomycetes). Am. J. Bot. 67, 1137-1144.

Ladrón de Guevara, M., Lázaro, R., Quero, J.L., Ochoa, V., Gozalo, B., Berdugo, M., Uclés, O., Escolar, C., Maestre, F.T., 2014. Simulated climate change reduced the capacity of lichen-dominated biocrusts to act as carbon sinks in two semi-arid Mediterranean ecosystems. Biodivers. Conserv. 23(7), 1787-1807.

Lafuente, A., Berdugo, M., Ladrón de Guevara, M., Gozalo, B., Maestre, F.T., 2018. Simulated climate change affects how biocrusts modulate water gains and desiccation dynamics after rainfall events. Ecohydrology 11, e1935.

Laguna-Defior, C., 2016. Ecofisiología y diversidad molecular de los líquenes neuropogonoides del género *Usnea* en Tierra del Fuego y la Antártida marítima. Universidad Complutense de Madrid. PhD Thesis.

Laguna-Defior, C., Pintado, A., Green, T.G.A., Blanquer, J.M., Sancho, L.G., 2016. Distributional and eco-physiological study on the Antarctic lichens species pair *Usnea antarctica/Usnea aurantiaco-atra*. Polar Biol. 39(7), 1183-1195.

Lange, O.L., Bertsch, A., 1965. Photosynthese der Wüstenflechte Ramalina maciformis nach Wasserdampfaufnahme aus dem Luftraum. Naturwissenschaften 52, 215-216.

Lange, O.L., Green, T.G.A., Ziegler, H., 1988. Water status related photosynthesis and carbon isotope discrimination in species of the lichen genus *Pseudocyphellaria* with green or blue-green photobionts and in photosymbiodemes. Oecologia 75, 494-501.

Lange, O.L., Meyer, A., Zellner, H., Ullmann, I. Wessels, D.C.J., 1990. Eight days in the life of a desert lichen: water relations and photosynthesis of *Teloschistes capensis* in the coastal fog zone of the Namib Desert. Madoqua 17(1), 17-30.

Lange, O.L., Meyer, A., Zellner, H., Heber, U., 1994. Photosynthesis and water relations of lichen soil crusts: field measurements in the coastal fog zone of the Namib Desert. Funct. Ecol. 8(2), 253-264.

Lange, O.L., Green, T.G.A., 1996. High thallus water content severely limits photosynthetic carbon gain of central European epilithic lichens under natural conditions. Oecologia 108(1), 13-20.

Lange, O.L., Green, T.G.A., Melzera, B. Meyera, A., Zellner, H., 1996. Water relations and CO2 exchange of the terrestrial lichen *Teloschistes capensis* in the Namib fog desert: Measurements during two seasons in the field and under controlled conditions. Flora 201, 268-280.

Lange, O.L., Belnap, J., Reichenberger, H., Meyer, A., 1997. Photosynthesis of green algal soil crust lichens from arid lands in southern Utah, USA: Role of water content on light and temperature responses of CO_2 exchange. Flora 192(1), 1-15.

Lange, O.L., Green, T.G.A., Reichenberger, H., 1999. The response of lichen photosynthesis to external CO_2 concentration and its interaction with thallus water-status. J. Plant Physiol. 154, 157-166.

Lange, O.L., 2001. Photosynthesis of soil-crust biota as dependent on environmental factors. In: Belnap, J., Lange, O.L. (Eds.), Biological Soil Crusts: Structure, function, and management. Springer, Berlin, pp 217-240.

Lange, O.L., Green, T.G.A., Heber, U., 2001. Hydration-dependent photosynthetic production of lichens: what do laboratory studies tell us about field performance? J. Exp. Bot. 52(363), 2033-2042.

Lange, O.L., 2002. Photosynthetic productivity of the epilithic lichen *Lecanora muralis*: long term field monitoring of CO_2 exchange and its physiological interpretation. I. Dependence of photosynthesis on water content, light, temperature, and CO_2 concentration from laboratory measurements. Flora 197, 233-249.

Lange, O.L., 2003. Photosynthetic productivity of the epilithic lichen *Lecanora muralis*: long-term field monitoring of CO_2 exchange and its physiological interpretation. III. Diel, seasonal, and annual carbon budgets. Flora 198, 277- 292.

Lange, O.L., Wagenitz, G., 2004. Vernon Ahmadjian introduced the term 'chlorolichen'. Lichenologist, 36(2), 171-171.

Lange, O.L., Green, T.G.A., 2005. Lichens show that fungi can acclimate their respiration to seasonal changes in temperature. Oecologia 142(1), 11-19.

Larena, I., Salazar, O., González, V., Julián, M.C., Rubio. V., 1999. Design of a primer for ribosomal DNA internal transcribed spacer with enhanced specificity for ascomycetes. J. Biotechnol. 75(2-3), 187-194.

Larigauderie, A., Körner, C., 1995. Acclimation of leaf dark respiration to temperature in alpine and lowland plant species. Ann. Bot. 76, 245-252.

Larson, D.W., Kershaw, K.A., 1975. Acclimation in arctic lichens. Nature 254, 421-423.

Lázaro, R., Cantón, Y., Solé-Benet, A., Bevan, J., Alexander, R., Sancho, L.G., Puigdefabregas, J., 2008. The influence of competition between lichen colonization and erosion on the evolution of soil surfaces in the Tabernas badlands (SE Spain) and its landscape effects. Geomorphology 102(2), 252-266.

Leavitt, S.D., Johnson, L.A., Goward, T., St. Clair, L.L., 2011a. Species delimitation in taxonomically difficult lichen-forming fungi: an example from morphologically and chemically diverse *Xanthoparmelia* (Parmeliaceae) in North America. Mol. Phylogenet. Evol. 60(3), 317-332.

Leavitt, S.D., Johnson, L., Clair, L., 2011b. Species delimitation and evolution in morphologically and chemically diverse communities of the lichen-forming genus *Xanthoparmelia* (Parmeliaceae, Ascomycota) in Western North America. Am. J. Bot. 98(2), 175-188.

Leavitt, S.D., Kraichak, E., Nelsen, M.P., Altermann, S., Divakar, P.K., Alors. D., Esslinger, T.L., Crespo, A., Lumbsch, T., 2015. Fungal specificity and selectivity for algae play a major role in determining lichen partnerships across diverse eco-geographic regions in the lichen-forming family *Parmeliaceae* (Ascomycota). Mol. Ecol. 24(14), 3779-3797.

Leavitt, S.D., Kirika, P., Amo de Paz, G., Huang, J., Hur, J., Elix, J., Grewe, F., Divakar, P.K., Lumbsch, H.T., 2018. Assessing phylogeny and historical biogeography of the largest genus of lichen-forming fungi, *Xanthoparmelia* (Parmeliaceae, Ascomycota). Lichenologist 50(3), 299-312.

Lee, J.R., Raymond, B., Bracegirdle, T.J., Chadès, I., Fuller, R.A., Shaw, J.D., Terauds, A., 2017. Climate change drives expansion of Antarctic ice-free habitat. Nature 547(7661), 49-54.

Leigh, J., Bryant, D., 2015. PopArt: full-feature software for haplotype network construction. Methods Ecol. Evol. 6, 1110-1116.

Lekouch, I., Muselli, M., Kabbachi, B., Ouazzani, J., Melnytchouk-Milimouk, I., Beysens, D., 2011. Dew, fog, and rain as supplementary sources of water in southwestern Morocco. Energy 36(4), 2257-2265.

Lenné, T., Bryant, G., Hocart, C.H., Huang, C.X., Ball, M.C., 2010. Freeze avoidance: a dehydrating moss gathers no ice. Plant. Cell. Environ. 33(10), 1731-1741.

Longton, R.E., 1970. Growth and productivity of the moss *Polytrichum alpestre* Hoppe in Antarctic regions. In: Holdgate, M.W. (Ed.), Antarctic Ecology. Academic Press, London, pp 818-837.

Longton, R.E., 1988. Biology of polar bryophytes and lichens. Cambridge University Press, Cambridge.

Love, M.I., Huber, W., Anders, S., 2014. Moderated estimation of fold change and dispersion for RNA-seq data with DESeq2. Genome Biol. 15, 550.

Lovelock, C.E., Jackson, A.E., Melick, D.R. Seppelt, R., 1995a. Reversible photo-inhibition in Antarctic moss during freezing and thawing. Plant Physiol. 109, 955-961.

Lovelock, C.E., Osmond, C.B. Seppelt, R.D., 1995b. Photo-inhibition in the Antarctic moss *Grimmia antarctici* Card. when exposed to cycles of freezing and thawing. Plant Cell Environ. 18, 1395-1402.

Lovelock, C., Robinson, S., 2002. Surface reflectance properties of Antarctic moss and their relationship to plant species, pigment composition and photosynthetic function. Plant. Cell. Environ. 25(10), 1239-1250.

Lud, D., Moerdijik, T.C.W., Van de poll, W.H., Buma, A.G.J., Huiskes, A.H.L., 2002. DNA damage and photosynthesis in Antarctica and Arctic *Sanionia uncinata* (Hedw.) Loeske under ambient and enhanced levels of UV-B radiation. Plant Cell Environ. 25, 1579-1589.

Lud, D., Schlensog, M., Schroeter, B., Huiskes, A.H.L., 2003. The influence of UV-B radiation on light dependent photosynthetic performance in *Sanionia unicinata* (Hedw.) Loeske in Antarctica. Polar Biol. 26, 225-232.

Lutsak, T., Fernández-Mendoza, F., Kirika, P., Wondarash, M., Printzen, C., 2016. Mycobiont-photobiont interactions of the lichen *Cetraria aculeata* in high alpine regions of East Africa and South America. Symbiosis 68, 25-37.

Lutzoni, F., Miadlikowska, J., 2009. Lichens. Curr. Biol. 19(13), R502-R503.

Maestre, F.T., Escolar, C., Ladrón de Guevara, M., Quero, J.L., Lázaro, R., Delgado-Baquerizo, M., Ochoa, V., Berdugo, M., Gozalo, B., Gallardo, A., 2013. Changes in

biocrust cover drive carbon cycle responses to climate change in drylands. Glob. Change Biol. 19(12), 3835-3847.

Mahé, F., Rognes, T., Quince, C., Vargas, C., Dunthorn, M., 2015. Swarm v2: highly-scalable and high-resolution amplicon clustering. PeerJ 3, e1420.

Maphangwa, K.W., Musil, C.F., Raitt, L., Zedda, L., 2012. Differential interception and evaporation of fog, dew and water vapour and elemental accumulation by lichens explain their relative abundance in a coastal desert. J. Arid Environ. 82, 71e80.

Maraun, D., 2016. Bias correcting climate change simulations - a critical review. Curr. Clim. Chang. Rep. 2(4), 211-220.

Marks, D., Winstral, A., Reba, M., Pomeroy, J., Kumar, M., 2013. An evaluation of methods for determining during-storm precipitation phase and the rain/snow transition elevation at the surface in a mountain basin. Adv. Water Resour. 55, 98-110.

Marschall, M., 2017. Ecophysiology of bryophytes in the changing environment. Acta. Biol. Plant. Agriensis. 5(2), 61-70.

Masella, A.P., Bartram, A.K., Truszkowski, J.M., Brown, D.G., Neufeld, J.D., 2012. PANDAseq: PAired-eND Assembler for Illumina sequences. BMC Bioinform. 13-31.

Matos, P.M., Pinho, P., Aragón, G., Martínez, I., Nunes, A., Soares, A.M., Branquinho, C., 2015. Lichen traits responding to aridity. J. Ecol. 103, 451-458.

Maxwell, K., Johnson, G.N., 2000. Chlorophyll fluorescence - a practical guide. J. Exp. Bot. 51(345), 659-668.

McDaniel, S.F., Shaw, A.J., 2005. Selective sweeps and intercontinental migration in the cosmopolitan moss *Ceratodon purpureus* (Hedw.) Brid. Mol. Ecol. 14(4), 1121-1132.

Midgley, G.F., Veste, M., Willert, D.J., Davis, G.W., Steinberg, M., Powrie, L.W., 1997. Comparative field performance of three different gas exchange systems. Bothalia 271, 83-89.

Miller, M, Pfeiffer, W., Schwartz, T., 2010. Creating the CIPRES Science Gateway for inference of large phylogenetic trees. Gateway Computing Environments Workshop (GCE), 1-8.

Molina-Montenegro, M.A., Carrasco-Urra, F., Acuña-Rodriguez, I., Oses, R., Torres-Diaz, C., Chwedorzewska, K.J., 2014. Assessing the importance of human activities for the establishment of the invasive *Poa annua* in Antarctica. Polar Res. 33, 1-7.

Molina-Montenegro, M.A., Galleguillos, C., Oses, R., Acuña-Rodríguez, I.S., Lavín, P., Gallardo-Cerda, J., Torres-Díaz, C., Diez, B., Pizarro, G.E., Atala, C., 2016. Adaptive

phenotypic plasticity and competitive ability deployed under a climate change scenario may promote the invasion of *Poa annua* in Antarctica. Biol. Invasions 18(3), 603-618.

Moya, P., Chiva, S., Molins, A., Jadrná, I., Skaloud, P., Peksa, O., Barreno, E., 2018. *Myrmecia israeliensis* as the primary symbiotic microalga in squamulose lichens growing in European and Canary Island terricolous communities. Fottea 18, 72-85.

Muggia, L., Pérez-Ortega, S., Fryday, A., Spribille, T., Grube, M., 2014. Global assessment of genetic variation and phenotypic plasticity in the lichen-forming species *Tephromela atra*. Fungal Divers. 64, 233-251.

Muggia, L., Candotto-Carniel, F., Grube, M., 2016. The lichen photobiont *Trebouxia*: Towards and appreciation of species diversity and molecular studies. In: Grube, M., Seckbach, J., Muggia, L. (Eds.), Algal and cyanobacteria symbioses. World Scientific, London, pp 111-146.

Murchie, E.H., Lawson, T., 2013. Chlorophyll fluorescence analysis: a guide to good practice and understanding some new applications. J. Exp. Bot. 64(13), 3983-3998.

Myllys, L., Lohtander, K., Tehler, A., 2001. *β-tubulin*, ITS and group I intron sequences challenge the species pair concept in *Physcia aipolia* and *P. caesia*. Mycologia 93, 335-343.

Nakatsubo, T., 2002. Predicting the impact of climatic warming on the carbon balance of the moss *Sanionia uncinata* on a maritime Antarctic island. J. Plant Res. 115, 0099-0106.

Navarro-Racines, C., Tarapues, J., Thornton, P., Jarvis, A., Ramirez-Villegas, J., 2020. High-resolution and bias-corrected CMIP5 projections for climate change impact assessments. Sci. Data 7(1), 7.

Nicotra, A.B., Atkin, O.K., Bonser, S.P., Davidson, A.M., Finnegan, E.J., Mathesius, U., Poot, P., Purugganan, M.D., Richards, C.L., Valladares, F., van Kleunen, M., 2010. Plant phenotypic plasticity in a changing climate. Trends Plant. Sci. 15(12), 684-692.

Niinemets, U., Valladares, F., 2004. Photosynthetic acclimation to simultaneous and interacting environmental stresses along natural light gradients: optimality and constraints. Plant. Biol. 6(3), 254-268.

Nimis, P.L., Martellos, S., 2021. ITALIC - The Information System on Italian Lichens. Version 5.0. University of Trieste, Dept. of Biology, (http://dryades.units.it/italic), accessed on 2021/09/06.

Ochyra, R., Smith, R.I.L., Bednarek-Ochyra, H., 2008. The illustrated moss flora of Antarctica. Cambridge University Press, Cambridge.

Oechel, W.C., 1976. Seasonal patterns of temperature response of CO_2 flux and acclimation in arctic mosses growing *in situ*. Photosynthetica 10, 447-456.

Oksanen, J., Blanchet, F.G., Friendly, M., Kindt, R., Legendre, P., McGlinn, D., Minchin, P.R., O'Hara, R.B., Simpson, G.L., Solymos, P., Henry, M., Stevens, H., Szoecs, E., Wagner, H., 2017. Vegan: community ecology package. R package version 2.2-1.

Oliva, M., Navarro, F., Hrbáček, F., Hernández, A., Nývlt, D., Pereira, P., Ruiz-Fernández, J., Trigo, R., 2017. Recent regional climate cooling on the Antarctic Peninsula and associated impacts on the cryosphere. Sci. Total Environ. 580, 210-223.

Oliver, M.J., Velten, J., Mishler, B.D., 2005. Desiccation tolerance in bryophytes: A reflection of the primitive strategy for plant survival in dehydrating habitats. Integr. Comp. Biol. 45, 788-799.

Onuț-Brännström, I., Benjamin, M., Scofield, D.G., Heiðmarsson, S., Andersson, M., Lindström, E.S., Johannesson, H., 2018. Sharing of photobionts in sympatric populations of *Thamnolia* and *Cetraria* lichens: evidence from high-throughput sequencing. Sci. Rep. 8(1), 4406.

Osyczka, P., Rola, K., Lenart-Boroń, A., Boroń, P., 2014. High intraspecific genetic and morphological variation in the pioneer lichen *Cladonia rei* colonising slag dumps. Cent. Eur. J. Biol. 9, 579-591.

Osyczka, P., Boroń, P., Lenart-Boroń, A., Rola, K., 2018. Modifications in the structure of the lichen *Cladonia* thallus in the aftermath of habitat contamination and implications for its heavy-metal accumulation capacity. Environ. Sci. Pollut. Res. 25(2), 1950-1961.

Øvstedal, D.O., Smith, R.L.I., 2001. Lichens of Antarctica and South Georgia: A guide to their identification and ecology. Cambridge University Press.

Pannewitz, S., Green, T.G.A., Scheidegger, C., Schlensog, M., Schroeter, B., 2003a. Activity pattern of the moss *Hennediella heimii* (Hedw.) Zand. in the Dry Valleys, southern Victoria Land, Antarctica, during the mid-austral summer. Polar. Biol. 26, 545-551.

Pannewitz, S., Schlensog, M., Green, T.G.A., Sancho, L.G., Schroeter, B., 2003b. Are lichens active under snow in continental Antarctica? Oecologia 135(1), 30-38.

Pannewitz, S., Green, T.G.A., Maysek, K., Schlensog, M., Seppelt, R., Sancho, L.G., Türk, R., Schroeter, B., 2005. Photosynthetic responses of three common mosses from continental Antarctica. Antarct. Sci. 17(03), 341-352.

Pannewitz, S., Green, T.G.A., Schlensog, M., Seppelt, R., Sancho, L.G., Schroeter, B., 2006. Photosynthetic performance of *Xanthoria mawsonii* C. W. Dodge in coastal habitats, Ross Sea region, continental Antarctica. Lichenologist 38(1), 67-81.

Paoli, L., Pinho, P., Branquinho, C., Loppi, S., Munzi, S., 2017. The influence of growth form and substrate on lichen eco-physiological responses along an aridity gradient. Environ. Sci. Pollut. Res. 24(34), 26206-26212.

Papaioannou, G., Papanikolaou, N., Retalis, D., 1993. Relationships of photosynthetically active radiation and shortwave irradiance. Theor. Appl. Climatol. 48, 23-27.

Paul, F., Otte, J., Schmitt, I., Dal Grande, F., 2018. Comparing Sanger sequencing and high-throughput meta-barcoding for inferring photobiont diversity in lichens. Sci. Rep. 8(1), 8624.

Peat, H.J., Clarke, A., Convey, P., 2007. Diversity and biogeography of the Antarctic flora. J. Biogeogr. 34, 132-146.

Perera-Castro, A.V., Waterman, M.J., Turnbull, J.D., Ashcroft, M.B., McKinley, E., Watling, J.R., Bramley-Alves, J., Casanova-Katny, A., Zuniga, G., Flexas, J., Robinson, S.A., 2020. It is hot in the sun: Antarctic mosses have high temperature optima for photosynthesis despite cold climate. Front. Plant Sci. 11, 1178.

Perera-Castro, A.V., Flexas, J., González-Rodríguez, Á.M., Fernández-Marín, B., 2021. Photosynthesis on the edge: photo-inhibition, desiccation and freezing tolerance of Antarctic bryophytes. Photosynth. Res. 149, 135-153.

Pérez-Ortega, S., Fernández-Mendoza, F., Raggio, J., Vivas, M., Ascaso, C., Sancho, L.G., Printzen, C., de Los Ríos, A., 2012. Extreme phenotypic variation in *Cetraria aculeata* (lichenized Ascomycota): adaptation or incidental modification? Ann. Bot. 109(6), 1133-1148.

Pharo, E.J., Beattie, A.J., 2002. The association between substrate variability and bryophyte and lichen diversity in eastern Australian forests. Bryologist 105(1), 11-26.

Phinney, N.H., Solhaug, K.A., Gauslaa, Y., 2018. Rapid resurrection of chlorolichens in humid air: specific thallus mass drives rehydration and reactivation kinetics. Environ. Exp. Bot. 148, 184-191.

Pino-Bodas, R., Burgaz, A.R., Martín, M.P., Lumbsch, H.T., 2011. Phenotypical plasticity and homoplasy complicate species delimitation in the *Cladonia gracilis* group (Cladoniaceae, Ascomycota). Org. Divers. Evol. 11(5), 343-355.

Pintado, A., Valladares, F., Sancho, L.G., 1997. Exploring phenotypic plasticity in the lichen *Ramalina capitata*: Morphology, water relations and chlorophyll content in north- and south-facing populations. Ann. Bot. 80(3), 345-353,

Pintado, A., Sancho, L.G., Green, T.G.A., Blanquer, J.M., Lázaro, R., 2005. Functional ecology of the Biological Soil Crusts in semi-arid SE Spain: sun and shade populations of *Diploschistes diacapsis* (Ach.) Lumbsch. Lichenologist 37(5), 425-432.

Pintado, A., Sancho, L.G., Blanquer, J., Green, T.G.A., Lázaro, R., 2010. Microclimatic factors and photosynthetic activity of crustose lichens from the semi-arid southeast of Spain: long-term measurements for *Diploschistes diacapsis*. Bibl. Lichenol. 105, 211-224.

Poelt, J., 1969. Bestimmungsschliissel europilischer Flechten. Cramer, Lehre.

Porada, P., Weber, B., Elbert, W., Pöschl, U., Kleidon, A., 2013. Estimating global carbon up-take by lichens and bryophytes with a process-based model. Biogeosciences 10(11), 6989-7033.

Porada, P., Weber, B., Elbert, W., Pöschl, U., Kleidon, A., 2014. Estimating impacts of lichens and bryophytes on global biogeochemical cycles. Glob. Biogeochem. Cycl. 28(2), 71-85.

Post, A., 1990. Photoprotective pigment as an adaptive strategy in the Antarctic moss *Ceratodon purpureus*. Pol. Biol. 10, 241-245.

Potter, K.A., Arthur Woods, H., Pincebourde, S., 2013. Microclimatic challenges in global change biology. Glob. Chang. Biol. 19(10), 2932-2939.

Prăvălie, R., 2016. Drylands extent and environmental issues. A global approach. Earth-Sci. Rev. 161, 259-278.

Printzen, C., Domaschke, S., Fernández-Mendoza, F., Pérez-Ortega, S., 2013. Biogeography and ecology of *Cetraria aculeata,* a widely distributed lichen with a bipolar distribution. MycoKeys 6, 33-53.

Proctor, M.C.F., 1982. Physiological ecology: Water relations, light and temperature responses, carbon balance. In: Smith, A.J.E. (Ed.), Bryophyte ecology. Chapman & Hall, London, pp 333-381.

Proctor, M.C.F., 2000. The bryophyte paradox: tolerance of desiccation, evasion of drought. Plant. Ecol. 151(1), 41-49.

Puillandre, N., Lambert, A., Brouillet, S., Achaz, G., 2012. ABGD, Automatic Barcode Gap Discovery for primary species delimitation. Mol. Ecol. 21(8), 1864-1877.

Raggio, J., Green, T.G.A., Sancho, L.G., 2016. In situ monitoring of microclimate and metabolic activity in lichens from Antarctic extremes: a comparison between South Shetland Islands and the McMurdo dry valleys. Polar Biol. 39(1), 113-122.

Raggio, J., Pintado, A., Vivas, M., Sancho, L., Büdel, B., Colesie, C., Weber, B., Schroeter, B., Lázaro, R., Green T.G.A., 2014. Continuous chlorophyll fluorescence, gas exchange and microclimate monitoring in a natural soil crust habitat in Tabernas badlands, Almería, Spain: progressing towards a model to understand productivity. Biodivers. Conserv. 23, 1809-1826.

Raggio, J., Green, T.G.A., Sancho, L.G., Pintado, A., Colesie, C., Weber, B., Büdel, B., 2017. Metabolic activity duration can be effectively predicted from macroclimatic data for Biological Soil Crusts habitats across Europe. Geoderma 306, 10-17.

Raggio, J., Green, T.G.A., Pintado, A., Sancho, L.G., Büdel, B., 2018. Environmental determinants of biocrust carbon fluxes across Europe: possibilities for a functional type approach. Plant Soil 429, 147-157.

Rambaut, A., 2018. FigTree v1.4.4. Institute of Evolutionary Biology University of Edinburgh, Edinburgh. http://tree.bio.ed.ac.uk/software/figtree/ (31 January 2021, date last accessed).

Rambaut, A., Drummond, A.J., Xie, D., Baele, G., Suchard, M.A., 2018. Posterior summarization in bayesian phylogenetics using Tracer 1.7. Syst. Biol. 67(5), 901-904.

Rizzi, G., Giordani, P., 2012. The ecology of the lichen genus *Xanthoparmelia* in Italy: An investigation throughout spatial scales. Plant Biosyst., 1-7.

Robinson, S.A., Wasley, J., Tobin, A.K., 2003. Living on the edge - plants and global change in continental and maritime Antarctica. Glob. Chang. Biol. 9(12), 1681-1717.

Rodríguez-Caballero, E., Castro, A., Chamizo, S., Quintas-Soriano, C., García-Llorente, M., Cantón, Y., Weber, B., 2017. Ecosystem services provided by biocrusts: From ecosystem functions to social values. J. Arid Environ. 159(4), 45-53.

Rognes, T., Flouri, T., Nichols, B., Quince, C., Mahé, F., 2016. VSEARCH: a versatile open source tool for metagenomics. PeerJ 4, e2584.

Rozas, J., Ferrer-Mata, A., Sánchez-Del Barrio, J.C., Guirao-Rico, S., Librado, P., Ramos-Onsins, S.E., Sánchez-Gracia, A., 2017. DnaSP6: DNA sequence polymorphism analysis of large data sets. Mol. Biol. Evol. 34(12), 3299-3302.

Rundel, P.W., 1978. Ecological relationships of desert fog zone lichens. Bryologist 81(2), 277-293.

Running S.W., Thornton P.E., Nemani R., Glassy J.M., 2000. Global terrestrial gross and net primary productivity from the earth observing system. In: Sala, O.E., Jackson, R.B., Mooney, H.A., Howarth, R.W. (Eds.), Methods in ecosystem science. Springer, New York, pp 44-57.

Sadowska-Des, A., Bálint, M., Otte, J., Schmitt, I., 2014. Assessing intraspecific diversity in a lichen-forming fungus and its green algal symbiont: evaluation of eight molecular markers. Fungal Ecol. 6, 141-151.

Sadowsky, A., Mettler-Altmann, T., Ott, S., 2016. Metabolic response to desiccation stress in strains of green algal photobionts *Trebouxia* from two Antarctic lichens of southern habitats. Phycologia 55(6), 703-714.

Sager, J.C., Mc Farlane, C., 1997. Radiation. In: Langhans, R.W., Tibbitts, T.W. (Eds.), Plant growth chamber handbook. Iowa Agricultural and Home Economics Experiment Station, pp 1-29.

Sala-Carvalho, W.R., Montessi-Amaral, F.P., Esposito, M.P., Campestrini, R., Rossi, M., Peralta, D.F., Furlan, C.M., 2022. Metabolome of *Ceratodon purpureus* (Hedw.) Brid., a cosmopolitan moss: the influence of seasonality. Planta 255(4), 77.

Sancho, L.G., Belnap, J., Colesie, C., Raggio, J., Weber, B., 2016. Carbon budgets of Biological Soil Crusts at micro-, meso-, and global scales. In: Weber, B. Büdel, B., Belnap, J. (Eds.), Biological Soil Crusts: An organizing principle in drylands. Springer, Cham, pp 287-304.

Sancho, L.G., Pintado, A., Navarro, F., Ramos, M., De Pablo, M.A., Blanquer, J.M., Raggio, J., Valladares, F., Green, T., 2017. Recent warming and cooling in the Antarctic Peninsula region has rapid and large effects on lichen vegetation. Sci. Rep. 7(1), 5689.

Sancho, L.G., Rios, A.D., Pintado, A., Colesie, C., Raggio, J., Ascaso, C., Green, T.G.A., 2020. *Himantormia lugubris,* an Antarctic endemic on the edge of the lichen symbiosis. Symbiosis 82, 49-58.

Sanders, W.B., 1999. Thallus organization and development in the fruticose lichen *Aspicilia californica*, with comparisons to other taxa. Lichenologist 31, 149-162.

Scheidegger, C., Schroeter, B., Frey, B., 1995. Structural and functional processes during water vapour uptake and desiccation in selected lichens with green algal photobionts. Planta 197, 399-409.

Schimel, D., 1995. Terrestrial ecosystems and the carbon cycle. Glob. Change Biol. 1(1), 77-91.

Schlensog, M., Pannewitz, S., Green, T.G.A., Schroeter, B., 2004. Metabolic recovery of continental Antarctic cryptogams after winter. Polar Biol. 27, 399-408.

Schlensog, M., Green, T.G.A., Schroeter, B., 2013. Life form and water source interact to determine active time and environment in cryptogams: an example from the maritime Antarctic. Oecologia 173(1), 59-72.

Schmitt, I., Crespo, A., Divakar, P.K., Fankhauser, J.D., Herman-Sackett, E., Kalb, K., Nelsen, M.P., Nelson, N.A., Rivas-Plata, E., Shimp, A.D., Widhelm, T., Lumbsch, H.T., 2009. New primers for promising single-copy genes in fungal phylogenetics and systematics. Persoonia 23, 35-40.

Schoch, C., Seifert, K., Huhndorf, S., Robert, V., Spouge, J., Lévesque, C.A., Chen, W., 2012. Nuclear ribosomal internal transcribed spacer (ITS) region as a universal DNA barcode marker for Fungi. Proc. Natl. Acad. Sci. 109, 6241-6246.

Schofield, W.B., Crum, H.A., 1972. Disjunctions in bryophytes. Ann. Missouri Bot. Gard. 59, 174-202.

Schreiber, U., Bilger, W., 1993. Progress in chlorophyll fluorescence research: major developments during the past years in retrospect. In: Behnke, H.D., Lüttge, U., Esser, K., Kadereit, J.W., Runge, M. (Eds.), Progress in Botany. Springer, Berlin, pp 151-173.

Schreiber, U., Schliwa, U., Bilger, W., 1986. Continuous recording of photochemical and non-photochemical chlorophyll fluorescence quenching with a new type of modulation fluorometer. Photosynth. Res. 10(1-2), 51-62.

Schroeter, B., Scheidegger, C., 1995. Water relations in lichens at sub-zero temperatures: structural changes and carbon dioxide exchange in the lichen *Umbilicaria aprina* from continental Antarctica. New Phytol. 131, 273-285.

Schroeter, B., Olech, M., Kappen, L., Heitland, W., 1995. Eco-physiological investigations of *Usnea antarctica* in the maritime Antarctic. I. Annual microclimatic conditions and potential primary production. Antarct. Sci. 7(3), 251-260.

Schroeter, B., 1997. Grundlagen der stoffproduktion von kryptogamen unter besonderer berücksichtigung der flechten. Aus dem Botanischen Institut der Universität Kiel.

Schroeter, B., Kappen, L., Schulz, F., Sancho, L.G., 2000. Seasonal variation in the carbon balance of lichens in the maritime Antarctic: long-term measurements of photosynthetic activity in *Usnea aurantiaco-atra*. In: Davison, W., Howard-Williams, C., Broady, P. (Eds.), Antarctic Ecosystems: Models for Wider Ecological Understanding. Caxton Press, Christ- church, pp 258-262.

Schroeter, B., Green, T.G.A., Pannewitz, S., Schlensog, M., Sancho, L.G., 2010. Fourteen degrees of latitude and a continent apart: Comparison of lichen activity over two years at continental and maritime Antarctic sites. Antarct. Sci. 22(6), 681-690.

Schroeter, B., Green, T.G.A., Pannewitz, S., Schlensog, M., Sancho, L.G., 2011. Summer variability, winter dormancy: lichen activity over 3 years at Botany Bay, 77°S latitude, continental Antarctica. Polar Biol. 34, 13-22.

Schroeter, B., Green, T.G.A., Kulle, D., Pannewitz, S., Schlensog, M., Sancho, L.G., 2012. The moss *Bryum argenteum* var. *muticum* Brid. is well adapted to cope with high light in continental Antarctica. Antarct. Sci. 24, 281-291.

Schroeter, B., Green, T.G.A., Pintado, A., Türk, R., Sancho, L.G., 2017. Summer activity patterns for mosses and lichens in maritime Antarctica. Antarct. Sci. 29(6), 517-530.

Schroeter, B., Green, T.G.A., Pintado, A., Roman, T. Sancho, L.G., 2021. Summer activity patterns for a moss and lichen in the maritime Antarctic with respect to altitude. Polar Biol. 44, 2117-2137.

Schuster, G., Ott, S., Gassmann, A., Romeike, J., 2002. *In situ* measurement of the water content of lichens. In: Kranner, I.C., Beckett, R.P., Varma, A.K. (Eds.), Protocols in lichenology. Springer, Berlin, pp 224-235.

Semikhatova, O.A., Gerasimenko, T.V., Ivanova, T.I., 1992. Photosynthesis, respiration, and growth of plants in the Soviet Arctic. In: Chapin, F., Jeffereis, R., Reynolds, J., Shaver, G., Svoboda, J. (Eds.), Arctic ecosystems in a changing climate: An eco-physiological perspective. Academic Press, San Diego, pp 169-192.

Sérgio, C., Figueira, R., Menezes, R., 2011. Modeling the distribution of *Sematophyllum substrumulosum* (Hampe) E. Britton as a signal of climatic changes in Europe. In: Tuba, Z., Slack, N., Stark, L. (Eds.), Bryophyte ecology and climate change. Cambridge University Press, Cambridge, pp 427-440.

Shaw, J., Beer, S.C., 1999. Life history variation in gametophyte populations of the moss *Ceratodon purpureus* (Ditrichaceae). Am. J. Bot. 86(4), 512-521.

Siegert, M., Atkinson, A., Banwell, A., Brandom, M., Convey, P., Davies, B., Downie, R., Edwards, T., Hubbard, B., Marshall, G., Rogelj, J. Rumble, J. Stroeve, J., Vaughan, D., 2019. The Antarctic Peninsula under a 1.5°C global warming scenario. Front. Environ. Sci. 7, 1-7.

Singh, J., Singh, R.P., Khare, R., 2018. Influence of climate change on Antarctic flora. Polar Sci. 18, 94-101.

Skotnicki, M., Mackenzie, A., Ninham, J.A., Selkirk, P., 2004. High levels of genetic variability in the moss *Ceratodon purpureus* from continental Antarctica, sub-Antarctic Heard and Macquarie Islands, and Australasia. Polar. Biol. 27, 687-698.

Smellie, J.L., Liesa, M., Muñoz, J.A., Sàbat, F., Pallàs, R., Willan, R.C.R., 1995. Lithostratigraphy of volcanic and sedimentary sequences in central Livingston Island, South Shetland Islands. Antarctic Sci. 7(1), 99-113.

Smith, C.W., Smith, C.W., 2009. The lichens of Great Britain and Ireland. British Lichen Society.

Smith, N.G., Dukes, J.S., 2013. Plant respiration and photosynthesis in global-scale models: incorporating acclimation to temperature and CO_2. Glob. Change Biol. 19(1), 45-63.

Smith, R.I.L., 1972. Vegetation of the South Orkney Islands with particular reference to Signy Island. British Antarctic Survey Scientific Reports, 68.

Smith, R.I.L., 1984. Terrestrial plant biology of the sub-Antarctic and Antarctic. In: Laws, R.M. (Ed.), Antarctic ecology. Academic Press, London, pp 61-162.

Smith R.I.L., 1990. Signy Island as a paradigm of biological and environmental change in Antarctic terrestrial ecosystems. In: Kerry, K.R., Hempel, G. (Eds.), Antarctic Ecosystems. Springer, Berlin, pp 32-50.

Smith, R.I.L., 1999. Biological and environmental characteristics of three cosmopolitan mosses dominant in continental Antarctica. J. Veg. Sci. 10(2), 231-242.

Smith, R.I.L., 2001. Plant colonization response to climate change in the Antarctic. Folia Facultatis Scientiarium Naturalium Universitatis Masarykianae Brunensis. Geographia 25, 19-33.

Smith, R.I.L, Richardson, M., 2011. Fuegian plants in Antarctica: natural or anthropogenically assisted immigrants? Biol. Invasions 13, 1-5.

Solé-Benet, A., Cantón, Y., Lázaro, R., del Barrio, G., Puigdefábregas, J., Vidal, S., 2009. Estación experimental 'El Cautivo' (Desierto de Tabernas, Almería). Ministerio de Medio Ambiente.

Solhaug, K.A., Asplund, J., Gauslaa, Y., 2021. Apparent electron transport rate - a non-invasive proxy of photosynthetic CO_2 uptake in lichens. Planta 253(1), 14.

Souza-Egipsy, V., Valladares, F., Ascaso, C., 2000. Water distribution in foliose lichen species: interactions between method of hydration, lichen substances and thallus anatomy. Ann. Bot. 86, 595-601.

Souza-Egipsy, V., Sancho, L.G., 2001. Descripción del microclima en dos comunidades liquénicas del SE semiárido de la Península Ibérica. Nimbus 7-8, 187-212.

Stamatakis, A., 2014. RAxML v8: a tool for phylogenetic analysis and post-analysis of large phylogenies. Bioinformatics 30, 1312-1313.

Sultan, S.E., 2000. Phenotypic plasticity for plant development, function and life history. Trends Plant Sci. 5(12), 537-42.

Szaniszlo, P.J., 1985. An introduction to dimorphism among zoopathogenic fungi. In: Szaniszlo, P.J., Harris, J.L. (Eds.), Fungal dimorphism. Springer, Boston, pp 3-13.

Taiyun, W., Viliam, S., 2017. R package 'corrplot': Visualization of a correlation matrix. Available at: from https://github.com/taiyun/corrplot.

Tamm, A., Caesar, J., Kunz, N., Colesie, C., Reichenberger, H., Weber, B., 2018. Eco-physiological properties of three Biological Soil Crusts types and their photoautotrophs from the Succulent Karoo, South Africa. Plant and Soil 429(1-2), 127-146.

Tamura, K., Peterson, D., Peterson, N., Stecher, G., Nei, M., Kumar, S., 2011. MEGA5: Molecular evolutionary genetics analysis using maximum likelihood, evolutionary distance, and maximum parsimony methods. Mol. Biol. Evol. 28(10), 2731-2739.

Tarnawski, M.G., Melick, D.R., Roser, D.J., Adamson, E., Adamson, H., & Seppelt, R.D., 1992. In situ carbon dioxide levels in cushion and turf forms of *Grimmia antarctici* at Casey Station, East Antarctica. J. Bryol. 17, 241-249.

Thomas, E.R., Dennis, P.F., Bracegirdle, T.J., Franzke, C., 2009. Ice core evidence for significant 100-year regional warming on the Antarctic Peninsula. Geophys. Res. Lett. 36(20), 1-5.

Tolpysheva, T.Y., Timofeeva, A.K., 2008. The effect of the substrate on the growth and reproduction of the lichens *Cladonia rangiferina* and *C. mitis.* Moscow Univ. Biol. Sci. Bull. 63, 170-177.

Tretiach, M., Brown, D.H., 1995. Morphological and physiological differences between epilithic and epiphytic populations of the lichen *Parmelia pastillifera*. Ann. Bot. 75(6), 627-632.

Turner, J., Barrand, N.E., Bracegirdle, T.J., Convey, P., Hodgson, D.A., Jarvis, M., Jenkins, A., Marshall, G., Meredith, M.P., Roscoe, H., Shanklin, J., French, J., Goosse, H., Guglielmin, M., Gutt, J., Jacobs, S., Kennicutt, M.C., Masson-Delmotte, V., Mayewski, P., Navarro, F., Robinson, S., Scambos, T., Sparrow, M., Summerhayes,

C., Speer, K., Klepikov, A., 2005. Antarctic climate change during the last 50 years. Int. J. Climatol. 25(3), 279-294.

Turner, J., Overland, J.E., Walsh, J.E., 2007. An Arctic and Antarctic perspective on recent climate change. Int. J. Climatol. 27(3), 277-293.

Turner, J., Lu, H., White, I., King, J.C., Phillips, T., Hosking, J.S., Bracegirdle, T.J., Marshall, G.J., Mulvaney, R., Deb, P., 2016. Absence of 21st century warming on Antarctic Peninsula consistent with natural variability. Nature 535(7612), 411-415.

Uchida, M., Nakatsubo, T., Kanda, H., Koizumi, H., 2006. Estimation of the annual primary production of the lichen *Cetrariella delisei* in a glacier foreland in the High Arctic, Ny-Ølesund, Svalbard. Polar Res. 25, 39-49.

Ueno, T., Bekku, Y., Uchida, M., Kanda, H., 2006. Photosynthetic light responses of a widespread moss, *Sanionia uncinata*, from contrasting water regimes in the high Arctic tundra, Svalbard, Norway. J. Bryol. 28(4), 345-349.

Ure, J.D., Stanton, D.E., 2019. Co-dominant anatomically disparate lichens converge in hydrological functional traits. Bryologist 122(3), 463-470.

Valanne, N., 1976a. Development of chloroplast structure and photosynthetic competence in dark-adapted moss protonemata after exposure to light. Protoplasma 89, 359-369.

Valanne, N., 1976b. Effect of continuous light on CO_2 fixation, chlorophyll content, growth and chloroplast structure in *Ceratodon purpureus*. Z. Pflanzenphysiol. 81, 347-357.

Valanne, N., 1977. The combined effects of light intensity and continuous light on the CO_2 fixation, chlorophyll content and chloroplast structure of the protonema of *Ceratodon purpureus*. Z. Pflanzenphysiol. 83, 275-283.

Valanne, N. Aro, E.-M., Repo, E., 1978. Changes in photosynthetic capacity and activity of RuBPC-ase and glycolate oxidase during the early growth of moss protonemata in continuous and rhythmic light.

Valladares, F., Balaguer, L., Martinez-Ferri, E., Perez-Corona, E., Manrique, E., 2002. Plasticity, instability and canalization: Is the phenotypic variation in seedlings of sclerophyll oaks consistent with the environmental unpredictability of Mediterranean ecosystems? New Phytol. 156(3), 457-467.

Vančurová, L., Peksa, O., Němcová, Y., Škaloud, P., 2015. *Vulcanochloris* (*Trebouxiales, Trebouxiophyceae*), a new genus of lichen photobiont from La Palma, Canary Islands, Spain. Phytotaxa 219, 118.

Vanderwel, M.C., Slot, M., Lichstein, J.W., Reich, P.B., Kattge, J., Atkin, O.K., Bloomfield, K.J., Tjoelker, M.G., Kitajima, K., 2015. Global convergence in leaf respiration from estimates of thermal acclimation across time and space. New Phytol. 207(4), 1026-1037.

Vaughan, D.G., Marshall, G.J., Connolley, W.M., Parkinson, C., Mulvaney, R., Hodgson, D.A., King, J.C., Pudsey, C.J., Turner, J., 2003. Recent rapid regional climate warming on the Antarctic Peninsula. Clim. Chang. 60, 243-274.

Velmala, S., Myllys, L., Halonen, P., Goward, T., Ahti, T., 2009. Molecular data show that *Bryoria fremontii* and *B. tortuosa* (Parmeliaceae) are conspecific. Lichenologist 41(3), 231-242.

Vignon, É., Roussel, M.L., Gorodetskaya, I.V., Genthon, C., Berne, A., 2021. Present and future of rainfall in Antarctica 48(8), e2020GL092281.

Violle, C., Navas, M.L., Vile, D., Kazakou, E., Fortunel, C., Hummel, I., Garnier, E., 2007. Let the concept of trait be functional. Oikos 116, 882-892.

Wagner, S., Zotz, G., Bader, M.Y., 2013a. The temperature acclimation potential of tropical bryophytes. Plant Biol. 16(1), 117-124.

Wagner, S., Zotz, G., Salazar Allen, N., Bader, M.Y., 2013b. Altitudinal changes in temperature responses of net photosynthesis and dark respiration in tropical bryophytes. Ann. Bot. 111(3), 455-465.

Walker, F.J., 1985. The lichen genus *Usnea* subgenus neuropogon. Bull. Br. Mus. Nat. Botany 13, 1-130.

Walther, G.R., Post, E., Convey, P., Menzel, A., Parmesan, C., Beebee, T.J., Fromentin, J.M., Hoegh-Guldberg, O., Bairlein, F., 2002. Ecological responses to recent climate change. Nature 416(6879), 389-395.

Watanabe, M., Suzuki, T., O'ishi, R., Komuro, Y., Watanabe, S., Emori, S., Takemura, T., Chikira, M., Ogura, T., Sekiguchi, M., Takata, K., Yamazaki, D., Yokohata, T., Nozawa, T., Hasumi, H., Tatebe, H., Kimoto, M., 2010. Improved climate simulation by MIROC5: mean states, variability, and climate sensitivity. J. Clim. 23(23), 6312-6335.

Watson, R.T., Zinyowera, M.C., Moss, R.H., Dokken, D.J., 1996. Technical summary: impacts, adaptations, and mitigation options. Intergovernmental Panel on Climate Change, United Kingdom.

Weber, B., Graf, T., Bass, M., 2012. Eco-physiological analysis of moss-dominated Biological Soil Crusts and their separate components from the Succulent Karoo, South Africa. Planta 236(1), 129-139.

Wedin, M., Westberg, M., Crewe, A.T., Tehler, A., Purvis, O.W., 2009. Species delimitation and evolution of metal bioaccumulation in the lichenized *Acarospora smaragdula* (Ascomycota, Fungi) complex. Cladistics 25(2), 161-172.

Werth, S., Sork, V.L., 2014. Ecological specialization in *Trebouxia* (Trebouxiophyceae) photobionts of *Ramalina menziesii* (Ramalinaceae) across six range-covering ecoregions of western North America. Am. J. Bot. 101, 1127-1140.

Werth, S.; Miao, V.P.W.; Jónsson, Z.O.; Andrésson, Ó.S., 2015. High-Throughput Sequencing in studies of lichen population biology. In: Upreti, D., Divakar, P., Shukla, V., Bajpai, R. (Eds.), Recent advances in lichenology. Springer, New Delhi, pp 61-94.

Williams, L., Colesie, C., Ullmann, A., Westberg, M., Wedin, M., Büdel, B., 2017. Lichen acclimation to changing environments: Photobiont switching vs. climate-specific uniqueness in *Psora decipiens*. Ecol. Evol. 7(8), 2560-2574.

Wood, A.J., Oliver, M.J., Cove, D.J., 2000. Bryophytes as model systems. Bryologist 103(1), 128-133.

Wood, S.N., 2019. Mixed GAM computation vehicle with automatic smoothness estimation. retrieved from https://cran.r-project.org/web/packages/mgcv/mgcv.pdf.

Xiong, F.S., Mueller, E.C., Day, T.A., 2000. Photosynthetic and respiratory acclimation and growth response of Antarctic vascular plants to contrasting temperature regimes. Am. J. Bot. 87(5), 700-710.

Yahr, R., Vilgalys, R., De Priest, P.T., 2006. Geographic variation in algal partners of *Cladonia subtenuis* (Cladoniaceae) highlights the dynamic nature of a lichen symbiosis. New Phytol. 171(4), 847-860.

Ye, H., Mather, J.R., 1997. Polar snow cover changes and global warming. Int. J. Climatol. 17(2), 155-162.

Supplementary data

APPENDIX A. Supplementary data of Chapter 1

Table S1 Best fitting model found using CurveExpert Professional software for each light response curve of *C. purpureus*.

Temperature (ºC)	Model	R² adjusted	Standard error	Replicates
0	Rational Model	0.71	0.46	4
5	Exponential Plus Linear	0.94	0.35	4
10	Rational Model	0.98	0.22	4
15	Rational Model	0.95	0.53	4
20	Rational Model	0.96	0.47	4
25	Rational Model	0.89	0.68	4

Table S2 Factor loadings from a PCA of five physiological traits measured at four different temperatures in maritime Antarctica, continental Antarctica and the Succulent Karoo semi-arid Desert.

Physiological traits	PC1	PC2
DRopt	0.39	-0.74
NP$_{1300}$	0.59	0.07
GP	-0.44	-0.67
Photosynthetic efficiency	0.55	-0.09

Fig. S1 Correlation plot of the photosynthetic parameters of *C. purpureus* in maritime Antarctica, continental Antarctica and the Succulent Karoo semi-arid Desert. The correlations with a p-value lower than 0.05 were statistically significant (*). The colour gradient indicates if the correlation is positive, negative or if there is no-correlation.
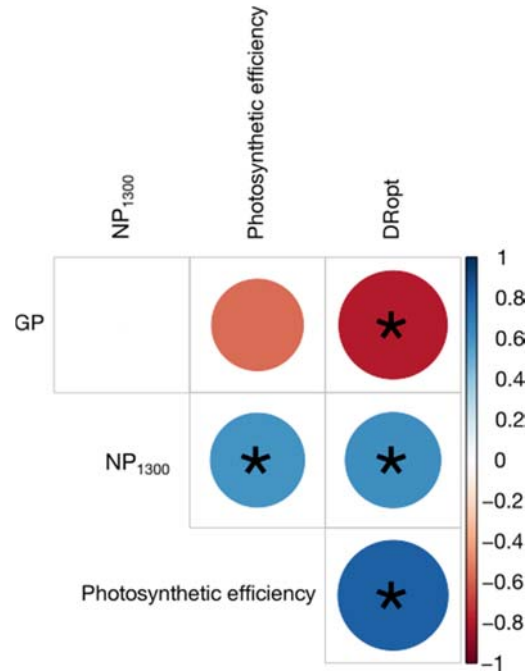
Fig. S2 Microclimatic temperature of *C. purpureus* at Livingston Island (maritime Antarctica) from February 27th to March 24th 2018. Four replicates were recorded simultaneously (I1, I2, I3 and I4).
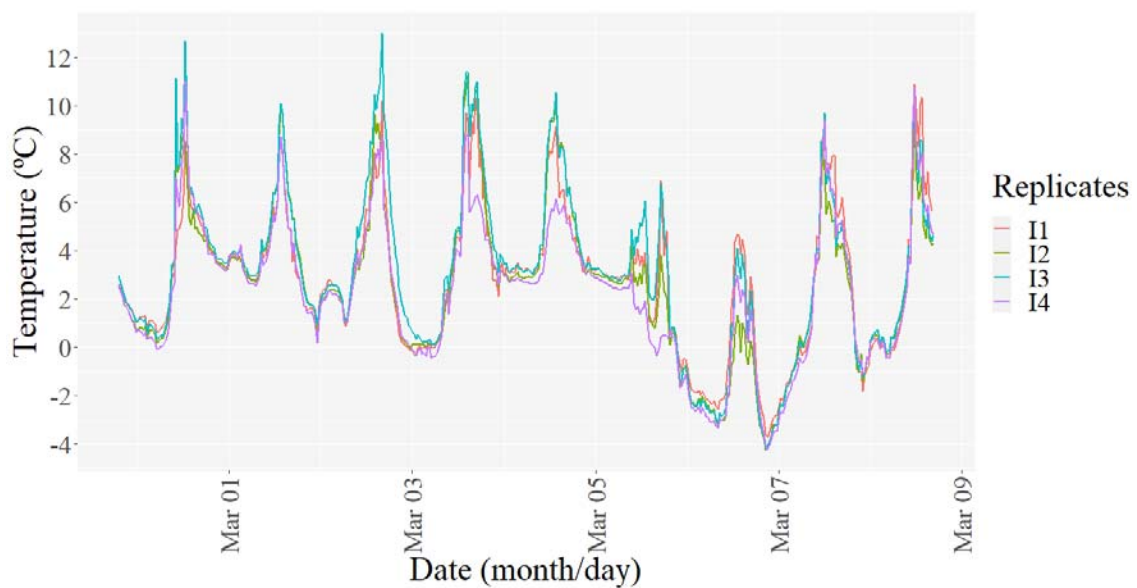
Fig. S3 Microclimatic relative humidity of *C. purpureus* at Livingston Island (maritime Antarctica) from February 27th to March 24th 2018. Four replicates were recorded simultaneously (I1, I2, I3 and I4).
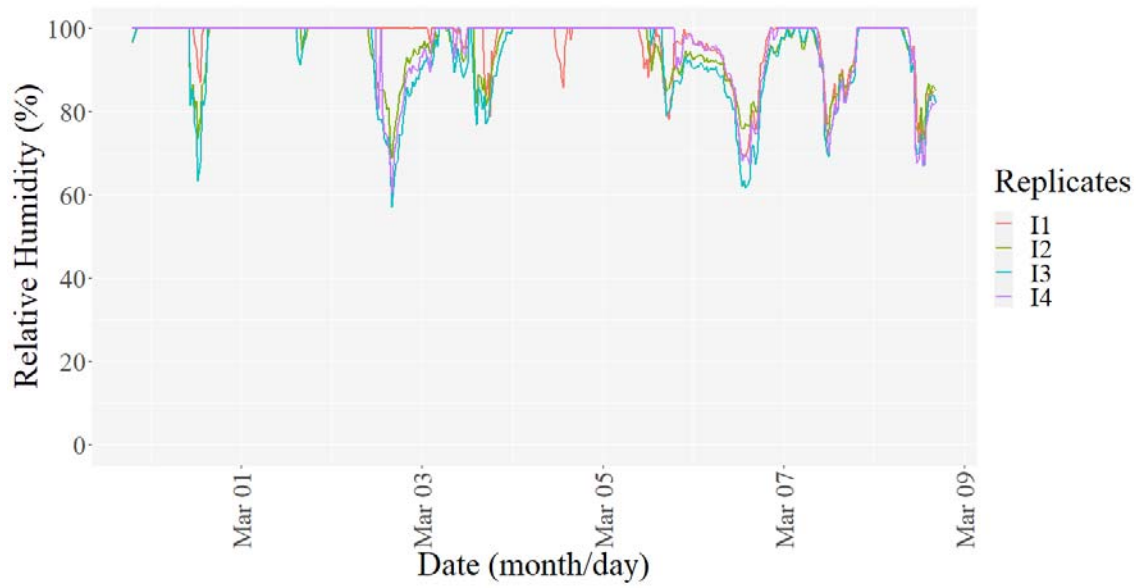
APPENDIX B. Supplementary data of Chapter 2

Table S1 Equations to calculate the physiological parameters of the response desiccation curve.

Parameter	Units	Concept
NP_{400}	$\mu mol\ CO_2\ m^{-2}\ s^{-1}$	Maximum net photosynthetic rate: Maximum rate measured in the lab.
Area below the response desiccation curve		Area below the response desiccation curve on time bases calculated from the starting of the curve at time zero (t_0) to its ending $t_{(n)}$.
Duration of the optimal conditions		Period of time in which the lichen is photosynthesizing within 90% of the NP_{400} (Colesie et al., 2017).
Starting of the optimal conditions	minutes	Time elapsed until achieving to 90% of the NP_{400} (Colesie et al., 2017).
Total duration of the desiccation curve		-

MWC	mm	Maximum water content: Amount of water retained in the lichen thallus when it is suprasaturated of water (Solhaug et al., 2021).$$MWC[mm] = \frac{\frac{(Wsat[gr] - Wdry[gr]) * 1000}{area[cm^2]}}{100}$$
OWC		Optimal water content: Amount of water retained in the lichen thallus at which NP_{400} occurs (Solhaug et al., 2021).$$OWC[mm] = \frac{\frac{(Wopt[gr] - Wdry[gr]) * 1000}{area[cm^2]}}{100}$$

'Wsat' is the sample weight when it is suprasaturated of water;

'Wdry' is the dry weight obtained by gravimetric determination following Schuster et al. (2002) procedure, in which samples were dried in an oven at 105 °C for 24h;

'area' is the area of the lichen thallus surface;

'Wopt' is the lichen weight when it achieves to the maximum net photosynthesis.

Table S2 Best fitting model found using CurveExpert Professional software for each response curve of *Xanthoparmelia*.

Habitat	Replicates	Temperature (ºC)	Model	R² adjusted	Standard error
Desiccation response curves					
Desert	12 specimens	15	Hoerl	0.53	0.54
Coast	12 specimens		Rational Model	0.71	0.50
Light response curves					
Desert	12 specimens	5	Exponential Plus Linear	0.87	0.37
Coast	12 specimens		MMF	0.77	0.57
Desert	12 specimens	10	Exponential Plus Linear	0.91	0.49
Coast	12 specimens		Exponential Plus Linear	0.92	0.37
Desert	12 specimens	15	Exponential Plus Linear	0.92	0.50
Coast	12 specimens		Exponential Plus Linear	0.88	0.66

Table S3 Equations to calculate the physiological parameters of the light response curve.

Parameter	Units	Concept
DRopt		Dark respiration at the optimal water content: Rate obtained in the lab measurements.
NP$_{1500}$		Net photosynthetic rate at PPFD of 1500 µmols photons m^{-2} s^{-1}: Rate obtained in the lab measurements.
GP	µmol CO$_2$ m^{-2} s^{-1}	Gross photosynthetic rate. $$GP\left[\frac{\mu mols\ CO_2}{m^2.s}\right] = \left|NP_{1500} + DR_{opt}\right|$$
Photosynthetic efficiency	Adimensional	Ratio between NP$_{1500}$ and DRopt (Green and Lange, 1995). $$K_F = \frac{(NP_{1500} + DRopt)}{DR_{opt}}$$
Φ	mol CO$_2$ mol^{-1} quanta	Quantum yield of photosynthesis: Measure of the light use efficiency of absorbed quanta. It is the slope of the line of the light limited part (from 0 µmols photons m^{-2} s^{-1} to 32 µmols photons m^{-2} s^{-1}). $$\Phi\left[\frac{\mu mols\ CO_2}{mol\ quanta}\right] = \frac{\Delta_{NP}}{\Delta_{PPFD}} = \frac{NP_{PPFD=32} - NP_{PPFD=0}}{32 - 0}$$

LCP	μmol photons m^{-2} s^{-1}	Light compensation point: light intensity in which the photosynthetic rate is zero. It was obtained graphically.
LSP		Light saturation point: light intensity in which the maximum net photosynthetic rate is constant. It was obtained graphically as the light intensity in which NP$_{1500}$ achieve at 95% of the total net photosynthesis.

Table S4 Loci and primers used in the present study.

Locus	Primer name	Orientation (F/R)	Primer sequence (5'– 3')	Reference
MYCOBIONT				
nrITS	ITS1F	F	CTTGGTCATTTAGAGGAAGTAA	Gardes and Burns (1993)
	ITS4A	R	CGCCGTTACTGGGGCAATCCCTG	Larena et al. (1999)
β-tubulin	Bt3-LM	F	GAACGTCTACTTCAACGAG	Myllys et al. (2001)
	Bt10-LM	R	TCGGAAGCAGCCATCATGTTCTT	Myllys et al. (2001)
MCM7	X_Mcm7_F	F	CGTACACYTGTGATCGATGTG	Leavitt et al. (2011b)
	X_Mcm7_R	R	GTCTCCACGTATTCGCATTCC	Leavitt et al. (2011b)
PHOTOBIONT				
ITS2	ITS-Cha3	F	CAACTCTCRRCAACGGATA	Cheng et al. (2016)
	ITS-u4	R	RGTTTCTTTTCCTCCGCTTA	Cheng et al. (2016)

Table S5 PCR settings.

PCR	PCR protocol	Reference
MYCOBIONT		
nrITS	94°C (5 min), 5 cycles of 94°C (30 sec) + 55°C (30 sec) + 72°C (60 sec), 30 cycles of 94°C (30 sec) + 55°C (30 sec) + 72°C (60 sec), 72°C (300 min),	Wedin et al. (2009)
β-tubulin	94°C (5 min), 5 cycles of 94°C (30 sec) + 60°C (30 sec) + 72°C (60 sec), 30 cycles of 94°C (30 sec) + 55°C (30 sec) + 72°C (60 sec), 72°C (300 sec),	Wedin et al. (2009)
MCM7	94°C (10 min), 38 cycles of 94°C (45 sec) + 56°C (50 sec) + 72°C (60 sec), 72°C (5 min),	Schmitt et al. (2009)
PHOTOBIONT		
ITS2	95ºC (4 min) 35 cycles of 95ºC (30 sec) 35 cycles of 50/63°C (20 sec) 35 cycles of 72°C (20 sec) 35 cycles of 72°C (5 min)	Dal Grande et al. (2018)

Table S6 GenBank accession numbers of the mycobiont sequences generated in this study and download from Leavitt et al. (2018) and Amo de Paz et al. (2012).

Taxon	nrITS	nuLSU	*β-tubulin*	*MCM7*	mtSSU	Reference
Xanthoparmelia adhaerens	HM125744	HM125766	-	-	HM125722	Leavitt et al. (2018)
Xanthoparmelia atroviridis '1'	JQ912314	JQ912415	-	-	-	Leavitt et al. (2018)
Xanthoparmelia atroviridis '2'	JQ912320	JQ912419	-	-	MG695790	Leavitt et al. (2018)
Xanthoparmelia atroviridis '3'	JQ912329	JQ912425	-	-	MG695791	Leavitt et al. (2018)
Xanthoparmelia caliginosa	JQ912315	-	-	-	-	Leavitt et al. (2018)
Xanthoparmelia hypopsila	MG695552	MG695653	MG695424	MG695719	MG695806	Leavitt et al. (2018)
Xanthoparmelia hypopsila	MG695553	MG695654	-	-	MG695807	Leavitt et al. (2018)
Xanthoparmelia hypopsila	MG695554	MG695655	-	-	MG695808	Leavitt et al. (2018)
Xanthoparmelia imitatrix	JQ912344	JQ912441	-	-	-	Leavitt et al. (2018)
Xanthoparmelia lineella	JQ912319	JQ912418	-	-	-	Leavitt et al. (2018)
Xanthoparmelia loxodes '1'	AY581076	AY578940	-	-	AY582313	Leavitt et al. (2018)
Xanthoparmelia loxodes '2'	AY581070	AY578933	-	-	AY582306	Leavitt et al. (2018)
Xanthoparmelia mougeotii	AY581100	AY578967	-	KR995696	AY582336	Leavitt et al. (2018)
Xanthoparmelia mougeotii	HM578964	HM579371	HM577851	HM579755	-	Leavitt et al. (2018)
Xanthoparmelia mougeotina	MG695560	MG695661	MG695430	MG695725	MG695814	Leavitt et al. (2018)
Xanthoparmelia pokornyi 2	AY581075	AY578939	-	KR995697	EU562707	Leavitt et al. (2018)
Xanthoparmelia pseudoglabrans	JQ912316	JQ912416	-	-	MG695820	Leavitt et al. (2018)
Xanthoparmelia pulla	MXG695565	MG695667	MG695434	MG695729	MG695821	Leavitt et al. (2018)

Xanthoparmelia quintarioides	JQ912318	JQ912417	-	-	-	Leavitt et al. (2018)
Xanthoparmelia squamans	JQ912343	JQ912440	-	-	MG695842	Leavitt et al. (2018)
Xanthoparmelia subimitatrix	JQ912328	JQ912424	-	-	MG695847	Leavitt et al. (2018)
Xanthoparmelia subproxila	AY581074	AY578938	-	-	AY582311	Leavitt et al. (2018)
Xanthoparmelia subproxila	MG695585	MG695685	MG695444	MG695739	MG695849	Leavitt et al. (2018)
Xanthoparmelia tegeta	AY581107	AY578975	-	-	AY582342	Leavitt et al. (2018)
Xanthoparmelia verrucella	MG695594	MG695694	MG695448	MG695743	MG695859	Leavitt et al. (2018)
Xanthoparmelia xanthomelaena	HM125740	HM125761	-	-	HM125717	Leavitt et al. (2018)
Xanthoparmelia delisei 1	JQ912307	JQ912408	-	-	AY582304	Amo de Paz et al. (2012)
Xanthoparmelia delisei 3	AY581068	AY578931	-	-	-	Amo de Paz et al. (2012)
Xanthoparmelia delisei 4	JQ912308	JQ912409	-	-	-	Amo de Paz et al. (2012)
Xanthoparmelia delisei 5	JQ912305	JQ912406	-	-	-	Amo de Paz et al. (2012)
Xanthoparmelia glabrans 5	AY581072	AY578935	-	-	AY582308	Amo de Paz et al. (2012)
Xanthoparmelia glabrans 6	JQ912306	JQ912407	-	-	-	Amo de Paz et al. (2012)
Xanthoparmelia glabrans 7	JQ912286	JQ912388	-	-	-	Amo de Paz et al. (2012)
Xanthoparmelia luteonotata 1	JQ912341	JQ912438	-	-	-	Amo de Paz et al. (2012)
Xanthoparmelia luteonotata 4	JQ912340	JQ912437	-	-	-	Amo de Paz et al. (2012)
Xanthoparmelia perrugata	JQ912324	-	-	-	-	Amo de Paz et al. (2012)
Xanthoparmelia pokornyi 1	AY037005	AY578934	-	-	AY582307	Amo de Paz et al. (2012)
Xanthoparmelia pokornyi 3	JQ912310	JQ912411	-	-	-	Amo de Paz et al. (2012)
Xanthoparmelia pokornyi 4	JQ912323	-	-	-	-	Amo de Paz et al. (2012)

Xanthoparmelia pokornyi 5	JQ912313	JQ912414	-	-	-	Amo de Paz et al. (2012)
Xanthoparmelia pokornyi 6	JQ912312	JQ912413	-	-	-	Amo de Paz et al. (2012)
Xanthoparmelia pokornyi 7	JQ912304	JQ912405	-	-	-	Amo de Paz et al. (2012)
Xanthoparmelia pulla 1	-	JQ912420	-	-	-	Amo de Paz et al. (2012)
Xanthoparmelia pulla 5	AY581071	AJ42X1433	-	-	AF351169	Amo de Paz et al. (2012)
Xanthoparmelia pulloides 1	JQ912347	JQ912444	-	-	-	Amo de Paz et al. (2012)
Xanthoparmelia pulloides 2	AY037004	AY578936	-	-	AY582309	Amo de Paz et al. (2012)
Xanthoparmelia ryssolea 1	JQ912311	JQ912412	-	-	-	Amo de Paz et al. (2012)
Xanthoparmelia ryssolea 2	JQ912309	JQ912410	-	-	-	Amo de Paz et al. (2012)
Xanthoparmelia ryssolea 3	JQ912322	-	-	-	-	Amo de Paz et al. (2012)
Xanthoparmelia verruculifera 1	JQ912334	JQ912431	-	-	-	Amo de Paz et al. (2012)
Xanthoparmelia verruculifera 2	JQ912336	JQ912433	-	-	-	Amo de Paz et al. (2012)
Xanthoparmelia verruculifera 3	JQ912338	JQ912435	-	-	-	Amo de Paz et al. (2012)
Xanthoparmelia verruculifera 4	JQ912335	JQ912432	-	-	-	Amo de Paz et al. (2012)
Xanthoparmelia verruculifera 5	JQ912321	-	-	-	-	Amo de Paz et al. (2012)
Xanthoparmelia pulla 1	MZ367274	-	MZ402522	MZ402566	-	New sequences
Xanthoparmelia pulla 2	MZ367275	-	MZ402523	MZ402567	-	New sequences
Xanthoparmelia pulla 3	MZ367276	-	MZ402524	MZ402568	-	New sequences
Xanthoparmelia pulla 4	MZ367277	-	MZ402525	MZ402569	-	New sequences
Xanthoparmelia pulla 5	MZ367278	-	MZ402526	MZ402570	-	New sequences
Xanthoparmelia pulla 6	MZ367279	-	MZ402527	MZ402571	-	New sequences

165

Xanthoparmelia pulla 7	MZ367280	-	MZ402528	MZ402572	-	New sequences
Xanthoparmelia pulla 8	MZ367281	-	MZ402529	MZ402573	-	New sequences
Xanthoparmelia pulla 9	MZ367282	-	MZ402530	MZ402574	-	New sequences
Xanthoparmelia pulla 10	MZ367283	-	MZ402531	MZ402575	-	New sequences
Xanthoparmelia pulla 11	MZ367284	-	MZ402532	MZ402576	-	New sequences
Xanthoparmelia pulla 12	MZ367285	-	MZ402533	MZ402577	-	New sequences
Xanthoparmelia pulla 13	MZ367286	-	MZ402534	MZ402578	-	New sequences
Xanthoparmelia pulla 14	MZ367287	-	MZ402535	MZ402579	-	New sequences
Xanthoparmelia pulla 15	MZ367288	-	MZ402536	MZ402580	-	New sequences
Xanthoparmelia pulla 16	MZ367289	-	MZ402537	MZ402581	-	New sequences
Xanthoparmelia pulla 17	MZ367290	-	MZ402538	MZ402582	-	New sequences
Xanthoparmelia pulla 18	MZ367291	-	MZ402539	MZ402583	-	New sequences
Xanthoparmelia pulla 19	MZ367292	-	MZ402540	MZ402584	-	New sequences
Xanthoparmelia pulla 20	MZ367293	-	MZ402541	MZ402585	-	New sequences
Xanthoparmelia pulla 21	MZ367294	-	MZ402542	MZ402586	-	New sequences
Xanthoparmelia pulla 22	MZ367295	-	MZ402543	MZ402587	-	New sequences
Xanthoparmelia pokornyi 1	MZ367296	-	MZ402516	MZ402560	-	New sequences
Xanthoparmelia pokornyi 2	MZ367297	-	MZ402517	MZ402561	-	New sequences
Xanthoparmelia pokornyi 3	MZ367298	-	MZ402518	MZ402562	-	New sequences
Xanthoparmelia pokornyi 4	MZ367299	-	MZ402519	MZ402563	-	New sequences
Xanthoparmelia pokornyi 5	MZ367300	-	MZ402520	MZ402564	-	New sequences

Xanthoparmelia pokornyi 6	MZ367301	-	MZ402521	MZ402565	-	New sequences
Xanthoparmelia pokornyi 7	MZ367302	-	MZ402544	MZ402588	-	New sequences
Xanthoparmelia pokornyi 8	MZ367303	-	MZ402545	MZ402589	-	New sequences
Xanthoparmelia pokornyi 9	MZ367304	-	MZ402546	MZ402590	-	New sequences
Xanthoparmelia pokornyi 10	MZ367305	-	MZ402547	MZ402591	-	New sequences
Xanthoparmelia pokornyi 11	MZ367306	-	MZ402548	MZ402592	-	New sequences
Xanthoparmelia pokornyi 12	MZ367307	-	MZ402549	MZ402593	-	New sequences
Xanthoparmelia pokornyi 13	MZ367308	-	MZ402550	MZ402594	-	New sequences
Xanthoparmelia pokornyi 14	MZ367309	-	MZ402551	MZ402595	-	New sequences
Xanthoparmelia pokornyi 15	MZ367310	-	MZ402552	MZ402596	-	New sequences
Xanthoparmelia pokornyi 16	MZ367311	-	MZ402553	MZ402597	-	New sequences
Xanthoparmelia pokornyi 17	MZ367312	-	MZ402554	MZ402598	-	New sequences
Xanthoparmelia pokornyi 18	MZ367313	-	MZ402555	MZ402599	-	New sequences
Xanthoparmelia pokornyi 19	MZ367314	-	MZ402556	MZ402600	-	New sequences
Xanthoparmelia pokornyi 20	MZ367315	-	MZ402557	MZ402601	-	New sequences
Xanthoparmelia pokornyi 21	MZ367316	-	MZ402558	MZ402602	-	New sequences
Xanthoparmelia pokornyi 22	MZ367317	-	MZ402544	MZ402603	-	New sequences
Xanthoparmelia pokornyi 23	-	-	-	MZ402559	-	New sequences

Table S7 Statistical analysis of the photosynthetic parameters obtained in the desiccation response curve of *Xanthoparmelia*, measured at PPFD of 400µmol photonsm^{-2} s^{-1} and temperature of 15 °C. The table shows the p-values obtained by comparing the specimens both habitats through ANOVA in the case of the data passed normal distribution (Shapiro-Wilks test) and equal variance test (Barlett test). For the data which failed normality and homoscedasticity, p-values were obtained through Kruskal-Wallis test. The asterisk (*) showed the parameters with p-value < 0.05.

Photosynthetic parameter	Shapiro-Wilks test	Bartlett test	Statistical model	p-value of the statistical model
NP$_{400}$	0.43	0.15	Anova	0.17
Duration of the optimal conditions	0.9	0.28	Anova	0.69
Total duration of the desiccation curve	0.06	0.02*	Kruskal-Wallis	0.52
Area below the response desiccation curve	0.88	0.33	Anova	0.10
Starting of the optimal conditions	0.41	0.22	Anova	0.23
MWC	0.88	0.009*	Kruskal-Wallis	0.33
OWC	0.10	0.06	Anova	0.051

Table S8 Statistical analysis of the photosynthetic parameters obtained in the light response curves of *Xanthoparmelia*, measured at 5, 10 and 15ºC. The table shows the p-values obtained by comparing the specimens both habitats through ANOVA in the case of the data passed normal distribution (Shapiro-Wilks test) and equal variance test (Barlett test). For the data which failed normality and homoscedasticity, p-values were obtained through Kruskal-Wallis test. The asterisk (*) showed the parameters with p-value < 0.05.

Photosynthetic parameter	Shapiro-Wilks test	Bartlett test	Statistical model	p-value of the statistical model
5ºC				
DRopt	7.9 e-06*	7.7 e-06*	Kruskall-Wallis	0.007*
NP1500	0.2	0.1	Anova	0.7
GP	0.02*	0.007*	Kruskall-Wallis	0.7
Photosynthetic efficiency	0.07	0.182	Kruskall-Wallis	0.002*
Φ	0.57	0.17	Anova	0.5
LSP	0.005*	0.6	Kruskall-Wallis	0.6
LCP	0.0008*	0.009*	Kruskall-Wallis	0.01*
10 ºC				
DRopt	0.0006*	0.001*	Kruskal-Wallis	0.15
NP1500	0.005*	0.001*	Kruskal-Wallis	0.0008*
GP	0.01*	0.19	Kruskal-Wallis	0.08
Photosynthetic efficiency	0.001*	0.26	Kruskal-Wallis	0.043*
Φ	0.17	0.85	Anova	0.45
LSP	0.9	0.27	Anova	0.051
LCP	0.0002*	0.0001*	Kruskal-Wallis	0.09
15 ºC				
DRopt	0.0006*	0.002*	Kruskall-Wallis	0.44
NP1500	0.04*	0.35	Kruskall-Wallis	0.6
GP	0.001*	0.07	Kruskall-Wallis	0.69

Photosynthetic efficiency	0.004*	0.01*	Kruskall-Wallis	0.18
Φ	0.14	0.44	Anova	0.69
LSP	0.03*	0.14	Kruskall-Wallis	0.69
LCP	0.003*	0.03*	Kruskall-Wallis	0.58

Table S9 Summary of genetic diversity statistics of nrITS, *β-tubulin*, and *MCM7* sequences of *Xanthoparmelia*, obtained using DNAsp software.

	nrITS	*β-tubulin*	*MCM7*
Number of sequences	44	43	44
Alignment length (bp)	503	592	442
Sites with alignment gaps or missing data	49	4	4
Singleton variable sites	9	5	1
Number of polymorphic (segregating) sites, S	13	11	8
Parsimony informative sites	4	6	7
Number of haplotypes, h	10	12	9
Haplotype diversity, Hd	0.613	0.721	0.840
Average number of nucleotide differences, k	1.123	2.228	1.584
Nucleotide diversity, Pi	0.00247	0.00379	0.00362
Nucleotide diversity (Jukes and Cantor), Pi(JC)	0.00248	0.00380	0.00363

Table S10 Summary of genetic diversity statistics of nrITS, *β-tubulin*, and *MCM7* sequences of *Xanthoparmelia* comparing both habitats.

	nrITS		*β-tubulin*		*MCM7*	
Genetic diversity for each habitat						
Habitat	Coast	Desert	Coast	Desert	Coast	Desert
Number of sequences	22	22	22	21	22	22
Number of polymorphic sites	13	1	11	0	6	3
Average number of nucleotide differences, k	1.926	0.247	1.801	0	1.411	1.186
Nucleotide diversity, Pi	0.00424	0.00054	0.00306	0	0.00322	0.00271
Genetic diversity between populations						
Mutations polymorphic in the desert, but monomorphic on the coast	0		0		2	
Mutations polymorphic on the coast but monomorphic in the desert	0		11		5	
Shared mutation	12		0		1	
Average number of nucleotide differences between populations	1		3.455		1.855	

Table S11 *Trebouxia*-OTU abundances associated with *Xanthoparmelia*.

Sample	OTU1	OTU2	OTU29	OTU31	OTU33	OTU37	OTU5	OTU61
1	33155	0	1	2	0	0	0	0
2	72613	0	1	8	0	0	0	5
3	65325	0	13	5	1	0	0	1
4	63229	0	24	21	0	0	1	0
5	125194	0	1	5	6	0	0	0
6	26811	1	4	3269	373	0	0	0
7	70291	0	1	5	3	0	0	0
8	80086	0	1	3	1	0	0	0
9	69082	0	0	1	0	0	0	4
10	63701	0	0	8	0	0	156	0
11	146153	0	4	35	12	0	0	0
13	67670	0	0	0	0	0	0	1
14	59158	0	7	41	3	0	8	7
15	7525	1	1	11	1	0	3	3
16	29078	0	3	1	0	0	2	42
17	30091	0	3634	0	1	0	0	0
18	106696	0	4	1	1	0	1	0
19	45305	0	1	0	0	0	0	0
20	26576	0	6	3	0	0	2	4
21	19418	0	22	14	0	0	0	24
22	177630	0	26	212	6	0	0	0
23	67435	0	1	5	1	0	0	1
24	465	0	0	14	1	0	0	0
25	44725	0	1	1	0	0	3	0
26	53852	0	2	16	0	0	21	0
27	94567	0	6	0	0	0	0	0
28	808	0	0	0	3	0	0	2
29	83604	0	0	0	0	0	0	0
30	0	0	0	0	0	0	25	0
31	309	0	0	0	0	0	4	0
33	62104	0	12	184	46	0	0	1

34	568	34630	1	0	0	0	29	0
35	137226	1	0	0	0	0	17	0
36	0	47932	3	3	0	0	1	0
37	28	2	0	0	0	0	34	2
38	1442	0	0	0	0	18	77398	0
40	0	2053	0	0	0	239	210	0
41	86725	68	0	1	0	847	3242	0
42	7162	98	0	0	0	43	45	0
43	66638	0	0	0	0	0	3	0
44	501	107	0	0	0	17	7	0
45	8862	0	0	0	0	0	10	0
46	0	1312	0	0	0	0	0	0
47	78927	0	0	0	0	10	5125	0
48	0	0	0	0	0	8	10337	0
51	1543	0	0	0	0	0	6204	1
54	20471	1	5	0	0	38	24	1
56	0	0	21	5	2	0	12457	3
57	130312	0	0	0	0	0	1	0
58	117485	1838	0	0	0	212	55	0
59	20964	32297	0	0	0	45	456	0
60	6359	46	1	0	0	0	0	3
61	7291	24902	0	0	0	33	2	0
62	55591	1000	0	0	0	0	4	0
63	1087	6955	0	0	0	0	2	0
64	138258	3	0	0	0	2	12	0
65	75005	1	0	0	0	1	0	1
66	19309	91	13	0	0	20	4	0
67	0	23208	0	0	0	11	0	0
68	17569	0	9	0	0	0	0	2
69	6016	751	3	0	0	0	0	0
70	0	19283	0	0	0	0	0	0
71	0	55082	0	0	0	78	5	0
72	132	1254	0	0	0	23	29	0

73	0	1240	0	0	0	162	27572	0
74	10777	1580	1	0	0	0	1	0
75	15506	8247	3	0	0	0	1	0
76	5588	3403	1	0	0	0	231	0
77	0	30292	0	0	0	13	0	0
78	0	23036	3	0	0	0	0	0
79	4632	1644	0	0	0	0	0	0
80	98164	1038	0	0	0	20	0	0
81	124414	23	0	0	0	3	4	0
82	101092	1	0	0	0	0	718	0
83	109446	0	0	0	0	4	14	1
84	18776	7	0	0	0	0	2	8
85	142943	1	0	0	0	73	0	3
86	0	20537	0	0	0	1	0	0
87	68184	2	0	0	0	2	0	0
88	79818	2	3	0	0	3	0	11
89	63877	12	0	0	0	0	0	0
90	57088	3	0	0	1	2	0	4
91	57003	15	0	0	0	0	7	1
92	18767	10636	0	0	0	8	0	2
93	78004	34	0	0	0	88	0	0
94	95130	0	0	0	0	0	0	0
95	54819	0	0	0	0	0	596	13
96	46137	0	0	0	0	0	0	30
97	88074	2	1	0	0	7	0	6
98	63670	1	0	0	0	0	1	2
99	0	38324	0	0	0	0	0	0
100	39059	4	5	0	0	4	19	233
101	0	50621	0	0	0	0	0	19
102	63959	3	0	0	0	28	0	39
103	53428	0	0	0	0	13	0	54
104	25729	3136	0	0	0	50	6	8
105	69257	1	0	0	0	6	1	2

106	4931	6780	0	0	0	0	0	0
107	0	48224	0	0	0	19	0	0
108	92512	2	0	0	0	109	1	7
109	71052	36	0	0	0	0	0	6
110	15982	3627	0	0	0	0	3	0
111	87979	0	1	0	0	0	0	1
112	170070	0	400	0	0	0	1	5
113	54938	1	10	40	8	0	0	1
114	84797	0	0	0	0	0	306	0
116	28964	0	3	0	1	3	1	0
117	83900	0	0	0	0	0	0	3
118	36238	0	19	4	3	0	0	5
119	36654	0	0	0	1	0	10	0
120	112676	0	29	16	0	0	2	1
121	50107	0	31	1	1	0	5	5
122	34183	0	18	3	0	0	0	3
123	120002	0	17	12	3	0	0	0
124	32718	1	7	0	0	0	0	5
125	91925	0	11	1	0	0	1	5
126	21243	0	31	4	0	1	0	4
127	51453	1	19	1	0	1	0	9
128	38958	0	16	13	1	0	0	3
129	108563	13	0	1	0	0	0	0
130	45272	2	8	5	0	0	0	4
131	74766	0	0	0	0	0	0	13
132	19515	0	3	6	0	0	0	3
133	80149	134	12	0	2	2	1	2
134	89053	21	1	3	1	0	0	2
136	69708	0	1	428	106	0	0	0
137	56921	0	16	171	207	0	1	1
138	31579	0	5	0	0	0	0	1
139	50441	0	3	18	2	0	0	8
140	59556	0	4	3	2	0	0	1

141	101712	1	44	35	0	0	0	1
142	80294	1	10	2	5	0	0	0
143	30313	0	3	2	1	0	0	1
144	49643	1	15	4	0	0	1	0
145	52160	0	0	0	0	0	0	2
146	97104	0	0	0	0	0	25	0
147	49900	0	0	0	5	0	0	1
148	86834	0	78	1	0	0	0	0
149	36484	0	3	4	19	0	1	1
150	64578	1	8	1	0	0	0	0
151	73165	0	0	0	0	0	0	0
152	75181	1	0	0	13	0	0	0
153	95940	0	0	0	3	0	0	0
154	36437	0	1	4	1208	0	0	1
155	17003	0	2	0	0	0	0	20
156	135866	0	0	0	2	0	0	0
157	167766	1	0	0	2	0	43	4
158	41291	0	0	0	0	0	0	0
159	88230	0	0	0	7	0	0	0
160	72526	0	0	0	0	0	0	0
161	86158	0	273	25	0	0	0	0
162	84471	0	0	0	0	0	0	1
163	119457	0	3	1	0	0	4	1
164	82406	0	2	1	1	0	0	0
165	69383	0	1	1	0	0	1	1
166	123139	0	0	0	0	0	1	0
167	87607	0	3	54	3	0	1	0
168	31322	0	0	0	0	0	0	0

Figure S1 Principal Coordinates Analysis (PCoA) of axes 1 (PCoA1) and 2 (PCoA2) of 19 BIOCLIM climatic variables and radiation for the six sampling site. Population 1, 6, and 7 are located in the desert, and population 3, 4, and 5 on the coast.
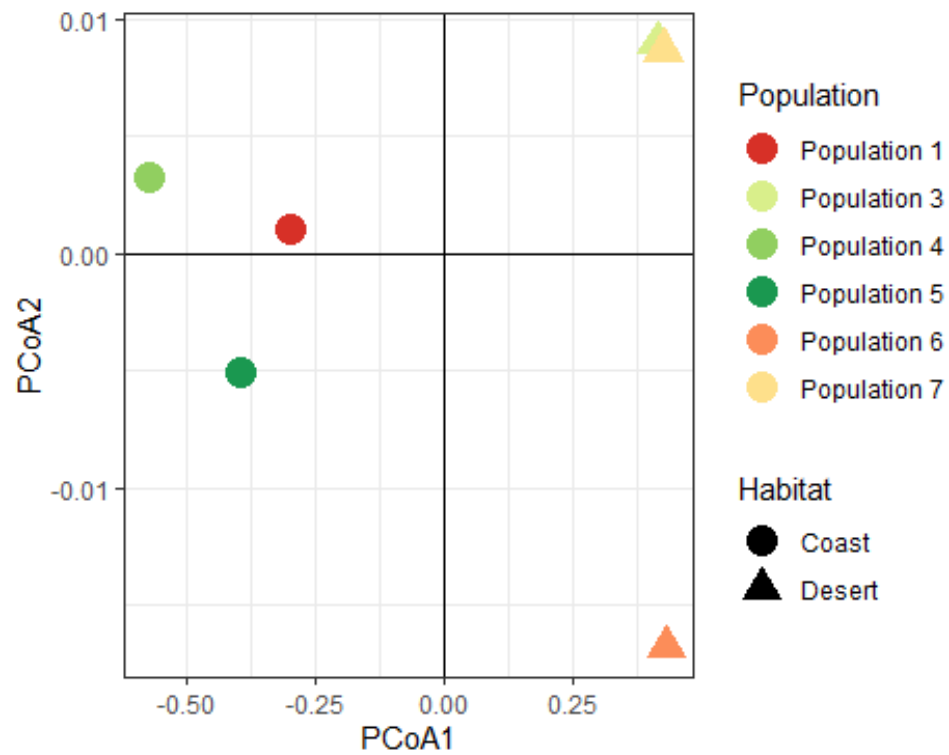
Figure S2 Principal Coordinates Analysis (PCoA) of axes 1 (PCoA1) and 2 (PCoA2) of the physiological performance analysis for the six sampling sites. In the PCoA, we included NP_{1500} and DRopt as the most explanatory photosynthetic parameters.
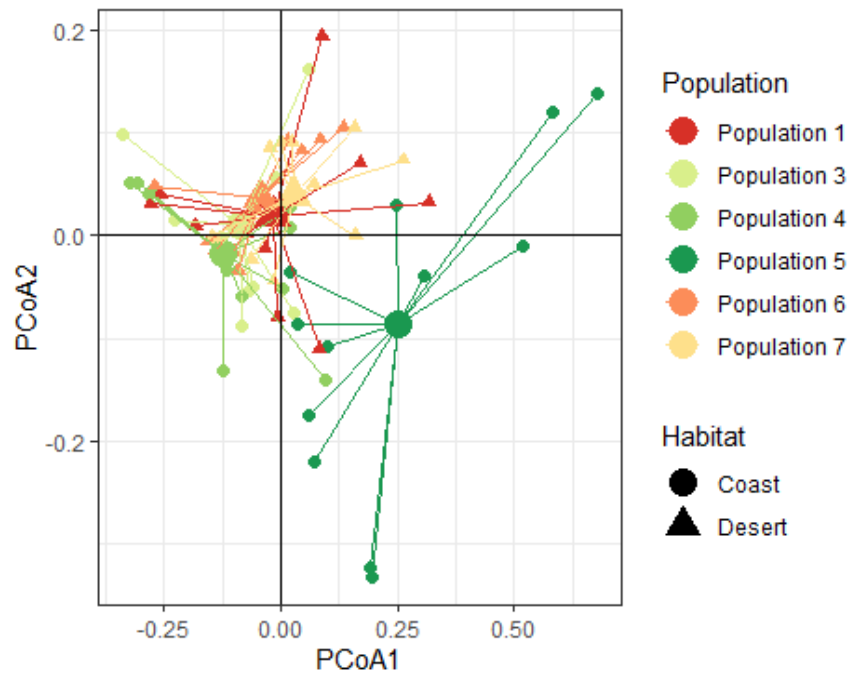

Figure S3 Tripartite network between host haplotypes, Trebouxia OTUs, and habitat.
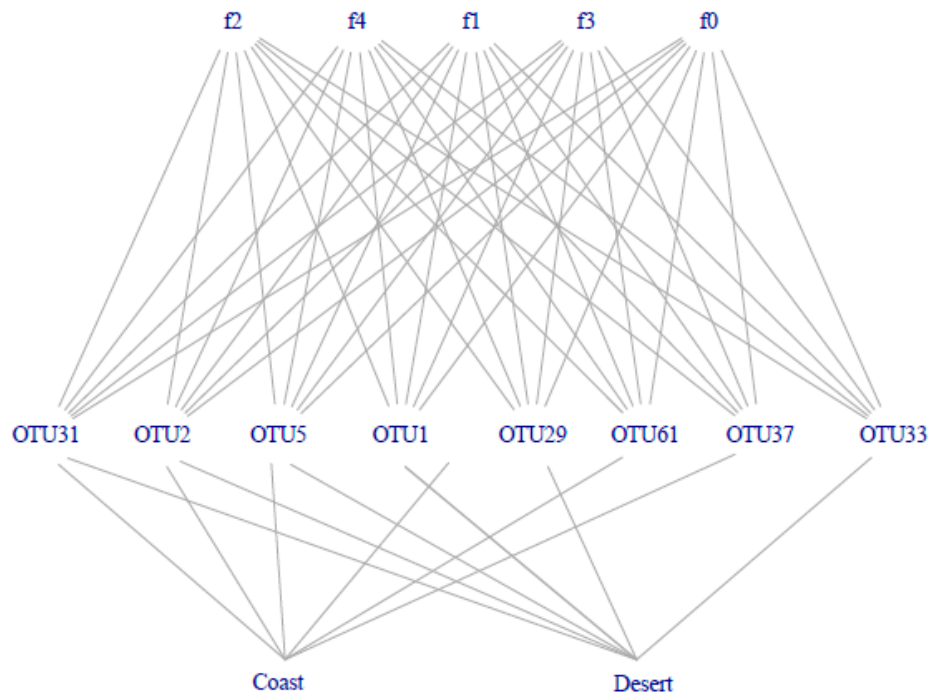
Figure S4 Dependence of net photosynthesis on time to incident PPFD of 400 µmol CO_2 m^{-2} s^{-1} at 15°C on the coast (green) and in the desert (blue). We analysed 12 samples for each locality (N =24). Colorized area showed the standard deviation of the mean net photosynthesis. The R^2-adjust and standard deviation of each curves is detailed in Table S2.
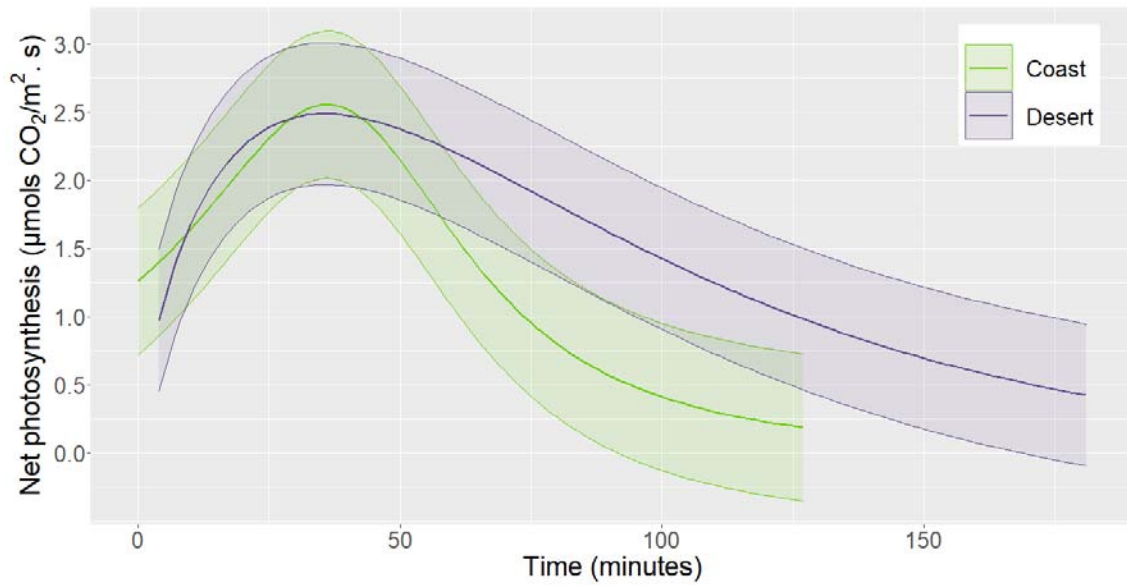
Figure S5 Maximum Likelihood phylogenetic tree of (A) *MCM7*, (B) nrITS and (C) *β-tubulin* of new generated sequences of *Xanthoparmelia pulla* and *X. pokornyi*. Bootstrap value higher than 70 % is showed in the node labels. Grey squares showed in which species is present the haplotype. Phylogenies were produced with RAxML and had a lnL value of -880.0010 for nrITS, -971.1340 for *β-tubulin* and -790.5756 for *MCM7*.
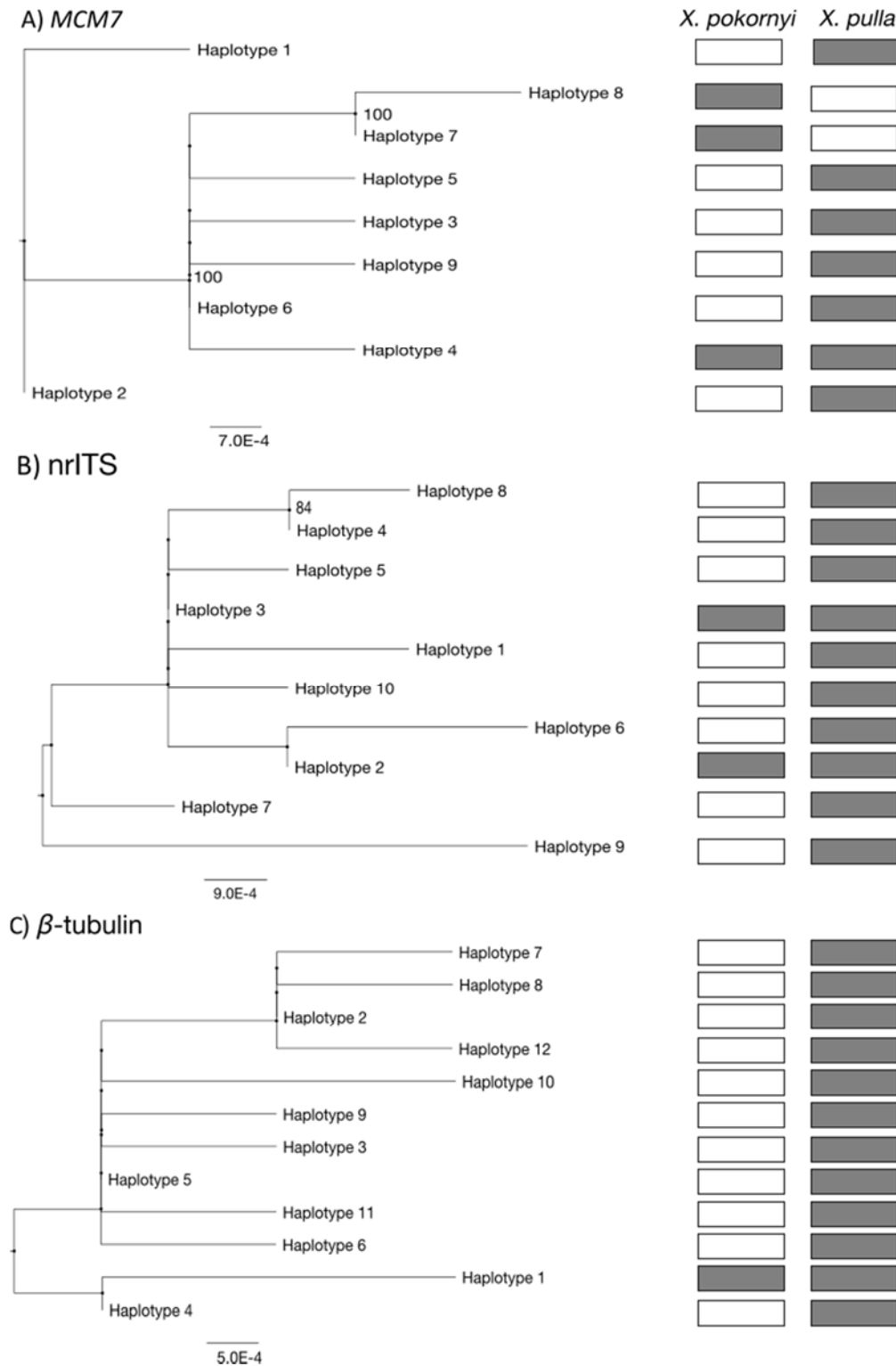
Figure S6 ITS2 secondary structure of the eight *Xanthoparmelia*-associated *Trebouxia* OTUs.
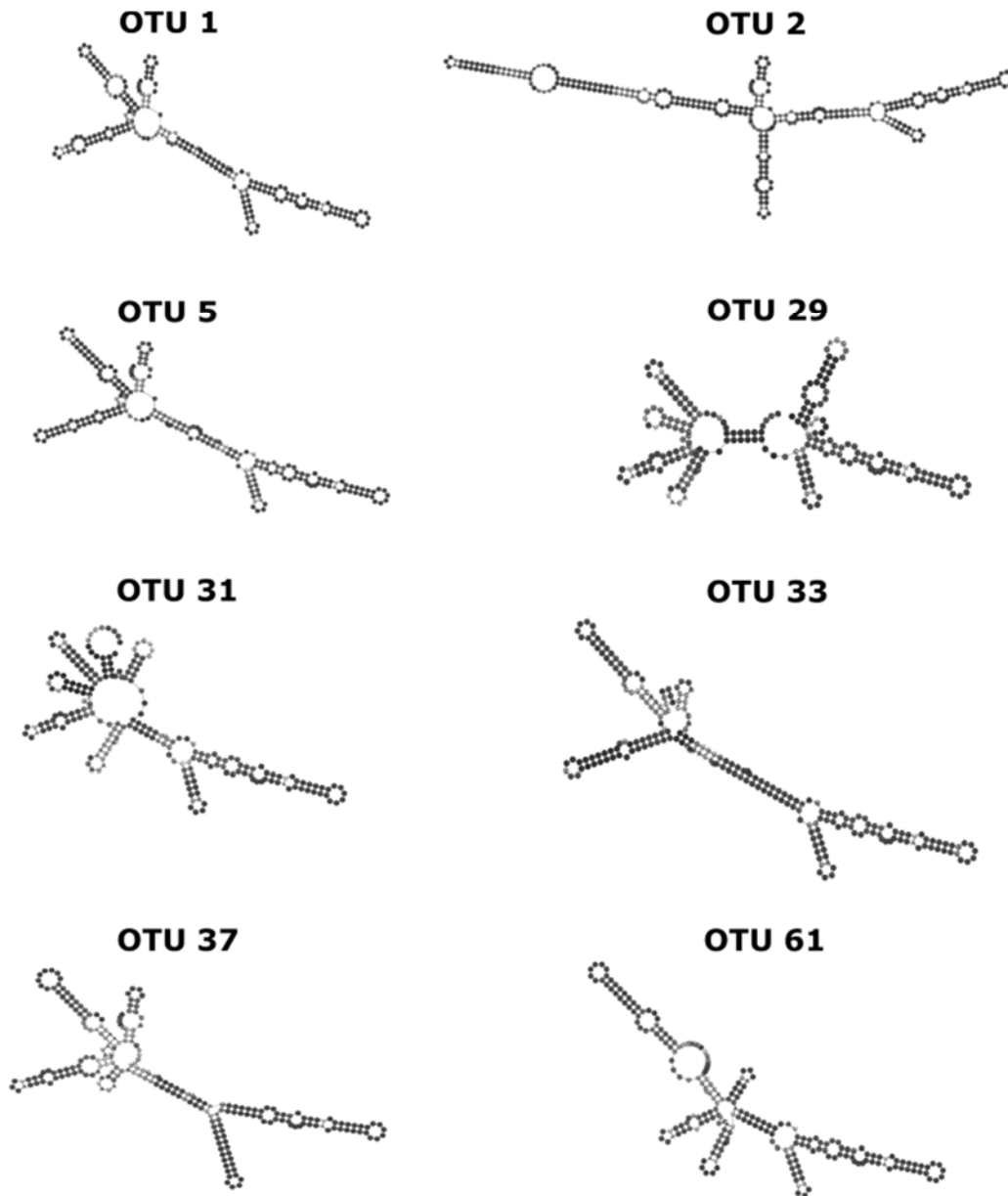
Figure S7 Phylogenetic placement of the *Xanthoparmelia*-associated *Trebouxia* OTUs. This is a maximum likelihood tree based on 8 *Trebouxia* OTUs and 69 OTUs representing the major, well-supported *Trebouxia* clades (i.e., 'A' – arboricola/gigantea, 'I' – impressa/gelatinosa, 'S' –simplex/'letharii'/jamesii, 'G' – galapagensis/usneae group) (Leavitt et al., 2015). *Trebouxia* OTUs retrieved for this study are marked in white inside of a black box.
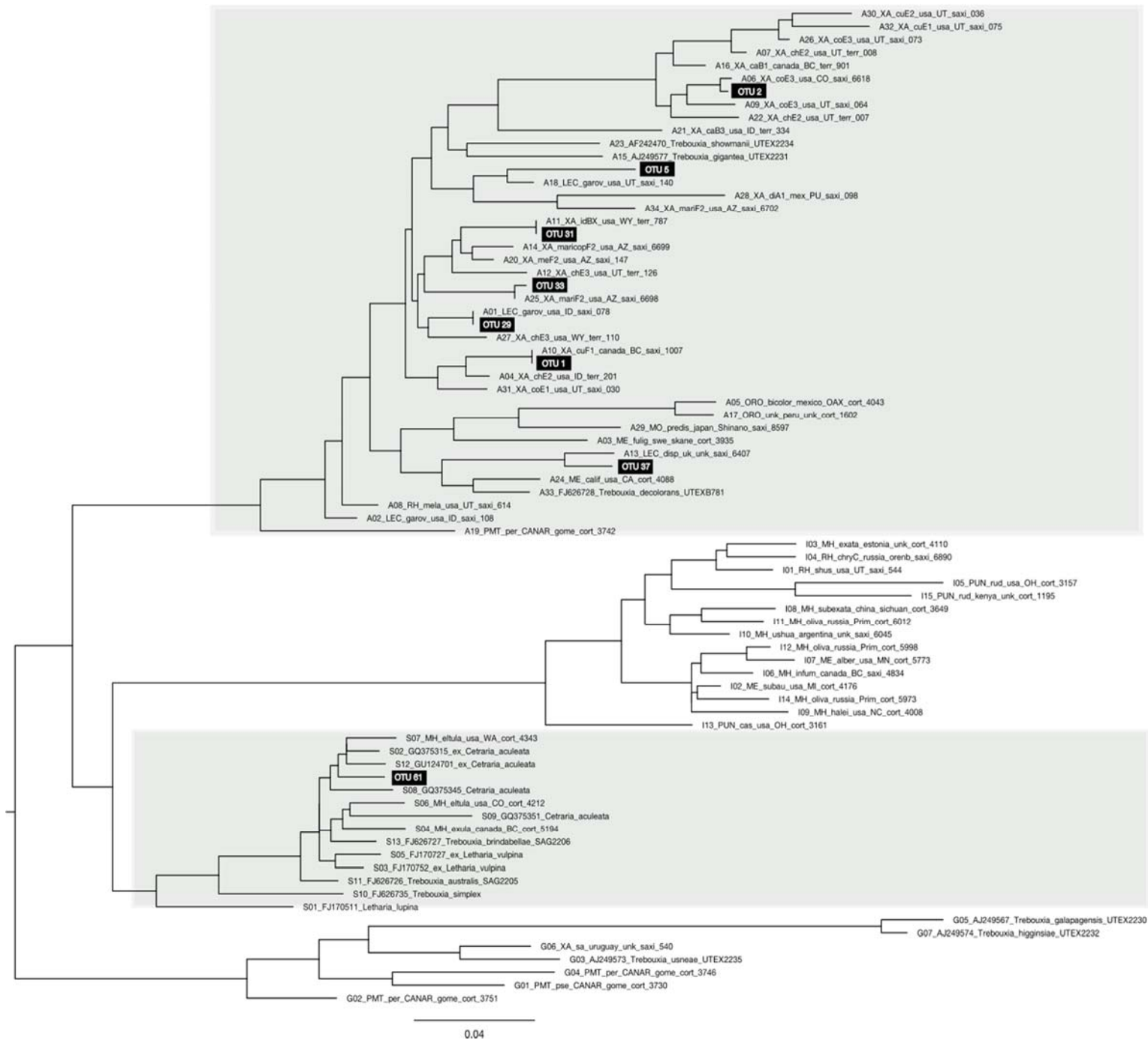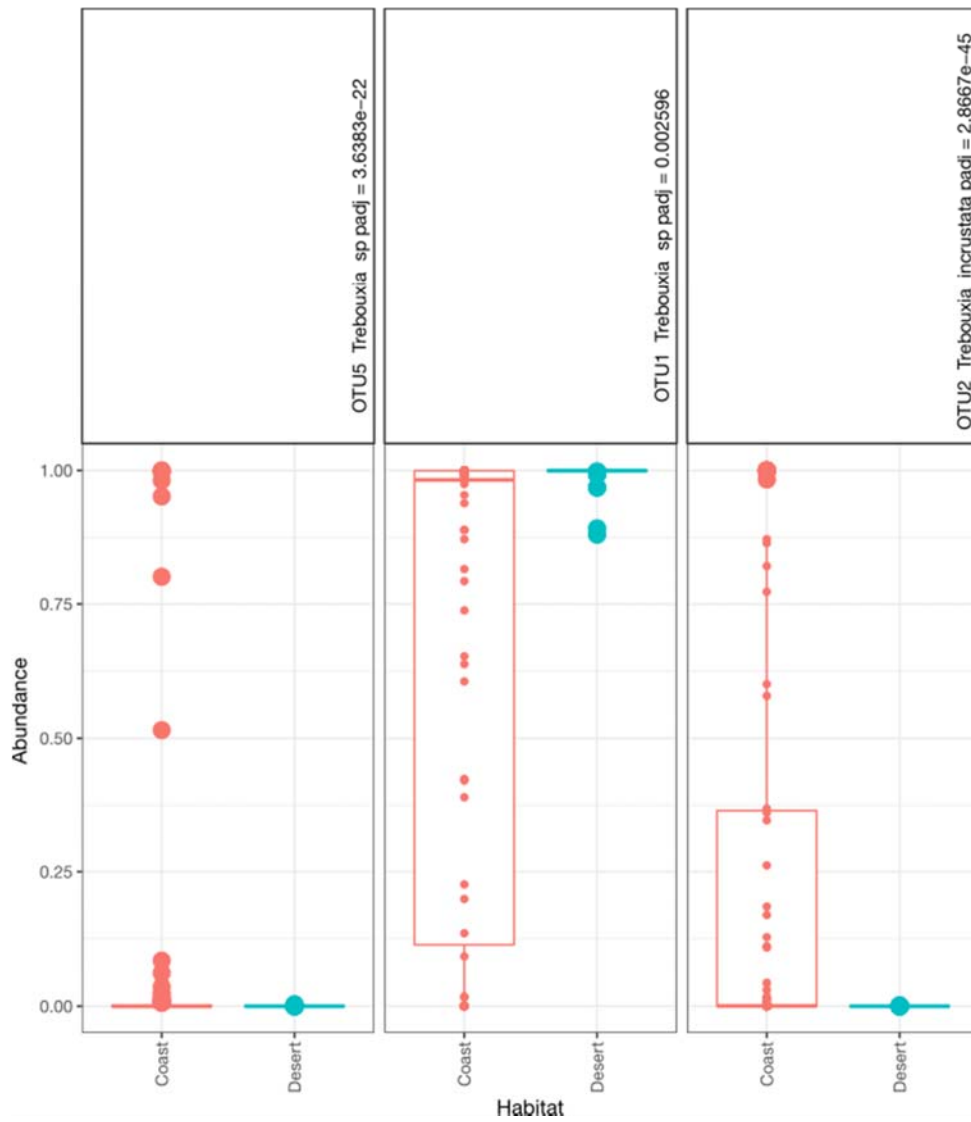
Figure S8 Significant differences in *Trebouxia* OTU abundance between habitats obtained from the DeSeq analysis.

APPENDIX C. Supplementary data of Chapter 3

Fig. S1 (a) Dependence of net photosynthesis (mg CO_2 gDW^{-1} hour^{-1}) on temperature (°C) and PAR (μmols photons m^{-2} s^{-1}) obtained from GAM 1. (b) GAM 1 statistical outcome. The edf corresponds to the estimated degrees of freedom. P-value < 0.05 is considered as the minimum level of significance. The model has an R^2 value of 0.99 and explains 100% of the total deviance.

(a)
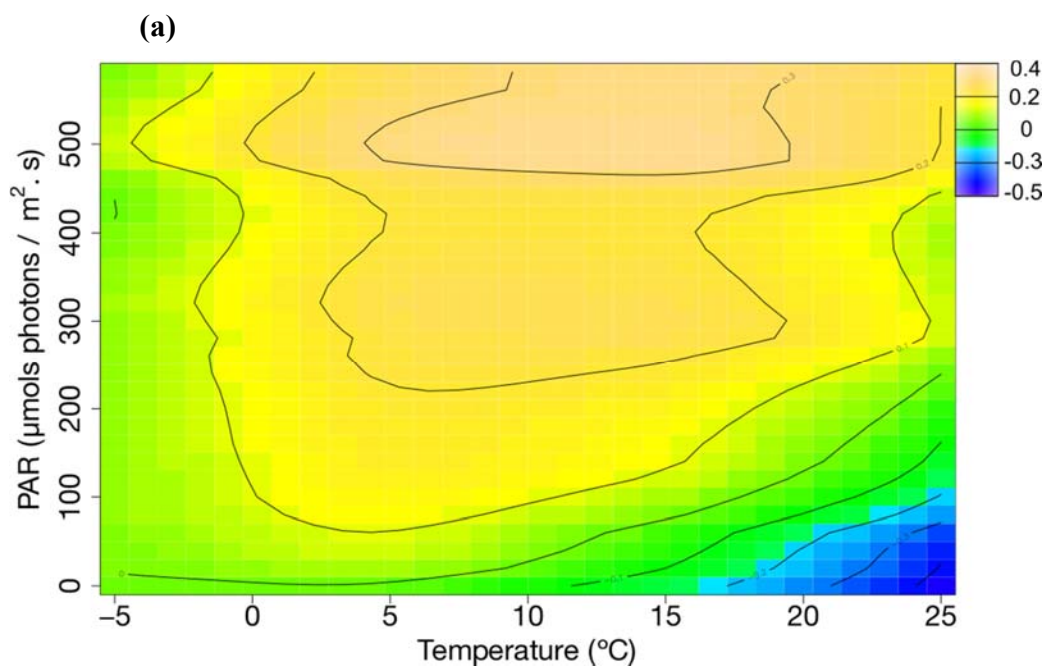
(b)

Smoothing terms	edf	F-test	p-value
s(PAR)	1	12.11	0.00316
s(Temperature)	7.569	121.44	< 2e-16
s(PAR, Temperature)	22.314	407.44	< 2e-16

Fig. S2 Macroclimate (black) and microclimate (red) from 2009 to 2014 at Livingston Island (maritime Antarctica). Daily means are given for (a) temperature, (b) PAR, and (c) relative humidity. The sum of daily precipitation is shown in (d).
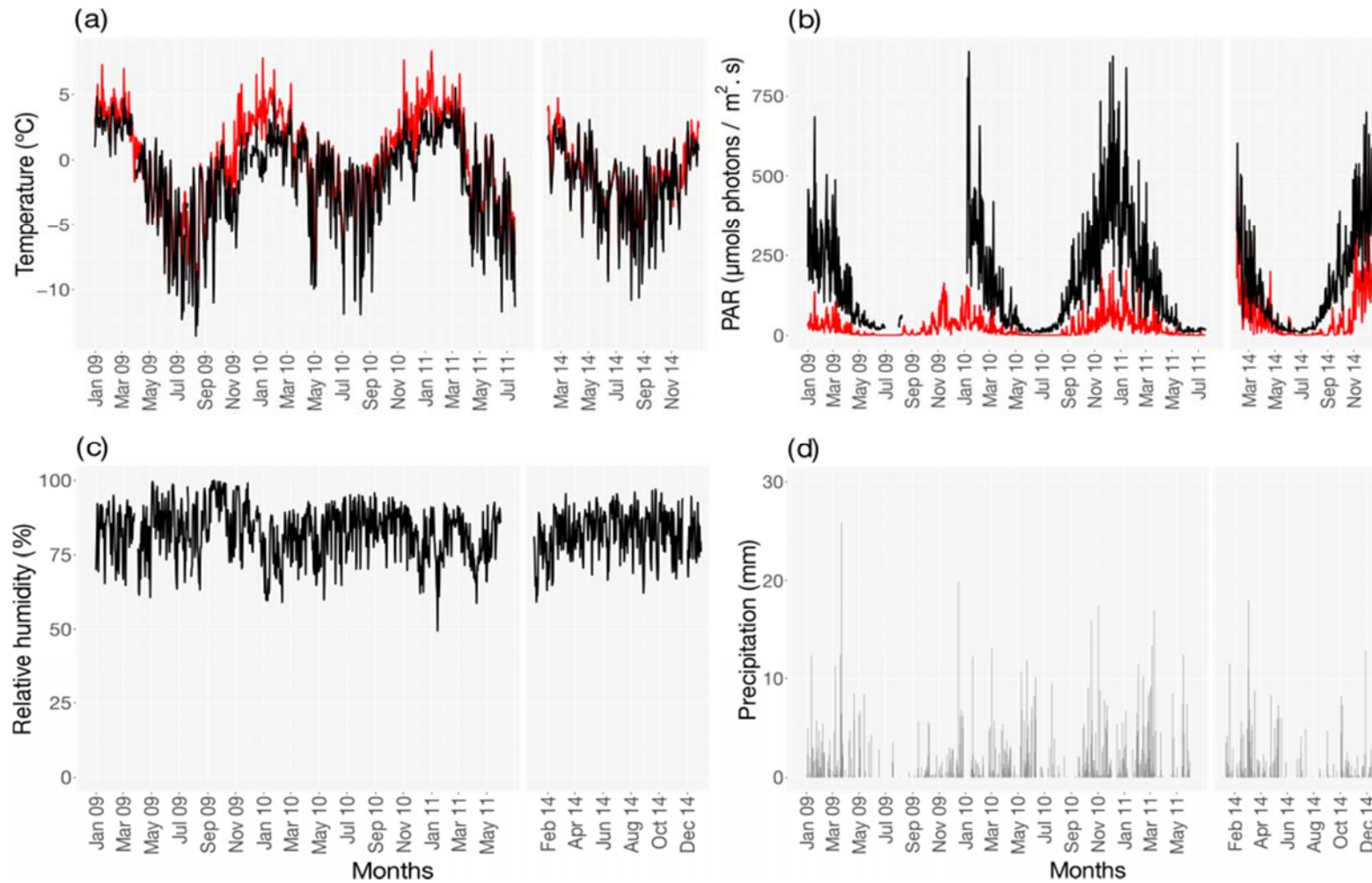
Fig. S3 Daily mean of metabolic activity measured for *Usnea aurantiaco-atra* at Livingston Island (maritime Antarctica) from 2009 to 2014.